Mathematical Modelling and Analysis of Different Food Chains of Sundarban Estuary, India

Thesis submitted

in partial fulfillment of the requirements

for the award of the degree of

DOCTOR OF PHILOSOPHY (SCIENCE)

Submitted By

TANUSHREE MURMU

Under the supervision of

PROF. (Dr.) ASHIS KUMAR SARKAR

Professor, Department of Mathematics
Jadavpur University, Kolkata-700032

Department of Mathematics
Jadavpur University
Kolkata-700032, India

September, 2024

যাদবপুর বিশ্ববিদ্যালয়

FACULTY OF SCIENCE
DEPARTMENT OF MATHEMATICS

JADAVPUR UNIVERSITY
Kolkata - 700 032, India
Telephone : 91 (33) 2457 2269

CERTIFICATE FROM THE SUPERVISOR

This is to certify that the thesis entitled "Mathematical Modelling and Analysis of Different Food Chains of Sundarban Estuary, India" submitted by Tanushree Murmu whose name was registered vide INDEX NO. 46/18/Maths./25 dated 13/02/2018 for the award of Doctor of Philosophy (Science) degree of Jadavpur University, Kolkata 700032. This thesis is absolutely based upon her own work under my supervision and is worthy of consideration for the award of Ph.D. (Sc.) degree. Neither this thesis nor any part of this work has been submitted to any other University or Institute for the award of any degree/diploma or any other academic award anywhere before.

09/09/2024

(Prof. ASHIS KUMAR SARKAR)
(Signature of the Supervisor date with official seal)

Professor
DEPARTMENT OF MATHEMATICS
Jadavpur University
Kolkata - 700 032, West Bengal

Dedicated to my parents…

Acknowledgement

It is with immense gratitude that I acknowledge the support of my supervisor, Prof. Ashis Kumar Sarkar, for his unwavering help throughout the research and writing process. I have greatly benefited from his open-door policy, his good nature, generosity, and inspirational academic thinking. His patience and guidance were invaluable in making my thesis possible.

I am truly appreciative of Prof. Dipak Kesh, Department of Mathematics, for his invaluable comments and suggestions that have significantly shaped my PhD journey.

My deepest gratitude goes to Prof. Sagnik Sinha, the Head of the Department of Mathematics, for providing all the facilities and helping carry out the research work. In this learning process, I am grateful to every teacher who has guided me down the way. I am grateful to the non-teaching staffs of the Department for their immense help during this journey.

I also express my gratitude to my friends, peers, and colleagues, including Dr. Bhuban Chandra Das. Without their company and encouragement, the trip to the finish line would have been very different and lonelier. A special thanks go to my lab colleagues, including Dr. Sudipta Sarkar, Smt. Srijita Mondal, Dr. Arunabha Sengupta, and Dr. Roshmi Das.

Most importantly, I am deeply grateful to my family members, especially my father Sri. Mahadev Murmu, my mother Smt. Sarimancha Murmu, and my five sisters Miss Bhabani Murmu, Mrs. Mamani Murmu, Mrs. Sonamoni Murmu, Miss Banashree Murmu, and Miss Jayashree Murmu for their unwavering support through the ups and downs of my PhD life. Their patience and encouragement have been a constant source of strength for me. Also, I sincerely thank my friend Sri. Sahadeb Das for bearing with all my mood swings.

There were times when I did not think it possible that this journey would end with a thesis written and bound. During this phase, we all experience hopelessness and despair, but we come out stronger, having roughed out the lows through the love of those around us and with the blessings of God. Thank you all once again.

Place: Jadavpur University   (**Tanushree Murmu**)

Date:

ABSTRACT

Sundarban mangrove forest is one of the largest mangrove forests, and it is very rich in dynamics due to its diversity. The forest and its adjacent estuary support detritus-based food chain, which is the most common and significant food chain to shape the dynamics of that ecosystem.

In this thesis, some non-spatial detritus-based prey-predator models in the Sundarban mangrove forest and the nearby estuary have been examined to study the dynamics of interaction between the micro-organism pool feeds on detritus and its invertebrate predators. This detritus is mainly produced from the plant litter of several mangrove trees by the decomposition process with the help of micro-organism pool. This detritus is the primary energy source of this ecosystem, and the energy is transferred from the detritus to the higher tropic levels. The rate of uptake of invertebrate predators is taken as Ivlev-type response function. We have also considered some models where the loss of detritus due to micro-organism pool is assumed to follow Holling type-II functional response. The mathematical analysis includes the existence of different feasible equilibria and their stability behaviour, including the existence of Hopf-bifurcation and limit cycle.

Next, we consider a model where it is assumed that besides the plant litter, a small amount of detritus is also formed from the dead bodies of invertebrate predators by the recycling process and the effect of single discrete-time delay is studied. Next, a model with multiple time delays is considered. These time delays play a pivotal role in building the dynamics as these delays can destabilize a stable ecosystem.

We have also formulated some models with Caputo fractional order derivatives. Due to its memory effect; these fractional order systems are more realistic and complicated than the integer order systems. Using the Homotopy perturbation method, the approximate solution of a fractional order model has been derived. Next, the effect of prey refuge is considered in a model in presence of toxicity. In mangrove estuary, tidal waves come twice a day, and due to tidal influence, some amount of micro-organisms of the adjacent estuary always washed out. As a result of this type of prey refuge, an amount of micro-organism is protected from predation. This prey refuge enhances the prey-predator coexistence and prevents the micro-organism from extinction. It is known that industries always release a huge amount of toxic substances into marine water. Due to the tidal influence of the adjacent Bay of Bengal, a huge amount of marine water enters in the estuary. The growth of micro-organism pool and invertebrate predators are affected because of this toxicity.

All the theoretical outcomes are verified by numerical simulations.

keywords: Detrtitus, Micro-organism pool, Ivlev-type functional response, Invertebrate predator, Time delay, Fractional order, Prey refuge, Toxicity.

Tanushree Murmu
09/09/2024
INDEX NO: 46/18/Maths./25
dated 13/02/2018

09/09/2024

Professor
DEPARTMENT OF MATHEMATICS
Jadavpur University
Kolkata - 700 032, West Bengal

Contents

Chapter 1

Introduction

Mathematical modeling is a powerful area of mathematics that deals with various real-world issues using mathematical expressions, equations, and terminology derived from mathematical ideas. Malthus (1798) applied mathematical modeling to population dynamics in the early 1800s. Malthus believed that population growth and decay are always exponential in nature. Later, Verhulst refined the Malthus model. Rather than focusing just on exponential growth, he included the horizontal asymptote of population increase or decay in his model. In his model, Verhulst used the phrase "carrying capacity of the environment." Subsequently, Volterra (1926) expanded mathematical modeling to include a prey-predator model. In this model, he primarily examined interspecies competition and the neutral stability of the interior equilibrium point, or center. Subsequently, a number of mathematicians created quadratic models, which included certain non-linear elements resulting from the feeding effect and more intricate interactions between the prey and predator species. These models included logistic-type growth equations. The field of mathematical ecology has grown significantly in the modern century, and numerous techniques and instruments have been created to thoroughly examine any prey-predator relationship.

1.1 Ecology

Ecology is the branch of science that focuses on the interactions that living things have with one another and their environment. A population is a group of individuals living in

a certain area who are members of the same class of species; a community is made up of individuals from different populations that share a particular area. Two key phrases that naturally accompany ecology are population and community. Certain characteristics are specific to a population, such as its growth, death, and reproduction rates. In 1866, the eminent biologist Ernst Haeckel created the term ecology. The construction of mathematical models for various ecological systems is of great interest due to the nonlinear interplay between living and non-living components and the consequent dynamical behaviour. In any ecological system, mathematical modeling is an organized approach that is essential to comprehending ecology through the use of certain state variables. This is the primary goal of mathematical modeling of an ecological system.

1.2 Food chain model

Certain creatures always prey on other organisms in any habitat. Predators are species that use prey as their food source, whereas prey are organisms that are consumed. Food energy is thus transferred from the lower member to the higher member. A food chain is a group of organisms that exchange energy with each other. The flow of food energy from lower to higher tropical levels and the interactions between predator and prey are portrayed by the food chain model, which is just a system of differential equations. There are two main types of food chain models:

1. Deterministic food chain model where time t is continuous.

2. The stochastic food chain model in the discrete-time domain.

1.3 Population dynamics

A subfield of theoretical biology known as population dynamics examines both short-term and long-term variations in a species' population size. It focuses mostly on population size and how it varies throughout time and space. In terms of evolutionary biology and biomathematics, this is the most important aspect. The Malthusian growth model was modeled in 1798 based on the first principle of population dynamics. Benjamin Gompertz (1825) later improved and changed this model. The prey-predator equations developed by Lotka and Volterra in 1925 and 1926 have the biggest impacts on the advancement of population biology. Immigration, emigration, and per capita birth and death rates all control the dynamics of any population. By creating a deterministic mathematical model, the dynamics of a population can be ascertained using this idea.

1.4 Mathematical ecology

A subfield of applied mathematics called mathematical ecology serves as a bridge between ecology and mathematics. It smoothly transforms the ecological condition in real life into a mathematical expression and then discusses the characteristics of the ecosystem's living and non-living components and how they relate to one another. An ecological problem can be converted into a mathematical problem and theoretically solved utilizing a variety of strategies, tools, and algorithms. Mathematical models of the food chain, prey-predator, fisheries, and epidemiological kinds have all been extensively investigated and analyzed in order to investigate various ecological facts.

1.5   Functional responses

The functional response is the rate at which a predator devours its prey. In each model system of prey and predator, this functional response is a necessary word. It significantly controls the dynamic stability of any predator-prey system. Prey-predator data are explained and interpreted using three distinct classes of functional responses in any predator-prey model.

1.5.1   Prey-dependent:

In prey-dependent models, the predation rate is thought to be exclusively reliant on prey density. This section discusses a few common prey-dependent functional responses that are frequently employed.

(i) **Holling type I**

The Holling type I functional response is thought to be represented by a bounded, one-dimensional linear curve. Predators either consume food at a constant rate or at a rate that grows linearly with increasing food density. In this instance, the predator's processing time for food is very short.

The Mathematical expression for the Holling type I function is

$$f(p(t)) = \eta p(t),$$

where the prey density is represented by $p(t)$, whereas the per capita rate of prey consumption by predators is denoted by η.

(ii) **Holling type II**

A bounded hyperbolic curve that is non-linear in nature is the characteristic of the Holling type II functional response. As the consumer's ability to process food is limited, the intake rate falls for this response function. Insects and micro-organisms are the primary examples

of this kind of functional response.

The mathematical expression for this type of functional response is

$$f(p(t)) = \frac{\eta p(t)}{\beta + p(t)}.$$

Here, the half-capturing saturation constant is denoted as β, and η, $p(t)$ are the same as described above.

(iii) **Holling type III**

When there is a large density of prey, the Holling type III functional response is almost the same as the Holling type II response. In low densities of prey populations, this kind of functional response is characterized by a sigmoid curve. This response function serves as a base for the model of vertebrate predators.

The following is an expression for this type of functional response.

$$f(p(t)) = \frac{\eta p^2(t)}{\beta + p^2(t)},$$

where the meaning of η, β, $p(t)$ have previously been explained.

(iv) **Holling type IV**

A non-monotonic function is the Holling type IV functional response, sometimes referred to as the Monod-Haldane type functional response.

In mathematics, this functional response is expressed as follows:

$$f(p(t)) = \frac{\eta p(t)}{\beta + bp(t) + p^2(t)},$$

where η, β, $p(t)$ are the previously indicated variables and b is the predator interference.

(v) **Ivlev-type**

The exponential character of the Ivlev-type functional response makes it appropriate for

5

modeling invertebrate predators.

Ivlev-type functional response, which is exponential, is what I have employed in my work. Its mathematical expression is

$$f(p(t)) = 1 - e^{-\delta p(t)}.$$

In this case, δ represents the hunting success, and $p(t)$ represents the prey species density at time t.

1.5.2 Predator-dependent:

The predator-dependent functional response has a predation rate, which is assumed to be influenced by the quantities of predators and prey. The following list includes a few highly utilized predator-dependent functional responses.

(i) **Beddington-DeAngelis**

The Beddington-DeAngelis response function and the Holling type II functional response are nearly similar; the Beddington-DeAngelis response function is dependent on mutual interference of predators, while the Holling type II functional response is not.

This response function's mathematical expression is as follows:

$$f(p(t), q(t)) = \frac{\eta p(t)}{\beta + ap(t) + bq(t)},$$

where η, β, $p(t)$, b are already described, and the terms a, $q(t)$ means prey saturation constant and predator density respectively.

(ii) **Crowley-Martin**

The Crowley-Martin functional response is dependent on predators, just like the Beddington-DeAngelis functional response.

The expression for this response function is

$$f(p(t), q(t)) = \frac{\eta p(t)}{\beta + ap(t) + abp(t)q(t)},$$

where all the variables and parameters have already been explained.

(iii) **Hassell-Varley:**

The Hassell-Varley functional response has the following mathematical expression:

$$f(p(t), q(t)) = \frac{\eta p(t)}{\beta q^{\gamma}(t) + p(t)}, \gamma \in (0, 1).$$

Every parameter and variable is the same as what was previously stated.

1.5.3   Ratio-dependent:

This is a unique example of a predator-dependent functional response where the ratio of prey to predator, rather than the total number of prey or predator, determines the rate of predation. Compared to prey-dependent response functions, these kinds of functional responses are more appropriate when predators are obligated to look for food. It is possible to alter the stability of a dynamic system by altering its functional responses. Therefore, finding a suitable functional response term to represent the stability of a prey-predator model is crucial.

1.6   Detritus

Detritus is dead organic stuff produced by the decomposition process of organisms. It is typically found in three distinct terrestrial ecosystems: chaparral, grassland, and forest. It can occasionally be found in aquatic environments as well. In forests, twigs and plant litter are the primary sources of detritus. These fall on the ground and are decomposed by a variety

of soil-dwelling micro-organisms, including bacteria, fungi, and protozoa. These microscopic organisms, known as decomposers, obtain their nourishment from the detritus. Fungi typically have a larger biomass in aquatic environments than that of bacteria. Fungi account for over 90% of the total biomass of micro-organisms (Findlay et al., 2002; Kominkova et al., 2000; Newell et al., 2002). Furthermore, fungi are primarily responsible for the breakdown process since their rate of production is higher than that of bacteria (Gulis and Suberkropp, 2003; Kuehn et al., 2000). Once more, bacteria have a turnover period that is shorter than fungi, which means that they are essential to decomposition (Baldy and Gessner, 1997; Findlay and Arsuffi, 1989; Hieber and Gessner, 2002). The recycling process also creates a tiny quantity of detritus from the animal corpses. In any detritus-based food chain, this detritus serves as the main and most important source of energy, moving energy from the lower to the upper tropical levels. The energy flow within a detritus food chain is constant, and it is substantially greater than that of other types of food chains seen in terrestrial environments.

1.7 Refuge

Predation constantly affects prey species in any ecosystem. The population growth of the prey species is negatively impacted by this predation. Prey species always have a tendency to hide and seek refuge in order to promote the growth of prey species. The refuge patch provides a safe place for prey species, shielding them from predators who are looking for food. The predator-prey model's dynamics in every ecosystem are greatly influenced by this prey refuge. Because of the less predation, this prey refuge has a favorable impact on prey growth and a negative impact on predator growth. Any ecosystem will primarily have two types of refuges: temporal refuge and spatial refuge. One of the most important and frequently utilized prey refuges is spatial refuge. Because of the fluctuating nature of the surrounding environment, spatial refuges exist in places that are more challenging

for predators to access. Thus, a portion of the prey species is shielded from predators to some extent (Gonzlez-Olivares and Ramos-Jiliberto, 2004). Temporal refuges result from the collective defense of prey species or from the simple reduction of predator species' mobility, which lowers the risk of predation. According to Maynard-Smith (1978), a prey refuge with a constant proportion has no effect on the impartially stable Lotka-Volterra model's stability behavior, but a constant number of prey refuges has. According to Hassell and May (1973), a model's oscillatory behavior can be changed into stable behavior by including a sizable refuge. It has been demonstrated that adding a prey refuge to any model of predator-prey can increase the stabilizing impact (Gonzlez-Olivares and Ramos-Jiliberto, 2004). In certain cases, this refuge can prevent the extinction of the prey species. Prey refuge regulates the prey-predator paradigm's dynamics to a significant extent.

1.8 Time delay

Time delays can cause oscillations in a variety of species and, generally, have an unstable impact on the dynamics of the species populations. In population dynamics, a species' growth does not happen instantly. It takes time for a predator to give birth to new offspring when it takes nourishment from its prey. It is known as the gestation delay. Each and every species of an ecosystem generally experiences different life stages in their whole life cycle, and the activities differ from one stage to another. Any population model can contain a variety of delays, such as those related to incubation, gestation, and maturation. Maturation delay and gestation delay are the most commonly used delays among them. The period of time a newly born species spends in its juvenile class before beginning to reproduce after it enters the adult class is known as the maturity delay. This indicates that the maturation delay is the amount of time needed for a species to reach maturity.

The differential equation with time delay τ can be expressed as follows for any population:

$$\dot{p}(t) = f(p(t), p(t - \tau)).$$

1.9 Fractional derivative

The study of integrals and derivatives of arbitrary orders, particularly fractional orders, is known as fractional calculus (Ishteva, 2005). For more than three centuries, it has been widely applied in several scientific domains. Fractional differential equations are more suitable than integer-order differential equations in real-world scenarios for any dynamical system. Since integer-order derivative models do not take memory effects into account, in general, the only time integer-order derivatives are utilized is when calculating the dependent variable's current rate of change with respect to the independent variable (Forde, 2005; Kuang, 1993; Milton, 2015). Certain models in ecological systems rely more on past data than on current data. Fractional derivatives and integrals make greater sense in this situation. The best method for including memory in a species where memory exists is to take into account the fractional derivative, which has a non-local feature. There are two basic components of the memory effect. One is memory rate, which can be derived via the derivative's order, and the other is memory function, which is connected to the fractional derivative's kernel. Leibniz originally presented the concept of fractional derivative in the 17th century in 1695 (Kilbas, 2006). In the 18th and 19th centuries, famous mathematicians Euler, Lagrange, Lacroix, and Fourier defined some fractional derivatives. When α is not an integer, Euler discovered a new interpretation for the derivative $\frac{d^\alpha x^\beta}{dx^\alpha}$ (Samko et al., 1993). In 1772, Lagrange observed that the law of exponents for differential operators of integer order can be changed into any arbitrary order (Miller and Ross , 1993). Laplace later provided a thorough explanation of the fractional derivative of the function $f(x) = x^n$,

which Lacroix had computed (Miller and Ross , 1993). He also covered the situation where $n = \frac{1}{2}$ (Miller and Ross , 1993). Fourier provided a thorough and useful formulation of the fractional order derivative in 1822, which was applicable to any function (Miller and Ross , 1993). Fractional derivatives have been applied in recent years by Letnikov, Abel, Liouville, Riemann, Grunwald, and Riemann to address many real-world issues. Abel used fractional order integration and differentiation to solve the tautochrone problem in 1823 (Caputo and Mainardi, 1971). Liouville used the infinite series with fractional derivatives in 1832 to find the solutions to various linear differential equations (Samko et al., 1993). A new definition of fractional integration in the Taylor series was presented by Riemann in 1876 (Samko et al., 1993). The definitions of Riemann and Liouville were joined later in the 19th century to form the Riemann-Liouville fractional derivative (Miller and Ross , 1993). The most famous and noteworthy Caputo derivative was then published in the literature in 1967 (Caputo, 1967).

We have applied the Caputo fractional derivative in our work. Since the derivative of any constant is zero, it is easy to derive the initial and boundary conditions to frame issues (Atangana and Secer, 2013). This makes the Caputo derivative convenient for fractional derivative. The equilibria of an integer order system and a Caputo fractional derivative system are exactly the same.

1.10   Objective of the thesis

Our primary goal in this thesis is to investigate the detritus-based prey-predator models in the Sundarban mangrove forest and the nearby estuary. The principal and crucial energy source in our study is detritus, from which energy is transferred to higher tropic levels of the food chain models. In this mathematical analysis, we have regarded the micro-organism pool as prey and the invertebrate as predator. The effect of the uptake function of inver-

tebrate predators is the main concern here. Here, the impact of discrete time delays on the stability behavior of models has also received attention. In addition, we have looked at fractional-order predator-prey models with different fractional orders. In order to obtain the model's approximate analytical solution, we have additionally utilized the Homotopy perturbation method. Understanding the stability behavior of equilibria, Hopf bifurcation, stability switching, and limit cycle for delayed as well as non-delayed systems would undoubtedly be aided by this research. Ultimately, numerical simulations have been run to verify the theoretical results and obtain a deeper comprehension of the stability behavior across a range of model system parameter values.

1.11   Highlights of the thesis

The present thesis covers seven chapters for a clear understanding of some mathematical models of ecological systems. A brief description of each chapter has been introduced here to give a rough view of the topics discussed in the thesis.

Chapter 1: Chapter 1 discusses some basic preliminaries and definitions of terms used in the whole thesis. It provides some fundamental ideas about the topics relevant to the thesis.

Chapter 2: In this chapter, we examine a prey-predator model in the Indian Sundarban mangrove forest based on detritus. In this case, detritus is essential because it provides the nutrients to the micro-organism pool. We have employed the Ivlev-type response function to describe the rate of invertebrate predator's intake and the Holling Type-II functional response to explain the detritus loss rate brought on by the micro-organism pool. The mathematical analysis consists of the existence of multiple equilibria, their local and global stability, and the existence of a stable periodic orbit around the interior equilibrium point. With respect to the growth rate parameter of the micro-organism pool, the system undergoes Hopf-bifurcation about the interior equilibrium point. To comprehend the qualitative study,

numerical simulations are performed with respect to various values of the system parameters.

Chapter 3: Similar to Chapter 2, this chapter describes a deterministic mathematical model of an invertebrate predator and non-spatial detritus-based micro-organism in the Sundarban estuarine habitat. In this case, we assume that the predation follows an Ivlev-type response function. Our research primarily aims to comprehend the dynamics of the micro-organism pool since it is essential in determining the dynamics of food chains by transferring energy to higher tropical levels. We have also attempted to comprehend how the invertebrate predator's loss rate affects the model. The presence of many feasible equilibria and their local and global stability are included in the mathematical study. It is demonstrated that the interior equilibrium point is surrounded by a stable limit cycle. Additionally, a critical value for the micro-organism pool's loss rate has been identified, and for this value, Hopf-bifurcation behaviour is observed near the equilibrium point. Afterward, we add a discrete time delay to the invertebrate predator's functional response term. Additionally, we have obtained periodic oscillations with tiny amplitudes, where the bifurcation parameter is the time delay. Numerical simulations are used to validate all analytical conclusions for some system parameter values.

Chapter 4: This chapter explains another predator-prey mathematical model based on the mangrove ecosystem with the Ivlev-type response function as the invertebrate predator's functional response. Here, we have incorporated two different-valued gestation delays in the equation of the prey (micro-organism pool) and predator (invertebrate predator) population. This study thoroughly explains the immense impact of time delays throughout the chapter. These delays play a pivotal role in building the dynamics of our model. These delays can destabilize the model system and generate Hopf-bifurcating periodic oscillations. The analytical results have been verified through the execution of numerical simulations.

Chapter 5: This chapter describes the same model of chapter 2 but fractional order system is considered in place of integer order system. Since, integer-order derivatives are only used

to calculate the dependent variable's present rate of change with regard to the independent variable because they do not account for memory effects in their models. In ecological systems, certain models not only depend upon recent data but also on historical data. In this case, fractional derivatives make more sense. That's why we consider our model with fractional order derivatives.

Here, we have derived the approximate solution of the fractional order system using Homotopy Perturbation method (HPM) with high accuracy. As HPM is a rapid convergence method, we have done only a few iterations to get the system's approximate analytical series solutions. Numerical simulations have been experimented with different valued fractional orders to better understand our analytical findings.

Chapter 6: In the Sundarban mangrove forest and the adjacent estuary, another detritus-based predator-prey paradigm is the subject of this chapter's discussion. The model of this food chain is formulated with the help of fractional order derivatives. The effects of prey refuge and toxicity are also discussed in this paper. At the end, numerical simulations are run in order to confirm the analytical findings.

Chapter 7: Chapter 7 contains the conclusion, which includes a summary of the theoretical and numerical findings of all the chapters discussed in the thesis. The future scope of the research is also mentioned in this chapter.

Chapter 2

Qualitative Behaviour of a Detritus-Based Prey-Predator Model of Sundarban Mangrove Forest, India *

2.1   Introduction

Sundarban is one of the most extensive mangrove forests in the world and lies in the Ganga-Brahmaputra-Meghna delta, particularly at the border of the northern margin of the Bay of Bengal. Mangroves are one particular type of tree that grows in brackish wetlands where the land meets with the sea. In the Sundarban estuary, mangrove forests are vital as they support the detritus-based food chain and play a crucial role in shaping the dynamics of the adjacent estuary. A lot of detritus is formed from the litter of several mangrove forest species, such as *B. gymnorhiza, Avicennia Sp., Heritiera Sp., Exocaria Sp., Sonneratia Sp.*. Among these species, *Avicannia alba, Avicannia marina*, and then *Avicennia officinalis* are the leading sources of detritus. The plant litter is decomposed by several micro-organisms, namely fungi, bacteria, and certain protozoa, and detritus is formed. The detritus is washed out by tidal flow into the adjacent estuary. This detritus plays a significant role in regulating the productivity of the forest and the estuary. Several invertebrate predators, such as nematodes

---

and certain insect larvae are in the ecosystem and feed on the micro-organisms. Invertebrate predators are one of the most important members of the ecosystem in regulating the level of nutrients in the food chain/web. In this way, a detritus-based prey-predator system works in the Sundarban estuary. A lot of theoretical work has been done on detritus-based prey-predator system in the Sundarban estuarine ecosystem (Bandyopadhyay et al., 2003; Das and Ray, 2008; Gazi and Bandyopadhyay, 2006; Sarkar et al., 1991).

The present study considers a non-spatial detritus-based prey-predator model, where detritus is the primary energy/food source for micro-organisms and invertebrate predators. Here, it is proposed that the loss rate of detritus due to the micro-organism pool follows the Holling Type-II functional response (Braza, 2003; Du and Hsu, 2004; Hsu and Huang, 1995; Ko and Ryu, 2007; Peng and Wang, 2005, 2007; Saez and Gonzalez-Olivares, 1999; Tanner, 1975), the functional response of invertebrate predators is taken as the Ivlev-type response function (Kooij and Zegeling, 1996; Wang et al., 2010). It is observed that the growth rate of micro-organisms plays a significant role in shaping the dynamics of the mangrove ecosystem.

The present study has been carried out sequentially as follows: At first, the basic assumption and formulation of the mathematical model have been described, and we derive the equilibria and their feasibility conditions. Then, we showed the boundedness of the solutions (Ghosh and Sarkar, 1997; Sarkar et al., 1991) and the dynamic behavior of the system. We have also shown the local as well as global stability of the interior equilibrium point, the existence criteria of Hopf-bifurcation (Roy et al., 2016; Sarwardi et al., 2012), criteria for non-constant large-amplitude periodic solutions, and the direction of flow of trajectory of the periodic orbit. Finally, numerical simulation is carried out with respect to different values of system parameters, and we discuss and interpret the results of the system.

2.2 Model formulation

We consider a deterministic mathematical model of a non-spatial detritus-based micro-organism pool and its invertebrate predators as:

$$
\begin{aligned}
\frac{dx}{dt} &= x(a_1 - bx) - \frac{hxy}{k+x}. \\
\frac{dy}{dt} &= y\left(a_2 - \frac{cy}{bx}\right) - gz\{1 - exp(-ey)\}. \\
\frac{dz}{dt} &= z\left[-m + g\{1 - exp(-ey)\}\right],
\end{aligned} \tag{2.1}
$$

with the initial conditions:

$x(0) = x_0 > 0$, $y(0) = y_0 > 0$ and $z(0) = z_0 > 0$,

where x, y, z are the biomass of detritus produced from plant litter of mangrove, population density of micro-organism pool and population density of invertebrate predators respectively at time t. Here, a_1, b, h, k, a_2, c, g, e, m are positive constants. In system (2.1), it is assumed that the loss rate of detritus due to the micro-organism pool follows the Holling type-II functional response. The functional response of the predator is taken as the Ivlev-type response function where e is the hunting success, g is the maximum no of micro-organisms that can be eaten by an invertebrate predator, and m is the mortality rate of the invertebrate predators.

We consider the following substitution to make the system (2.1) into a non-dimensional form:

$x = kX$, $y = \frac{mk}{h}Y$, $z = \frac{km^2Z}{hg}$, $t = \frac{T}{m}$.

Then the model system (2.1) reduces to

$$
\begin{aligned}
\frac{dX}{dT} &= X\left[(\alpha - \eta X) - \frac{Y}{1+X}\right]. \\
\frac{dY}{dT} &= Y\left(\beta - \frac{\gamma Y}{X}\right) - Z\{1 - exp(-\phi Y)\}. \\
\frac{dZ}{dT} &= Z\left[-1 + \sigma\{1 - exp(-\phi Y)\}\right],
\end{aligned} \tag{2.2}
$$

where $\alpha = \frac{a_1}{m}$, $\eta = \frac{bk}{m}$, $\beta = \frac{a_2}{m}$, $\gamma = \frac{c}{bh}$, $\sigma = \frac{g}{m}$, $\phi = \frac{emk}{h}$.

It is known that the qualitative behaviour of the system (2.1) and the non-dimensional system (2.2) are the same.

2.3 Equilibria

The system (2.2) has the following equilibria.

(i) The boundary equilibrium point $E_1(\frac{\alpha}{\eta}, 0, 0)$.

(ii) The invertebrate predator free equilibrium point $E_2(\overline{X}, \overline{Y}, 0)$,

where

$$
\begin{aligned}
\overline{X} &= \frac{-(\eta\gamma + \beta - \alpha\gamma) + \sqrt{(\eta\gamma + \beta - \alpha\gamma)^2 + 4\alpha\eta\gamma^2}}{2\eta\gamma}, \\
\overline{Y} &= \frac{\beta\left\{-(\eta\gamma + \beta - \alpha\gamma) + \sqrt{(\eta\gamma + \beta - \alpha\gamma)^2 + 4\alpha\eta\gamma^2}\right\}}{2\eta\gamma^2}.
\end{aligned}
$$

(iii) The interior equilibrium $E_3(X^*, Y^*, Z^*)$, where

$$
\begin{aligned}
X^* &= \frac{(\alpha - \eta) + \sqrt{(\alpha + \eta)^2 - \frac{4\eta}{\phi}ln\left(\frac{\sigma}{\sigma-1}\right)}}{2\eta}, \\
Y^* &= \frac{1}{\phi}ln\left(\frac{\sigma}{\sigma-1}\right), \\
Z^* &= \sigma\frac{1}{\phi}ln\left(\frac{\sigma}{\sigma-1}\right)\left[\beta - \frac{\frac{2\gamma\eta}{\phi}ln\left(\frac{\sigma}{\sigma-1}\right)}{(\alpha - \eta) + \sqrt{(\alpha+\eta)^2 - \frac{4\eta}{\phi}ln\left(\frac{\sigma}{\sigma-1}\right)}}\right].
\end{aligned}
$$

We see that the interior equilibrium $E_3(X^*, Y^*, Z^*)$ is feasible under the given conditions:

(i) $\sigma > 1$,

18

(ii) $Y^* > \alpha$,

(ii) $\beta > \dfrac{2\gamma\eta Y^*}{(\alpha-\eta)+\sqrt{(\alpha+\eta)^2-4\eta Y^*}} = \beta^*(\text{say})$.

2.4 Qualitative analysis of the model

2.4.1 Boundedness of the solutions

The boundedness of solutions of the system (2.2) is shown in the following lemma.

Lemma 2.1

The system (2.2) possesses uniformly bounded solutions.

Proof

Suppose $S(T) = X + \sigma Y + Z$.

Now

$$\frac{dS}{dT} = \frac{dX}{dT} + \sigma\frac{dY}{dT} + \frac{dZ}{dT}$$

$$\leq \alpha X - \eta X^2 + \beta\sigma Y - \frac{\sigma\gamma Y^2}{X} - Z$$

$$\leq \alpha X - \eta X^2 - Z - \sigma\gamma\left(\frac{Y}{\sqrt{X}} - \frac{\beta}{\gamma}\sqrt{X}\right)^2 + \frac{\sigma\beta^2}{\gamma}X - \beta\sigma Y$$

$$\leq 2\alpha X - \eta X^2 + \frac{\sigma\beta^2}{\gamma}X - \alpha X - \beta\sigma Y - Z$$

$$\leq -m_1 S(T) + 2\alpha X - \eta X^2 + \frac{\sigma\beta^2}{\gamma}X. \tag{2.3}$$

Let $F(X) = 2\alpha X - \eta X^2 + \frac{\sigma\beta^2}{\gamma}X$, then F has maximum value
$F_{max} = \frac{1}{\eta}\left(2\alpha + \frac{\sigma\beta^2}{\gamma}\right)\left\{\alpha - \frac{1}{4\eta}\left(2\alpha + \frac{\sigma\beta^2}{\gamma}\right) + \frac{\sigma\beta^2}{2\gamma}\right\}$ at $X = \frac{1}{2\eta}\left(2\alpha + \frac{\sigma\beta^2}{\gamma}\right)$.
Hence, it follows that $\frac{dS}{dT} + m_1 S(T) \leq F_{max}$,

where $m_1 = \min\{\alpha, \beta, 1\}$,

which implies

$$S(T) \leq F_{max} + e^{-m_1 T} S(X(0), Y(0), Z(0)).$$

Hence, $\limsup_{T \to \infty} S(T) \leq \frac{F_{max}}{m_1}$.

Hence, the lemma is proved.

2.4.2   Dynamic behaviour of the system

In this subsection, we will discuss the stability of the equilibria E_1, E_2, and E_3, respectively.

Let J_k be the Jacobian of the system (2.2) at the equilibrium points E_k, where $k = 1, 2, 3$.

At E_1, the Jacobian matrix is

$$J_1 = \begin{bmatrix} -\alpha & -\frac{\alpha}{\alpha+\eta} & 0 \\ 0 & \beta & 0 \\ 0 & 0 & -1 \end{bmatrix}.$$

So, the eigenvalues of the matrix J_1 are $-\alpha$, β, -1. So, E_1 is stable in the X and Z directions and unstable in the Y direction.

At E_2, the Jacobian matrix is

$$J_2 = \begin{bmatrix} \alpha - 2\eta\overline{X} - \frac{\overline{Y}}{(1+\overline{X})^2} & -\frac{\overline{X}}{1+\overline{X}} & 0 \\ \frac{\gamma\overline{Y}^2}{\overline{X}^2} & \beta - \frac{2\gamma\overline{Y}}{\overline{X}} & -1 + e^{-\phi\overline{Y}} \\ 0 & 0 & -1 + \sigma\left(1 - e^{-\phi\overline{Y}}\right) \end{bmatrix}.$$

At E_2, the characteristic equation of J_2 is

$$\left[-1+\sigma\left(1-e^{-\phi\overline{Y}}\right)-\lambda\right]\left[\lambda^2-\lambda\left\{\alpha-2\eta\overline{X}-\frac{\overline{Y}}{(1+\overline{X})^2}+\beta-\frac{2\gamma\overline{Y}}{\overline{X}}\right\}\right.$$
$$\left.+\left(\beta-\frac{2\gamma\overline{Y}}{\overline{X}}\right)\left\{\alpha-2\eta\overline{X}-\frac{\overline{Y}}{(1+\overline{X})^2}\right\}+\frac{\gamma\overline{Y}^2}{\overline{X}\left(1+\overline{X}\right)}\right]=0.$$
$$\Rightarrow\left[-1+\sigma\left(1-e^{-\phi\overline{Y}}\right)-\lambda\right]\left[\lambda^2+P\lambda+Q\right]=0,$$

where

$$P=-\alpha+2\eta\overline{X}+\frac{\overline{Y}}{(1+\overline{X})^2}-\beta+\frac{2\gamma\overline{Y}}{\overline{X}},$$
$$Q=\left(\beta-\frac{2\gamma\overline{Y}}{\overline{X}}\right)\left\{\alpha-2\eta\overline{X}-\frac{\overline{Y}}{(1+\overline{X})^2}\right\}+\frac{\gamma\overline{Y}^2}{\overline{X}\left(1+\overline{X}\right)}.$$

If $P>0$ and $Q>0$, the equilibrium $E_2(\overline{X},\overline{Y},0)$ is stable in the XY plane; otherwise, it is unstable.

In the Z direction, $E_2(\overline{X},\overline{Y},0)$ is unstable or stable according to the condition $\overline{Y}>Y^*$ or $\overline{Y}<Y^*$.

Through numerical simulation, we have shown for some parametric values where $P>0$ and $Q>0$, E_2 is stable in the XY plane.

At E_3, the Jacobian matrix is

$$J_3=\begin{bmatrix}\alpha-2\eta X^*-\frac{Y^*}{(1+X^*)^2} & -\frac{X^*}{1+X^*} & 0\\[2mm]\frac{\gamma Y^{*2}}{X^{*2}} & \beta-\frac{2\gamma Y^*}{X^*}-Z^*\phi e^{-\phi Y^*} & -\frac{1}{\sigma}\\[2mm]0 & \phi\sigma Z^* e^{-\phi Y^*} & 0\end{bmatrix}.$$

21

At E_3, the characteristic equation of J_3 is

$$\lambda^3 - \lambda^2 \left[\left\{ \alpha - 2\eta X^* - \frac{Y^*}{(1+X^*)^2} \right\} + \left\{ \beta - \frac{2\gamma Y^*}{X^*} - Z^* \phi e^{-\phi Y^*} \right\} \right]$$

$$- \lambda \left[- \left\{ \alpha - 2\eta X^* - \frac{Y^*}{(1+X^*)^2} \right\} \left\{ \beta - \frac{2\gamma Y^*}{X^*} - Z^* \phi e^{-\phi Y^*} \right\} - \phi Z^* e^{-\phi Y^*} \right.$$

$$\left. - \frac{X^*}{1+X^*} \frac{\gamma Y^{*2}}{X^{*2}} \right] - \phi Z^* e^{-\phi Y^*} \left\{ \alpha - 2\eta X^* - \frac{Y^*}{(1+X^*)^2} \right\} = 0.$$

$$\Rightarrow \lambda^3 + A\lambda^2 + B\lambda + C = 0, \tag{2.4}$$

where

$$A = - \left\{ \alpha - 2\eta X^* - \frac{Y^*}{(1+X^*)^2} \right\} - \left\{ \beta - \frac{2\gamma Y^*}{X^*} - Z^* \phi e^{-\phi Y^*} \right\},$$

$$B = \left\{ \alpha - 2\eta X^* - \frac{Y^*}{(1+X^*)^2} \right\} \left\{ \beta - \frac{2\gamma Y^*}{X^*} - Z^* \phi e^{-\phi Y^*} \right\} + \phi Z^* e^{-\phi Y^*} + \frac{X^*}{1+X^*} \frac{\gamma Y^{*2}}{X^{*2}},$$

$$C = - \phi Z^* e^{-\phi Y^*} \left\{ \alpha - 2\eta X^* - \frac{Y^*}{(1+X^*)^2} \right\}.$$

The system (2.2) is locally asymptotically stable if $A > 0$, $C > 0$, $AB - C > 0$.

Here, $A > 0$ if

$$\beta < \frac{1}{1 - \phi Y^* (\sigma - 1)} \left\{ - \alpha + 2\eta X^* + \frac{Y^*}{(1+X^*)^2} + \frac{2\gamma Y^*}{X^*} - \frac{\phi \gamma Y^{*2} (\sigma - 1)}{X^*} \right\} = \beta^{**}(say).$$

Here, $C > 0$ (always). Now $AB - C = \sigma_1 \beta^2 + \sigma_2 \beta + \sigma_3$,

where

$$\sigma_1 = \left\{ \phi Y^* (\sigma - 1) - 1 \right\} \left\{ - \eta X^* + \frac{X^* Y^*}{(1+X^*)^2} + \phi Y^* (\sigma - 1) \left(1 + \eta X^* - \frac{X^* Y^*}{(1+X^*)^2} \right) \right\},$$

22

$$\sigma_2 = \left\{ -\eta X^* + \frac{X^*Y^*}{(1+X^*)^2} + \phi Y^* (\sigma - 1) \left(1 + \eta X^* - \frac{X^*Y^*}{(1+X^*)^2} \right) \right\}$$
$$\left\{ -\frac{\phi \gamma (\sigma - 1) Y^{*2}}{X^*} + \eta X^* - \frac{X^*Y^*}{(1+X^*)^2} + \frac{2\gamma Y^*}{X^*} \right\} + \phi Y^* (\sigma - 1) \left(-\eta X^* + \frac{X^*Y^*}{(1+X^*)^2} \right)$$
$$+ \left\{ \phi Y^* (\sigma - 1) - 1 \right\} \left\{ -\frac{\phi \gamma (\sigma - 1) Y^{*2}}{X^*} \left(1 + \eta X^* - \frac{X^*Y^*}{(1+X^*)^2} \right) - \frac{2\alpha \gamma Y^*}{X^*} + 4\eta \gamma Y^* \right.$$
$$+ \left. \frac{2\gamma Y^{*2}}{X^*(1+X^*)^2} + \frac{\gamma Y^{*2}}{X^*(1+X^*)} \right\},$$

$$\sigma_3 = \left\{ \frac{-\phi \gamma (\sigma - 1) Y^{*2}}{X^*} + \eta X^* - \frac{X^*Y^*}{(1+X^*)^2} + \frac{2\gamma Y^*}{X^*} \right\} \left\{ \frac{-\phi \gamma (\sigma - 1) Y^{*2}}{X^*} \right.$$
$$\left(1 + \eta X^* - \frac{X^*Y^*}{(1+X^*)^2} \right) - \frac{2\alpha \gamma Y^*}{X^*} + 4\eta \gamma Y^* + \frac{2\gamma Y^{*2}}{X^*(1+X^*)^2} + \left. \frac{\gamma Y^{*2}}{X^*(1+X^*)} \right\}$$
$$- \frac{\phi \gamma (\sigma - 1) Y^{*2}}{X^*} \left(-\eta X^* + \frac{X^*Y^*}{(1+X^*)^2} \right).$$

Due to the complex form of A, B, and C, it is pretty unlikely to find an explicit parametric condition for which all those conditions are satisfied. However, through simulations, the result is obtained that there exists some threshold value of β, say $\beta = \beta_1$ such that for $0 < \beta < \beta_1$, all A, C and $AB - C$ are positive, and as β passes through β_1, then $AB - C$ becomes negative. Hence, it is concluded that for $\beta^* < \beta < \min\{\beta^{**}, \beta_1\}$, E_3 is locally stable. At $\beta > \min\{\beta^{**}, \beta_1\}$, E_3 is unstable and at $\beta = \beta_1$, $AB - C$ vanishes.

Now in the following theorem, we derive the condition for existence of small amplitude periodic oscillations for variation of parameters of the system (2.2).

Theorem 2.1

The necessary and sufficient condition for existence of Hopf-bifurcation is that there exists a $\beta = \beta_1$ such that $A(\beta_1) > 0, B(\beta_1) > 0, C(\beta_1) > 0, \psi(\beta_1) = AB - C = 0$, and $\frac{df}{d\beta}\big|_{\beta=\beta_1} \neq 0$.

Proof

To prove the existence of Hopf-bifurcation, at first we show that the characteristic polynomial has one real and two purely imaginary roots at $\beta = \beta_1$ (Rai et al., 1983).

Here, $AB - C = \sigma_1 \beta^2 + \sigma_2 \beta + \sigma_3$.

Now

$\sigma_1 \beta^2 + \sigma_2 \beta + \sigma_3 = 0$ has one positive root β_1 such that $A(\beta_1)B(\beta_1) - C(\beta_1) = 0$. Let us consider the real root is $\rho(\beta_1) = u(\beta_1) + iv(\beta_1)$.

We know that $u(\beta_1) = 0$. We have to show $\frac{du}{d\beta}|_{\beta=\beta_1} \neq 0$.

Now since $\rho(\beta_1)$ is a root of equation (2.4), So, it satisfies (2.4).

So, we get

$(u + iv)^3 + A(u + iv)^2 + B(u + iv) + C = 0.$

Now separating the real and imaginary parts, we get

$$u^3 - 3uv^2 + Au^2 - Av^2 + Bu + C = 0,$$

$$3u^2 v - v^3 + 2Auv + Bv = 0. \qquad (2.5)$$

Let us consider β is in the neighbourhood of β_1. Then (2.5) has a solution such that $v(\beta_1) \neq 0$ iff $v^2 = 3u^2 + 2Au + B$, which gives

$$8u^3 + 8Au^2 + 2(A^2 + B)u + AB - C = 0. \qquad (2.6)$$

Equation (2.5) has a root $u(\beta)$ such that $u(\beta) = 0$ iff $A(\beta_1)B(\beta_1) - C(\beta_1) = 0$, which implies $\sigma_1 \beta_1^2 + \sigma_2 \beta_1 + \sigma_3 = 0$.

Now at $\beta = \beta_1$, $u(\beta_1) = 0$ is the only root, since $12u^2 + 8Au + (A^2 + B) = 0$ has no real root.

Again, it is seen that $v(\beta_1) = \sqrt{B(\beta_1)}$ holds.

Our aim is to show $\frac{du}{d\beta}|_{\beta=\beta_1} \neq 0$.

Now from (2.6), we get

$24u^2\frac{du}{d\beta} + 16Au\frac{du}{d\beta} + 8\frac{dA}{d\beta}u^2 + 2(A^2 + B)\frac{du}{d\beta} + 2u(2A\frac{dA}{d\beta} + \frac{dB}{d\beta})u + 2\sigma_1\beta + \sigma_2 = 0.$

At $\beta = \beta_1$, using $u(\beta_1) = 0$, we get

$\frac{du}{d\beta}\big|_{\beta=\beta_1} = \frac{-(2\sigma_1\beta_1+\sigma_2)}{2(A^2(\beta_1)+B(\beta_1))} \neq 0$. This completes the proof of the lemma.

2.4.3 Criteria for non-constant large amplitude periodic solutions

When $AB - C$ is negative, then the characteristic equation (2.4) has one real negative root and two complex roots with a positive real part. Then, E_3 is locally unstable. Now using the stable manifold theorem (Hale, 1969), we can say that a one-dimensional stable manifold and a two- dimensional unstable manifold exist at E_3. We have already shown that there exists a bounded invariant domain $\Re \subset \mathbb{R}^3_+$. Now, to know the exact location of the stable manifold, and to describe the flow of trajectories of the system through octant in the positively invariant bounded set $\Re \subset \mathbb{R}^3_+$, we use the method of sub-boxes. To do that, we divide $\Re$ into eight octants as follows(see Figure 2.1)

$$
\begin{aligned}
I &= \big\{(X,Y,Z) : \epsilon_1 \leq X \leq X^*, 0 \leq Y \leq Y^*, 0 \leq Z \leq Z^*\big\}, \\
II &= \big\{(X,Y,Z) : X^* \leq X \leq \frac{\alpha}{\eta}, 0 \leq Y \leq Y^*, 0 \leq Z \leq Z^*\big\}, \\
III &= \big\{(X,Y,Z) : X^* \leq X \leq \frac{\alpha}{\eta}, Y^* \leq Y \leq \frac{\alpha\beta}{\eta\gamma}, 0 \leq Z \leq Z^*\big\}, \\
IV &= \big\{(X,Y,Z) : \epsilon_1 \leq X \leq X^*, Y^* \leq Y \leq \frac{\alpha\beta}{\eta\gamma}, 0 \leq Z \leq Z^*\big\}, \\
V &= \big\{(X,Y,Z) : \epsilon_1 \leq X \leq X^*, 0 \leq Y \leq Y^*, Z^* \leq Z \leq \frac{L}{m} - \epsilon_1\big\}, \\
VI &= \big\{(X,Y,Z) : X^* \leq X \leq \frac{\alpha}{\eta}, 0 \leq Y \leq Y^*, Z^* \leq Z \leq \frac{L}{m} - \epsilon_1\big\}, \\
VII &= \big\{(X,Y,Z) : X^* \leq X \leq \frac{\alpha}{\eta}, Y^* \leq Y \leq \frac{\alpha\beta}{\eta\gamma}, Z^* \leq Z \leq \frac{L}{m} - \epsilon_1\big\}, \\
VIII &= \big\{(X,Y,Z) : \epsilon_1 \leq X \leq X^*, Y^* \leq Y \leq \frac{\alpha\beta}{\eta\gamma}, Z^* \leq Z \leq \frac{L}{m} - \epsilon_1\big\},
\end{aligned}
$$
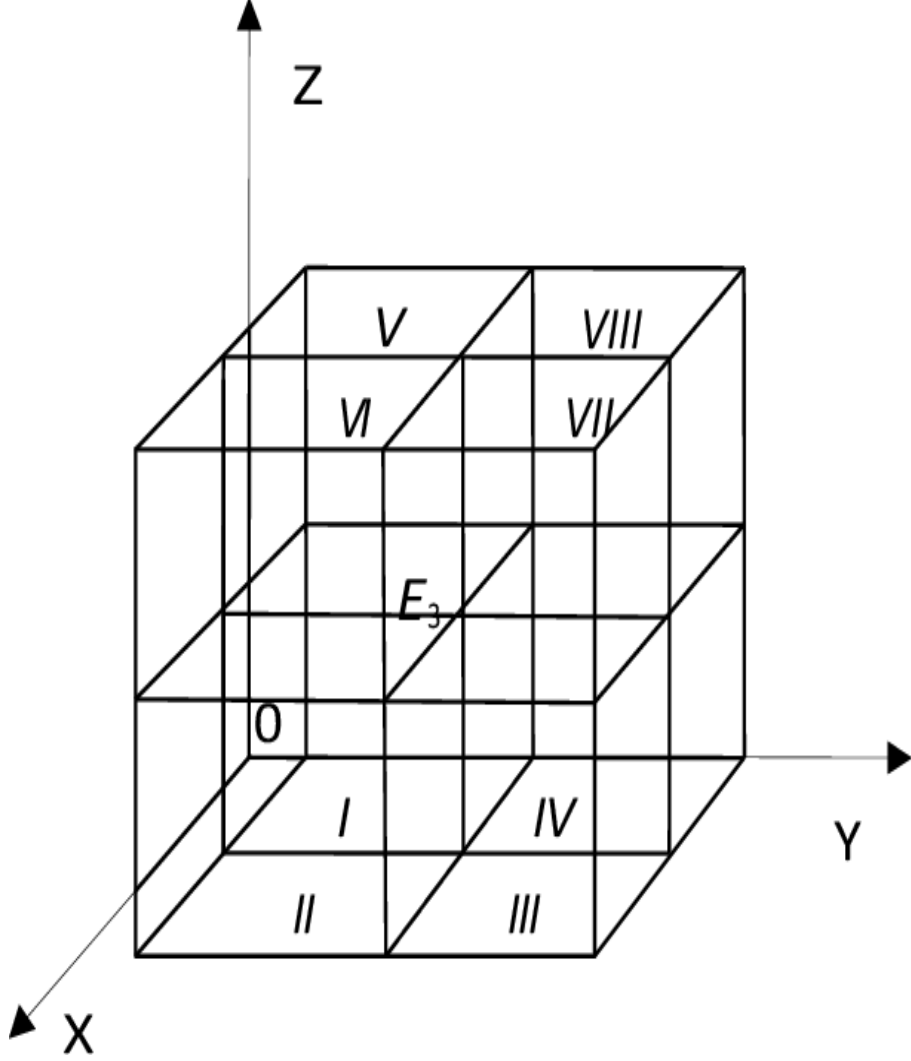
Figure 2.1: Rectangular region $\Re$ is divided into eight sub-boxes as defined in the text.

where $\epsilon_1 < \dfrac{(\alpha-\eta)-\sqrt{(\alpha-\eta)^2+4\alpha\eta\left(1-\frac{\beta}{\eta\gamma}\right)}}{2\eta}$.

Lemma 2.2

The eigenvector associated with the negative real eigenvalue of the Jacobian matrix at E_3, points into the boxes IV and VI.

Proof

Let λ_1 denote the unique real negative eigenvalue. Then, the vector $(x, y, z)^T$ must satisfy

$$\left[\alpha - 2\eta X^* - \frac{Y^*}{(1+X^*)^2} - \lambda_1\right]x = \frac{X^*}{1+X^*}y.$$

$$\frac{\gamma Y^{*2}}{X^{*2}}x + \left\{\beta - \frac{2\gamma Y^*}{X^*} - Z^*\phi e^{-\phi Y^*} - \lambda_1\right\}y = \frac{1}{\sigma}z.$$

$$\phi\sigma Z^* e^{-\phi Y^*}y = \lambda_1 z. \tag{2.7}$$

From the last equation of (2.7), we get that y and z are opposite signs.

Now $\alpha - 2\eta X^* - \frac{Y^*}{(1+X^*)^2} = X^*\left[\frac{Y^*}{(1+X^*)^2} - \eta\right]$.

Now let

$Y^* > \eta(1 + X^*)^2$

$\Rightarrow 0 > \sqrt{(\alpha + \eta)^2 - 4\eta Y^*}$

$\Rightarrow 0 > (\alpha + \eta)^2 - 4\eta Y^*,$

which can not be possible.

So, $\alpha - 2\eta X^* - \frac{Y^*}{(1+X^*)^2} < 0$.

So from (6.3), it can be seen that x and y are opposite signs when $\beta - \frac{2\gamma Y^*}{X^*} - Z^*\phi e^{-\phi Y^*} > 0$ for $\beta > \beta_1$ and $\lambda_1 > \alpha - 2\eta X^* - \frac{Y^*}{(1+X^*)^2}$. So, assuming these conditions we can say that the eigenvector associated with $\lambda_1 < 0$ points into the boxes IV and VI.

Lemma 2.3

Any positive solution of the system (2.2) except those on the stable manifold must eventually start oscillations according to the following sequence:

$I \to II \to III \to VII \to VIII \to V \to.$

Proof

Let F_{ij} denote the face between the boxes i and j. For the reason of the symmetry properties of boxes, we consider the trajectory that starts on face F_{23}, and we will show that the trajectory intersects the face F_{58}, excluding point E_3. We have seen that on F_{23}, $\dot{Y} > 0$, and on F_{37}, $\dot{Z} > 0$. So, it can be concluded that the trajectory does not return to II or III. Since the trajectory can not tend to E_3 from VII, it must intersect F_{78}. On the face F_{78}, we get $\dot{X} < 0$. So, we can say that the trajectory enters into box $VIII$. On the face F_{58}, $\dot{Y} < 0$. So, the trajectory enters into the box V. On the face F_{15}, $\dot{Z} < 0$. So, the trajectory enters the box I. Hence, the lemma is proved.

## 2.5   Numerical simulation and discussions

In this section, we perform some simulations to validate our analytical findings. We have done it using MATLAB-R2017a and the standard MATLAB differential equations integrator for Runge-Kutta method, i.e., MATLAB routine ODE 45. We have done it for a set of parameter values. For this purpose, we take $\alpha = 5$, $\eta = 0.2$, $\phi = 1$, $\sigma = 1.005$, $\gamma = 0.92$. Using this set of parameter values, we get the value of $\beta^* = 0.2038$, $\beta^{**} = 5.1212$, and $\beta_1 = 0.4229$. So, $\min\{\beta^{**}, \beta_1\} = \beta_1 = 0.4229$. Thus, for $\beta^* < \beta < \beta_1$, the system is locally asymptotically stable around the interior equilibrium E_3 and when $\beta > \beta_1$, then the system is unstable.

Figure 2.2 shows the solution curve of the system (2.2) around the interior equilibrium E_3 when $\beta^* < \beta < \beta_1$, and the phase portrait of the system (2.2) is shown in Figure 2.3. Figure 2.4 shows the oscillatory behaviour for detritus, micro-organism pool, and invertebrate predator population around E_3 for $\beta = 0.5 > \beta_1$. In Figure 2.5, we plot the phase portrait of the system for $\beta = 0.5 > \beta_1$, which shows the periodic orbit around E_3.
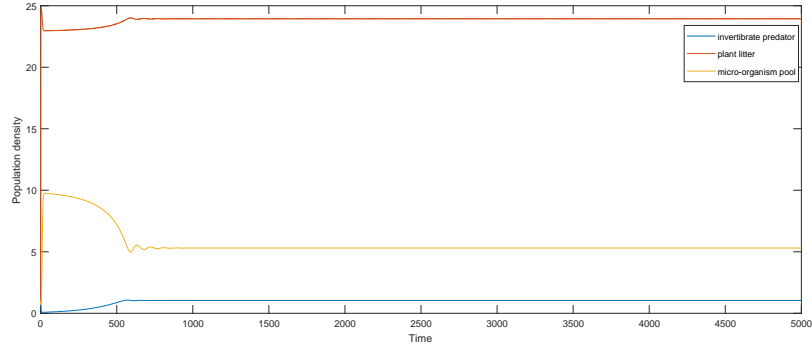
Figure 2.2: Globally asymptotically stable steady-state around E_3 for same initial values for $\alpha = 5$, $\beta = 0.4$, $\gamma = 0.92$, $\phi = 1$, $\eta = 0.2$, and $\sigma = 1.005$.
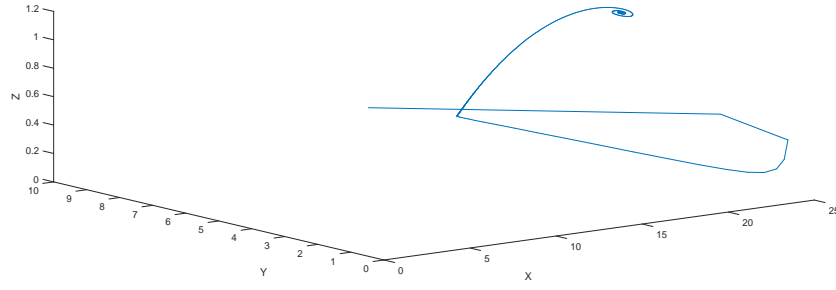
Figure 2.3: Globally asymptotically stable steady-state around E_3 for same initial values for $\alpha = 5$, $\beta = 0.4$, $\gamma = 0.92$, $\phi = 1$, $\eta = 0.2$, and $\sigma = 1.005$.

In Figure 2.6, we set the value of $\beta = \beta_1 = 0.4229$, and there exists a small amplitude
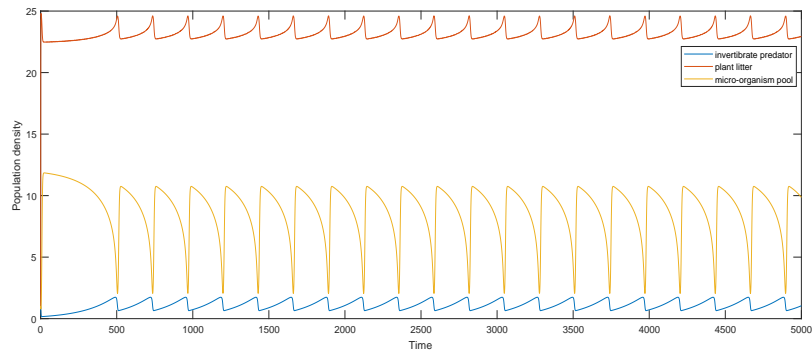
Figure 2.4: Oscillatory behaviour of the system (2.2) for same initial values for $\alpha = 5$, $\beta = 0.5$, $\gamma = 0.92$, $\phi = 1$, $\eta = 0.2$, and $\sigma = 1.005$.

Figure 2.5: existence of periodic orbit for same initial values for $\alpha = 5$, $\beta = 0.5$, $\gamma = 0.92$, $\phi = 1$, $\eta = 0.2$, and $\sigma = 1.005$.
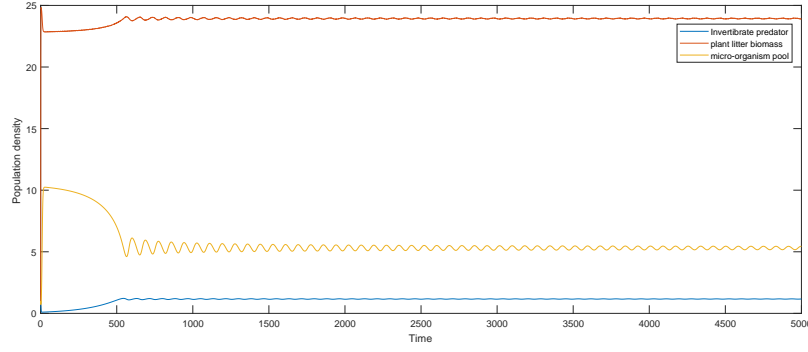
Figure 2.6: Hopf-bifurcating small-amplitude periodic solution for same initial values for $\alpha = 5$, $\beta = 0.4229$, $\gamma = 0.92$, $\phi = 1$, $\eta = 0.2$, and $\sigma = 1.005$.

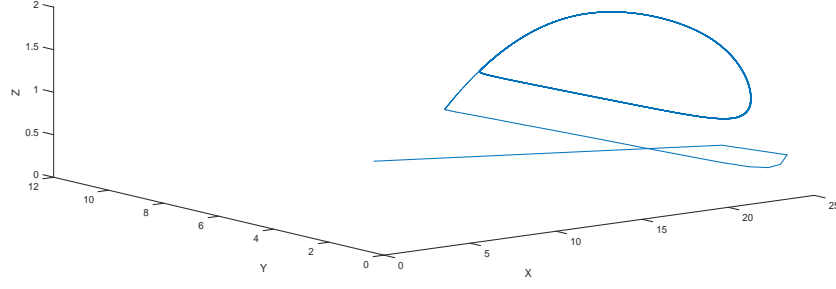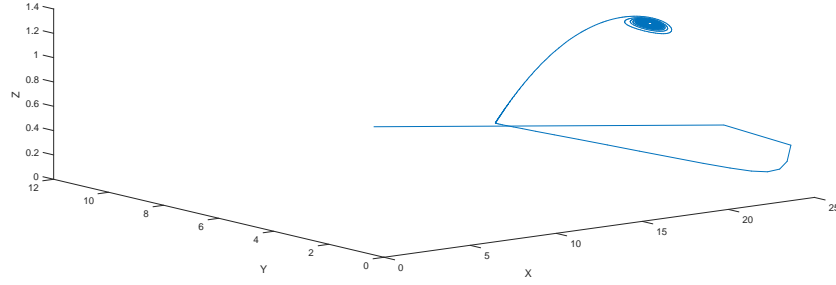**Figure 2.7:** Hopf-bifurcating small-amplitude periodic solution for same initial values for $\alpha = 5$, $\beta = 0.4229$, $\gamma = 0.92$, $\phi = 1$, $\eta = 0.2$, and $\sigma = 1.005$.

periodic oscillation which leads to Hopf-bifurcation whereas Figure 2.7 shows the phase portrait of Hopf-bifurcation with small amplitude periodic oscillation around E_3 for the same parameter values. Through the numerical simulation, it is shown that the parameter β plays an important role in shaping the dynamic behaviour of the model system (2.2).

2.6 Conclusions

We know that mangrove forests are very rich ecosystems due to the formation of detritus in the Sundarban estuary. Therefore, the formation of detritus from the litter of mangrove forests is significant since it plays a crucial role in maintaining the nutrient level of the estuary. In this study, we consider the mathematical model, which is completely based on some realistic situations from the viewpoint of biology. The general dynamical behavior of a homogeneous model of a detritus-based ecosystem comprised of a micro-organism pool and invertebrate predators with a deterministic environment is discussed. Here, The loss of detritus is assumed to follow the Holling type-II functional response, and the uptake function considered for the invertebrate predator is the Ivlev-type function. This uptake function has a dense ecological interpretation. It shows the complex nature of the model system, which leads us to some complicated mathematical results that are realistic from the ecological point of view. In the study, we derive the conditions of global attractor, periodic orbit, and Hopf-bifurcation under certain conditions. Here, we can see that the growth rate of the micro-organism pool acts as a bifurcation parameter, and it is an important factor that can affect the stability of the mangrove ecosystem. This study provides an overall view of the detritus-based food chain in the Sundarban estuary.

Chapter 3

Qualitative Analysis of Micro-Organism Pool and its Invertebrate Predator with Discrete Time-Delay in Sundarban Estuary, India *

3.1 Introduction

One of the greatest natural wonders of the global estuarine ecology is the Sundarban. It is a large mangrove forest located at the seaside of the Bay of Bengal. The main part of Sundarban is situated in Bangladesh, and the remaining part is located in India (about 4000 km^2). Sundarban estuarine complex is an important ecosystem, especially for its unique estuarine feature of the World's largest coastal mangrove forest. In this estuary, mangrove forest plays a very significant role in keeping the ecological balance of this estuary. The main sources of nutrients in this estuary are the litter from several mangroves, including *B. gymnorhiza, Avicennia Sp., Heritiera Sp., Exocaria Sp., Sonneratia Sp.*. Mangrove leaves fall to the ground, where they are decomposed by a variety of micro-organisms, including bacteria, fungus, and specific protozoa. In this region, tidal flow happens twice daily. The leaf detritus is transported to the nearby estuary by the tidal wave, which also regulates

the ecosystem's total production. These micro-organisms offer a source of food for a variety of invertebrates found in the Sundarban ecosystem, including *nematodes* and some insect larvae, particularly *chironomide.* The detritus food chain is maintained by a very large quantity of nutrients and decomposition of organic matter. A lot of analytical studies have been done on detritus-based ecosystems in the estuarine system (Bandyopadhyay et al., 2003; Das and Ray, 2008; Gazi and Bandyopadhyay, 2006; Sarkar et al., 1991). The current study is based on the construction of a deterministic mathematical model of an invertebrate predator, micro-organism pool and its non-spatial detritus source.

The Ivlev-type response function is used in this model to represent the functional response of the invertebrate predators (Kooij and Zegeling, 1996; Wang et al., 2010). The relationship between predation rate (i.e., no of micro-organisms eaten per invertebrate predator per unit of time) and micro-organism density is termed as the functional response. Here, the Ivlev-type response function has a major influence on the dynamics of Sundarban estuary. This function has negative curvature over the whole prey range. With the use of a basic nonlinear mathematical model consisting of invertebrate predators and micro-organisms based on detritus, we can describe the dynamics of the ecosystem.

In reality, it is observed that when a predator feeds on any prey, some time is needed for the digestion of food. There are two main types of delays in reality: gestation delay and maturation delay. Our addition of a gestation delay to the invertebrate predator's growth equation makes the model more realistic. There are many authors who have included time delays in prey-predator models in biological systems (Das and Ray, 2008; Gazi and Bandyopadhyay, 2006; Jana et al., 2012; Liu et al., 2016; Thingstad and Langeland, 1974). Hutchinson (1984) first used delay in a logistic differential equation.

The current investigation has been conducted in a sequential manner as outlined below: Section 3.2 focuses on the fundamental assumptions and construction of the model. The existence of equilibrium point is covered in Section 3.3. Section 3.4 encompasses the con-

dition of the solutions being bounded, as discussed by Sarkar et al. (1991) and Ghosh and Sarkar (1997). Section 3.5 provides an explanation of the local behaviour shown by the various equilibria of the system at a local level. This section also includes the concept of system permanence, as discussed by Hofbauer (1981) and Hutson and Vickers (1983). The system's global behaviour and the existence of periodic solutions resulting from Hopf bifurcation around the interior equilibrium are the main topics of Section 3.6. Roy et al. (2016) and Sarwardi et al. (2012) have both investigated this subject. In the absence of a time delay, this section also addresses the existence of a limit cycle for different values of the system parameters. We looked at the delay model in section 3.7 and showed how the dynamics of the population are affected by gestation delay. We have also calculated the length of time delay required to preserve stability in section 3.8. In section 3.9, the effects of different system parameters on the delayed and non-delayed systems are analyzed through numerical simulations. In section 3.10, we have finally clarified and examined the results of our research.

3.2   Formulation of model

Here, we examine a mathematical model of a non-spatial detritus based micro-organism and its invertebrate predator as follows:

$$
\begin{aligned}
\frac{dx}{dt} &= x(a_1 - bx). \\
\frac{dy}{dt} &= y\left(a_2 - \frac{cy}{bx}\right) - gz\{1 - exp(-ey)\}. \\
\frac{dz}{dt} &= z\big[-m + g\{1 - exp(-ey)\}\big],
\end{aligned}
\tag{3.1}
$$

considering the following initial conditions:

$x(0) = x_0 > 0, y(0) = y_0 > 0$ and $z(0) = z_0 > 0$, where x, y, and z represent the biomass of the detritus, the biomass of the micro-organisms, and the biomass of the invertebrate predators at time t respectively. e represents the hunting success. All of the system's parameters are thought to be positive. Here, a_2 represents the prey species' growth rate, $\frac{a_2 b}{c}$ their carrying capacity and g is the invertebrate predator's food conversion efficiency rate. It is considered that the growth of micro-organisms follows donor-controlled type function, while the growth of detritus follows logistic growth. In this instance, the predator's functional response is interpreted as an Ivlev-type response function. For mathematical simplicity, we consider the following non-dimensional system with the help of the following transformations:

$x = \frac{mX}{b}$, $y = \frac{Y}{e}$, $z = \frac{mZ}{eg}$, $t = \frac{T}{m}$.

Subsequently, the model system (3.1) becomes

$$
\begin{aligned}
\frac{dX}{dT} &= X(\alpha - X). \\
\frac{dY}{dT} &= Y\left(\beta - \frac{\gamma Y}{X}\right) - Z\{1 - exp(-Y)\}. \\
\frac{dZ}{dT} &= Z\left[-1 + \sigma\{1 - exp(-Y)\}\right],
\end{aligned}
\tag{3.2}
$$

where $\alpha = \frac{a_1}{m}$, $\beta = \frac{a_2}{m}$, $\gamma = \frac{c}{em^2}$, $\sigma = \frac{g}{m}$.

3.3   Equilibria and their feasibility

There exists only one axial equilibrium $E_1(\alpha, 0, 0)$ and one planar equilibrium point $E_2(\alpha, \frac{\alpha\beta}{\gamma}, 0)$. The interior equilibrium of the system (3.2) is given by $E_3(X^*, Y^*, Z^*)$, where $X^* = \alpha$,

$Y^* = ln(\frac{\sigma}{\sigma-1})$, $Z^* = \sigma \ln(\frac{\sigma}{\sigma-1})\left[\beta - \frac{\gamma}{\alpha}ln(\frac{\sigma}{\sigma-1})\right]$.

We may observe that, under the following criteria, the interior equilibrium $E_3(X^*, Y^*, Z^*)$ is feasible:

(i) $\sigma > 1$, (ii) $\gamma < \frac{\alpha\beta}{Y^*} = \gamma^*$(say).

3.4   Boundedness

The following lemma proves that the system's solutions are bounded.

Lemma 3.1

There are uniformly bounded solutions for system (3.2).

Proof

Suppose $S(T) = X + \sigma Y + Z$. Now

$$
\begin{aligned}
\frac{dS}{dT} &= \frac{dX}{dT} + \sigma\frac{dY}{dT} + \frac{dZ}{dT} \\
&\leq \alpha X - X^2 + \sigma\beta Y - \frac{\sigma\gamma Y^2}{X} - Z \\
&\leq \alpha X - X^2 - Z - \sigma\gamma\left(\frac{Y}{\sqrt{X}} - \frac{\beta}{\gamma}\sqrt{X}\right)^2 + \frac{\sigma\beta^2}{\gamma}X - \beta\sigma Y \\
&\leq 2\alpha X - X^2 + \frac{\sigma\beta^2}{\gamma}X - \alpha X - \beta\sigma Y - Z \\
&\leq -m_1 S(T) + 2\alpha X - X^2 + \frac{\sigma\beta^2}{\gamma}X.
\end{aligned}
$$

(3.3)

Let $F(X) = 2\alpha X - \eta X^2 + \frac{\sigma\beta^2}{\gamma}X$, then F has maximum value

$F_{max} = \left(2\alpha + \frac{\sigma\beta^2}{\gamma}\right)\left\{\alpha - \frac{1}{4}\left(2\alpha + \frac{\sigma\beta^2}{\gamma}\right) + \frac{\sigma\beta^2}{2\gamma}\right\}$ at $X = \frac{1}{2}\left(2\alpha + \frac{\sigma\beta^2}{\gamma}\right)$.

Hence, it follows that $\frac{dS}{dT} + m_1 S(T) \leq F_{max}$,

where $m_1 = \min\{\alpha, \beta, 1\}$.

which implies

$S(T) \leq F_{max} + e^{-m_1 T}S(X(0), Y(0), Z(0))$.

Hence, $\limsup_{T\to\infty} S(T) \leq \frac{F_{max}}{m_1}$.

Hence, the lemma is proved.

Theorem 3.1

If $\beta > max\left\{\sqrt{\gamma}, \frac{\gamma \ln\left(\frac{\sigma}{\sigma-1}\right)}{\alpha}\right\}$, then the system (3.2) is permanent.

Proof

We will prove the permanence of the system (3.2) by forming the 'average Lyapunov function' as elaborated by Hofbauer (1981) and Hutson and Vickers (1983).

In our model, we consider the average Lyapunov function of the form

$\phi(E) = X^{r_1} Y^{r_2} Z^{r_3}$,

where $\phi(E)$ is a non-negative C^1 function in $\mathbb{R}^3_+$ and each r_i is positive. Then

$$
\begin{aligned}
\eta(E) &= \frac{\dot{\phi}(E)}{\phi(E)} \\
&= r_1 \frac{\dot{X}}{X} + r_2 \frac{\dot{Y}}{Y} + r_3 \frac{\dot{Z}}{Z} \\
&= r_1(\alpha - X) + r_2\left(\beta - \frac{\gamma Y}{X}\right) - \frac{Z}{Y}\{1 - exp(-Y)\} + r_3\left[-1 + \sigma\{1 - exp(-Y)\}\right].
\end{aligned}
$$

From local behaviour, it is clear that there is no periodic trajectory in the boundary planes. Therefore, we can say that the system (3.2) is permanent if there exists $r_i > 0$ ($i = 1, 2, 3$) such that $\eta(E_j) > 0$, $j = 1, 2$. Now

$\eta(E_1) = r_2\beta - r_3$,

$\eta(E_2) = r_2\left(\beta - \frac{\gamma}{\beta}\right) - r_3\left[-1 + \sigma\left\{1 - exp\left(\frac{-\alpha\beta}{\gamma}\right)\right\}\right]$.

Therefore, we can find at least one positive $r = (r_1, r_2, r_3)$ such that $\eta(E_1) > 0$ and $\eta(E_2) > 0$, if $\beta > max\left\{\sqrt{\gamma}, \frac{\gamma \ln\left(\frac{\sigma}{\sigma-1}\right)}{\alpha}\right\}$. Hence, the theorem is proved.

3.5　Stability analysis of the system

Let J_k be the Jacobian matrices at the equilibrium points E_k, where $k = 1, 2, 3$. The eigenvalues of the Jacobian matrix J_1 are $-\alpha, \beta, -1$. So, E_1 is stable in the X and Z directions and unstable in the Y direction.

The eigenvalues of the Jacobian matrix J_2 are $-\alpha$,

$$\frac{1}{2}\left[-\left\{\beta + 1 - \sigma\left(1 - e^{-\frac{\alpha\beta}{\gamma}}\right)\right\} + \sqrt{\left\{\beta + 1 - \sigma\left(1 - e^{-\frac{\alpha\beta}{\gamma}}\right)\right\}^2 - 4\beta\left\{1 - \sigma\left(1 - e^{-\frac{\alpha\beta}{\gamma}}\right)\right\}}\right],$$

$$\frac{1}{2}\left[-\left\{\beta + 1 - \sigma\left(1 - e^{-\frac{\alpha\beta}{\gamma}}\right)\right\} - \sqrt{\left\{\beta + 1 - \sigma\left(1 - e^{-\frac{\alpha\beta}{\gamma}}\right)\right\}^2 - 4\beta\left\{1 - \sigma\left(1 - e^{-\frac{\alpha\beta}{\gamma}}\right)\right\}}\right].$$

So, E_2 is stable in the X direction and stable or unstable in the YZ plane according to the conditions: $\sigma > \dfrac{1-\beta}{\left(1-e^{-\frac{\alpha\beta}{\gamma}}\right)}$ or $\sigma < \dfrac{1-\beta}{\left(1-e^{-\frac{\alpha\beta}{\gamma}}\right)}$.

The characteristic equation corresponding to E_3 is

$$(-\alpha - \lambda)\left[\lambda^2 + \lambda\left\{-\beta + \frac{2\gamma Y^*}{\alpha} + Z^* e^{-Y^*}\right\} + \sigma Z^* e^{-Y^*}(1 - e^{-Y^*})\right] = 0$$

$$\Rightarrow (-\alpha - \lambda)\left[\lambda^2 + A\lambda + B\right] = 0,$$

where

$$A = -\beta + \frac{2\gamma Y^*}{\alpha} + Z^* e^{-Y^*},$$

$$B = \sigma Z^* e^{-Y^*}(1 - e^{-Y^*}).$$

If $A > 0$ and $B > 0$, we can conclude that the interior equilibrium $E_3(X^*, Y^*, Z^*)$ is locally asymptotically stable.

Here, $B > 0$ is always true.

Now $A > 0$ if the condition

$$\gamma > \frac{\alpha\beta\left[1 - (\sigma - 1)Y^*\right]}{Y^*\left[2 - (\sigma - 1)Y^*\right]} = \gamma^{**}(\text{say}) \tag{3.4}$$

holds, i.e., under condition (3.4), the populations do not go to extinction.

3.6   Global stability analysis

It is observed that when $T \to \infty$, the biomass of the detritus will reach its maximum value α, i.e.,

$$\lim_{T \to \infty} \sup X(T) = \alpha.$$

This case is not only true analytically but also in real situations in the Sundarban estuary. The biomass of detritus tends to a particular value, regardless of the species' original population. Therefore, studying the global behavior of the system's two-dimensional subsystem suffices. The subsystem in two dimensions is provided by

$$
\begin{aligned}
\frac{dY}{dT} &= Y\left(\beta - \frac{\gamma Y}{X}\right) - Z\{1 - exp(-Y)\}. \\
\frac{dZ}{dT} &= Z\left[-1 + \sigma\{1 - exp(-Y)\}\right].
\end{aligned}
\tag{3.5}
$$

Now we will show that under the condition (3.4), the equilibrium point E_3 is a global attractor in the positive octant.

Theorem 3.2

If $\gamma > \dfrac{\alpha\beta\left[1-(\sigma-1)Y^*\right]}{Y^*\left[2-(\sigma-1)Y^*\right]} = \gamma^{**}$, then the subsystem (3.5) is globally asymptotically stable.

Proof

Assume that Γ can represent any periodic orbit in the positive YZ plane around (Y^*, Z^*).

$$
\begin{aligned}
\Delta &= \int_\Gamma \operatorname{div}(\dot{Y}, \dot{Z}) dT \\
&= \int_\Gamma \left(\beta - \frac{2\gamma Y}{\alpha} - Ze^{-Y} - 1 + \sigma - \sigma e^{-Y} \right) dT \\
&= \int_\Gamma \left(1 - e^{-Y} \right) F_Y dT,
\end{aligned}
\tag{3.6}
$$

where $F = \frac{Y\left(\beta - \frac{\gamma Y}{\alpha}\right)}{1 - e^{-Y}}$ is the prey isocline $\dot{Y} = 0$.

Assuming that E_3 is locally stable when $\gamma > \gamma^{**}$, and applying the Rozenzueig and MacArthur conditions (Freedman, 1980), $F_Y < 0$. Hence, $\Delta < 0$. This creates a contradiction because, according to the Poincare criteria (Conway and Smoller, 1986), any periodic orbit Γ in the positive YZ plane is stable. Consequently, there isn't a periodic orbit on the positive YZ plane around (Y^*, Z^*). For this reason, the system (3.2) is globally asymptotically stable at point $E_3(X^*, Y^*, Z^*)$.

Theorem 3.3

Around the equilibrium point $E_3(X^*, Y^*, Z^*)$ in the positive octant, there exists at least one stable limit cycle if $\gamma < \frac{\alpha\beta \left[1 - (\sigma-1)Y^* \right]}{Y^* \left[2 - (\sigma-1)Y^* \right]} = \gamma^{**}$.

Proof

The equilibrium point $E_3(X^*, Y^*, Z^*)$ is unstable if $\gamma < \gamma^{**}$. Since $F_Y > 0$, we can determine that $\Delta > 0$ using theorem 3.1. It is now possible to declare any periodic orbit to be stable by applying the Poincare criteria (Conway and Smoller, 1986). Thus, in the positive octant, there is at least one stable limit cycle around the equilibrium point $E_3(X^*, Y^*, Z^*)$.

Theorem 3.4

A Hopf-bifurcating small amplitude periodic solution occurs at $E_3(X^*, Y^*, Z^*)$ if $\gamma = \dfrac{\alpha\beta\left[1-(\sigma-1)Y^*\right]}{Y^*\left[2-(\sigma-1)Y^*\right]} = \gamma^{**}$. We therefore draw the conclusion that, upon reaching a critical value for the micro-organism pool's loss rate, the biomass of the micro-organism pool, and the number of invertebrate predators fluctuate with little amplitudes around the steady state $E_3(X^*, Y^*, Z^*)$.

Proof

To prove this theorem, we have to show that the conditions of Hopf-bifurcation are satisfied. If $\gamma = \gamma^{**}$, then $A = 0$, where

$$A = -\beta + \frac{2\gamma Y^*}{\alpha} + Z^* e^{-Y^*}.$$

Then the roots of the equation $\lambda^2 + A\lambda + B = 0$ are purely imaginary, namely $\pm\sqrt{B}i$, where

$$B = \sigma z^* e^{-Y^*}(1 - e^{-Y^*}) = Z^* \frac{(\sigma - 1)}{\sigma}.$$

Also, we have $\left[\dfrac{d(Real\lambda)}{d\gamma}\right]_{\gamma=\gamma^{**}} = \dfrac{2Y^*}{\alpha}|_{\gamma=\gamma^{**}} = \dfrac{2}{\alpha}\ln\dfrac{\sigma}{(\sigma-1)} \neq 0$.

Thus, every requirement for a Hopf-bifurcation is met. Consequently, periodic solutions with little amplitudes exist close to $E_3(X^*, Y^*, Z^*)$. Thus, the theorem is established.

3.7   Qualitative analysis of the delay Model

In this part, we include a discrete time delay τ, assuming that it takes some time τ for the food conversion. Thus, we take into account a gestation delay τ in the invertebrate predator's uptake function term. Consequently, we have a modified version of the system

(3.1) in the form of a delay differential equation model.

$$\frac{dx}{dt} = x(a_1 - bx).$$

$$\frac{dy}{dt} = y\left(a_2 - \frac{cy}{bx}\right) - gz\{1 - exp(-ey)\}.$$

$$\frac{dz}{dt} = z\left[-m + g\{1 - exp(-e(y - \tau))\}\right]. \tag{3.7}$$

The non-dimensional model of the above system becomes as follows:

$$\frac{dX}{dT} = X(\alpha - X).$$

$$\frac{dY}{dT} = Y\left(\beta - \frac{\gamma Y}{X}\right) - Z\{1 - exp(-Y)\}.$$

$$\frac{dZ}{dT} = Z\left[-1 + \sigma\{1 - exp(-Y(T - \tau))\}\right], \tag{3.8}$$

where α, β, γ, σ are the same as described in section 3.2, and $\tau \geq 0$.

Let us assume that $P \equiv P(T)$, $Q \equiv Q(T)$, and $R \equiv R(T)$ are small deviations from the equilibrium values X^*, Y^*, and Z^*, respectively, in order to linearize the above system (3.8) about the equilibrium point E_3.

Now we substitute $X = X^* + P$, $Y = Y^* + Q$, and $Z = Z^* + R$, and we get the linearized system as follows :

$$\frac{dP}{dT} = a_{11}P.$$

$$\frac{dQ}{dT} = a_{21}P + a_{22}Q + a_{23}R.$$

$$\frac{dR}{dT} = a_{32}Q(T - \tau), \tag{3.9}$$

where a_{11}, a_{21}, a_{22}, a_{23}, a_{32} are as follows: $a_{11} = -X^*$, $a_{21} = \frac{\gamma Y^{*2}}{X^{*2}}$,
$a_{22} = \beta - \frac{2\gamma Y^*}{X^*} - Z^* e^{-Y^*}$, $a_{23} = -(1 - e^{-Y^*})$, $a_{32} = \sigma Z^* e^{-Y^*}$.

The characteristic equation of the system (3.9) is given by

$$\Delta(\lambda, \tau) = \lambda^3 + \lambda^2(-a_{11} - a_{22}) + \lambda(a_{11}a_{22} - a_{23}a_{32}e^{-\lambda\tau}) + a_{11}a_{23}a_{32}e^{-\lambda\tau} = 0$$

$$\implies \Delta(\lambda, \tau) = \lambda^3 + p\lambda^2 + q\lambda + r(\theta - \lambda)e^{-\lambda\tau} = 0, \tag{3.10}$$

where $p = -a_{11} - a_{22}$, $q = a_{11}a_{22}$, $r = a_{23}a_{32}$, $\theta = a_{11}$.

Assuming that the interior equilibrium point's existence criteria are met, we now examine two scenarios.

Case 1. When $\tau = 0$.

This case is already discussed earlier.

Case 2. When $\tau \neq 0$.

Let us put $\lambda = \mu + i\omega$ in the characteristic equation (3.10), where μ and ω are the functions of τ.

Thus, the characteristic equation becomes

$$\Delta(\lambda, \tau) = (\mu + i\omega)^3 + p(\mu + i\omega)^2 + q(\mu + i\omega) + r[\theta - (\mu + i\omega)]e^{-(\mu+i\omega)\tau} = 0. \tag{3.11}$$

Now separating real and imaginary parts, we get

$$\mu^3 - 3\mu\omega^2 + p(\mu^2 - \omega^2) + q\mu + re^{-\mu\tau}[(\theta - \mu)\cos\omega\tau - \omega\sin\omega\tau] = 0,$$

and

$$-\omega^3 + 3\mu^2\omega + 2p\mu\omega + q\omega + re^{-\mu\tau}[-\omega\cos\omega\tau - (\theta - \mu)\sin\omega\tau] = 0. \tag{3.12}$$

Now to satisfy the necessary and sufficient condition of Hopf-bifurcation of the interior equilibrium point, the characteristic equation should possess purely imaginary roots. To get

that, we put $\mu(\tau) = 0$, and $\omega(\tau) \neq 0$ in the system of equations (3.12), and we obtain

$$-p\omega^2 + r\theta cos\omega\tau - r\omega sin\omega\tau = 0,$$

$$-\omega^3 + q\omega - r\theta sin\omega\tau - r\omega cos\omega\tau = 0. \tag{3.13}$$

Eliminating $sin\omega\tau$ and $cos\omega\tau$ from the above equation (3.13), we get

$$\omega^6 + (p^2 - 2q)\omega^4 + (q^2 - r^2)\omega^2 - r^2\theta^2 = 0. \tag{3.14}$$

Putting $\omega^2 = \Omega$, we get

$$\Omega^3 + (p^2 - 2q)\Omega^2 + (q^2 - r^2)\Omega - r^2\theta^2 = 0. \tag{3.15}$$

Now regardless of the sign of the coefficients of Ω^2 and Ω, the equation (3.15) always has at least one positive root.

Let the root be ω^*.

So, from the system of equations (3.13), we get the critical value of the delay parameter τ, i.e.,

$$\hat{\tau} = \frac{1}{\omega^*} \arctan\left[\frac{\theta q - p\omega^{*2} - \theta\omega^{*2}}{\omega^*(q + p\theta - \omega^{*2})}\right] + \frac{n\pi}{\omega^*}, n = 0, 1, 2, 3, ...$$

If we choose $n = 0$, we get smallest value of $\hat{\tau}$ denoted by $\hat{\tau}^0$, where

$$\hat{\tau}^0 = \frac{1}{\omega^*} \arctan\left[\frac{\theta q - p\omega^{*2} - \theta\omega^{*2}}{\omega^*(q + p\theta - \omega^{*2})}\right].$$

We must differentiate equation (3.10), in order to validate the transversality criterion of Hopf-bifurcation (Hassard et al., 1981).

Thus, we get

$$\left(\frac{d\lambda}{d\tau}\right)^{-1} = \frac{3\lambda^2 + 2p\lambda + q}{-\lambda(\lambda^3 + p\lambda^2 + q\lambda)} - \frac{1}{\lambda(\theta - \lambda)} - \frac{\tau}{\lambda}.$$

Thus,

$$\left[\frac{d(Re\lambda)}{d\tau}\right]^{-1}_{\tau=\hat{\tau}^0} = Re\left(\frac{d\lambda}{d\tau}\right)^{-1}_{\tau=\hat{\tau}^0}$$

$$= Re\left[\frac{-3\omega^{*2} + 2p\omega^*i + q}{-i\omega^*(-\omega^{*3}i - p\omega^{*2} + q\omega^*i)} - \frac{1}{i\omega^*(\theta - i\omega^*)} - \frac{\tau}{i\omega^*}\right]$$

$$= \frac{2\omega^{*6} + \omega^{*4}(3\theta^2 - 2q + p^2) + \omega^{*2}(2p^2\theta^2 - 4q\theta^2) + q^2\theta^2}{\omega^{*2}\left[(-\omega^{*2} + q)^2 + p^2\omega^{*2}\right][\omega^{*2} + \theta^2]}$$

$$= \frac{H(\omega^*, \theta, p, q)\,(\text{say})}{\omega^{*2}\left[(-\omega^{*2} + q)^2 + p^2\omega^{*2}\right][\omega^{*2} + \theta^2]}.$$

Now

$$\text{Sign}\left[\frac{d(Re\lambda)}{d\tau}\right]_{\tau=\hat{\tau}^0} = \text{Sign}\left[\frac{d(Re\lambda)}{d\tau}\right]^{-1}_{\tau=\hat{\tau}^0}$$

$$= \text{Sign}H(\omega^*, \theta, p, q).$$

Now $3\theta^2 - 2q + p^2 = 4a_{11}^2 + a_{22}^2 > 0\,(\text{always})$,

and $2p^2\theta^2 - 4q\theta^2 = 2a_{11}^2(a_{11}^2 + a_{22}^2) > 0\,(\text{always})$.

Thus, we get Sign $\left[\frac{d(Re\lambda)}{d\tau}\right]_{\tau=\hat{\tau}^0} \neq 0$.

Lemma 3.2

For all non-negative values of τ, the interior equilibrium point $E_3(X^*, Y^*, Z^*)$ is locally asymptotically stable provided the following necessary and sufficient conditions are met.

(a) Assuming $\tau = 0$, the interior equilibrium point $E_3(X^*, Y^*, Z^*)$ remains stable.

(b) There are no purely imaginary roots in characteristic equation (3.10).

We derive the following theorem 3.5 from the above discussions.

Theorem 3.5

The interior equilibrium point $E_3(X^*, Y^*, Z^*)$ is unstable for $\tau > \hat{\tau}^0$ and stable for $\tau < \hat{\tau}^0$. As τ approaches $\hat{\tau}^0$, it experiences a Hopf-bifurcation.

3.8 Estimation for the length of delay to preserve the stability

In this part, we calculate the approximate value of the length of delay τ to maintain stability of the system. First, we make the assumption that the equilibrium $E_3(X^*, Y^*, Z^*)$ is locally asymptotically stable in the absence of delay, and all of the eigenvalues of the characteristic equation (3.10) have negative real parts for sufficiently small values of $\tau > 0$. Therefore, without losing generality, we can state that no eigenvalue with a positive real component bifurcates from infinity (sometimes it might be seen in retarded system (Sarkar et al., 1990)). By using Nyquist criteria (Thingstad and Langeland, 1974), we derive the length of time delay. For this, we assume that all the variables used in our model are continuous in (τ, ∞). Our linearized model:

$$
\begin{aligned}
\frac{dP}{dT} &= a_{11}P. \\
\frac{dQ}{dT} &= a_{21}P + a_{22}Q + a_{23}R. \\
\frac{dR}{dT} &= a_{32}Q(T - \tau),
\end{aligned}
\tag{3.16}
$$

where a_{11}, a_{21}, a_{22}, a_{23}, a_{32} are already described.

Let $\bar{P}(s)$, $\bar{Q}(s)$, $\bar{R}(s)$ are the Laplace transformations of P, Q, and R.

So, from the above-linearized system, we get

$$(s - a_{11})\bar{P} = P(0),$$

$$(s - a_{22})\bar{Q} = a_{21}\bar{P} + a_{23}\bar{R} + Q(0),$$

$$s\bar{R}(s) = a_{32}[\bar{Q}(s) + K(s)]e^{-s\tau} + R(0), \tag{3.17}$$

where $K(s) = \int_{-\tau}^{0} Q(T)e^{-sT}dT$.

Solving (3.17), we get

$\bar{R}(s) = \frac{F(s,\tau,a_{11},a_{21},a_{22},a_{32})}{s^3 + ps^2 + qs + r(\theta - s)e^{-s\tau}}$,

where $F = a_{21}a_{32}e^{-s\tau}P(0) + (s - a_{11})a_{32}e^{-s\tau}Q(0) + (s - a_{11})(s - a_{22})a_{32}e^{-s\tau}K(s)$

$\qquad + (s - a_{11})(s - a_{22})R(0).$

Let $E(s) = s^3 + ps^2 + qs + r(\theta - s)e^{-s\tau}$,

which is the same as the characteristic equation (3.10).

Using Nyquist Criteria (Thingstad and Langeland, 1974), we say that in the presence of delay, the equilibrium $E_3(X^*, Y^*, Z^*)$ is locally asymptotically stable, provided the following criteria are met.

$$ImE(iv_0) > 0, ReE(iv_0) = 0, \tag{3.18}$$

where v_0 is the smallest positive root of the equation $ReE(iv) = 0$.

Now $E(iv) = -iv^3 - pv^2 + qvi + r\theta cosv\tau - ir\theta sinv\tau - irvcosv\tau - vrsinv\tau$.

Using (3.18), we get

$$-v_0{}^3 + qv_0 > r\theta sinv_0\tau + rv_0 cosv_0\tau,$$

and

$$pv_0{}^2 = r\theta cosv_0\tau - rv_0 sinv_0\tau.$$

47

Also,

$$-v^3 + qv > r\theta sinv\tau + rvcosv\tau, \tag{3.19}$$

and

$$pv^2 = r\theta cosv\tau - rvsinv\tau. \tag{3.20}$$

To find the maximum value of v say v_+, we use the conditions that $|cosv\tau| \le 1$ and $|sinv\tau| \le 1$. Using (3.20), we get

$$pv^2 \le r(\theta + v). \tag{3.21}$$

Taking the equal sign, we get

$$pv^2 - r\theta - rv = 0. \tag{3.22}$$

the eqaution (3.22) has a unique positive root say $v_+ \ge v_0$.

Thus, we get $v_+ = \frac{1}{2p}\left[r + \sqrt{r^2 + 4pr\theta}\right]$.

Again from (3.19), we get

$$v^2 < q - rcosv\tau - \frac{r\theta}{v}sinv\tau. \tag{3.23}$$

Using (3.20) and (3.23), we get

$\frac{r}{p}[\theta cosv\tau - vsinv\tau] < q - rcosv\tau - \frac{r\theta}{v}sinv\tau$

$\Rightarrow \left|-\left(r + \frac{r\theta}{p}\right)\right|(1 - cosv\tau) + \left|\left(\frac{r\theta}{v} - \frac{rv}{p}\right)\right|sinv\tau < q + \left|-\left(r + \frac{r\theta}{p}\right)\right| = \eta_1(\text{say}).$

Using trigonometric inequalities $1 - cosv\tau \le \frac{1}{2}v^2\tau^2$ and $sinv\tau \le v\tau$, we get

$M(v, \tau)(\text{say}) \le \left|-\left(r + \frac{r\theta}{p}\right)\right|\frac{1}{2}v^2\tau^2 + \left|\left(\frac{r\theta}{v} - \frac{rv}{p}\right)\right|v\tau \equiv N(v, \tau)(\text{say})$, where

$$M(v, \tau) = \left|-\left(r + \frac{r\theta}{p}\right)\right|(1 - cosv\tau) + \left|\left(\frac{r\theta}{v} - \frac{rv}{p}\right)\right|sinv\tau.$$

48

So, $M(v, \tau) \leq N(v, \tau) \leq N(v, \tau_+)$.

Now if $N(v, \tau) < \eta_1$, then $N(v, \tau) - c\eta_1 = 0$, where $0 < c < 1$. Then we get

$$A\tau^2 + B\tau - c\eta_1 = 0, \tag{3.24}$$

where $A = \frac{1}{2}v_+{}^2 \left| -\left(r + \frac{r\theta}{p} \right) \right|$, $B = v_+{}^2 \left| \left(\frac{r\theta}{v_+{}^2} - \frac{r}{p} \right) \right|$.

Let τ_+ be the positive root of (3.24).

So, $\tau_+ = \frac{1}{2A}[-B + \sqrt{B^2 + 4Ac\eta_1}]$, which is the required maximum length of time delay τ to maintain the stability of the system.

3.9   Numerical simulation and discussions

Numerical simulations have been performed using MATLAB-R 2016a to comprehend the dynamics of the qualitative study, and all analytical results have been confirmed as indicated in the figures. We used the default MATLAB differential equations integrator for Runge-Kutta technique for the simulations. We employ a set of acceptable system parameter values in this numerical representation of the system (3.2) to validate our theoretical findings. In consideration of the equilibrium points' feasibility criteria, we have selected a range of parameter values, including $\alpha = 3.5$, $\beta = 1.5$, $\sigma = 1.05$. Also we have chosen the values of γ by using the following conditions:

$$(i) \gamma > \frac{\alpha\beta\left[1 - (\sigma - 1)Y^*\right]}{Y^*\left[2 - (\sigma - 1)Y^*\right]} = \gamma^{**},$$
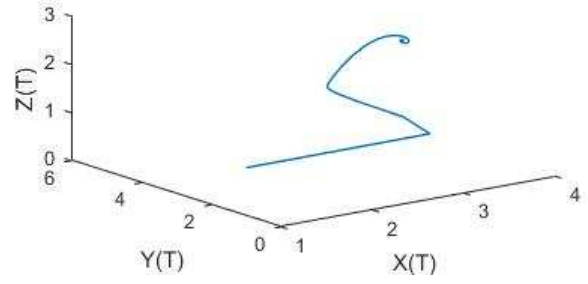$$(ii) \gamma < \gamma^{**},$$
$$(iii) \gamma = \gamma^{**}.$$

The system (3.2) has equilibrium point $E_3(3.5, 3.04, 2.29)$, for the set of parameter values. In Figure 3.1, we set the value of $\gamma = 0.9$, and we have shown the steady state of the detritus
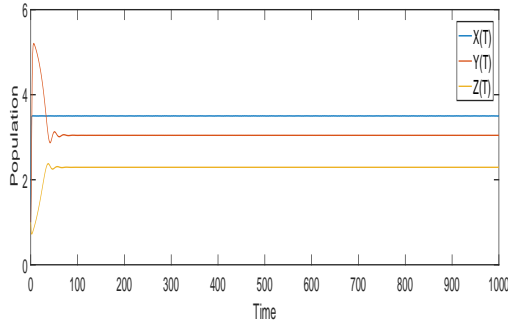
Figure 3.1: Stable state of the system (3.8) around E_3 for $\alpha = 3.5$, $\beta = 1.5$, $\sigma = 1.05$, $\gamma = 0.9$ when $\tau = 0$: (a) Time series plot, (b) Phase diagram plot.

Figure 3.2: Chaotic solution of the system (3.8) around E_3 for $\alpha = 3.5$, $\beta = 1.5$, $\sigma = 1.05$, $\gamma = 0.7$ when $\tau = 0$: (a) Time series plot, (b) Phase diagram plot.
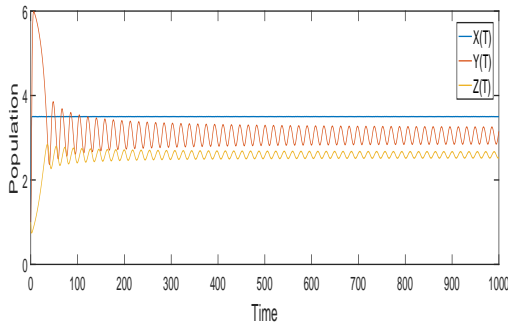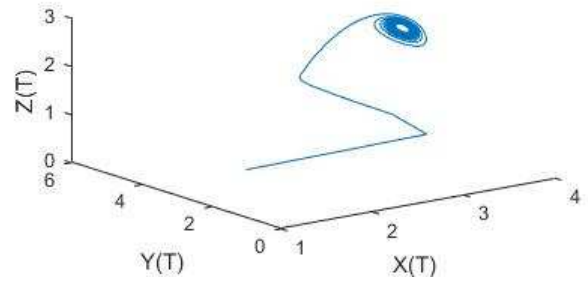
Figure 3.3: Hopf-bifurcation diagram of the model system (3.8) around E_3 for $\alpha = 3.5$, $\beta = 1.5$, $\sigma = 1.05$, $\gamma = 0.79$ when $\tau = 0$: (a) Time series plot, (b) Phase diagram plot.
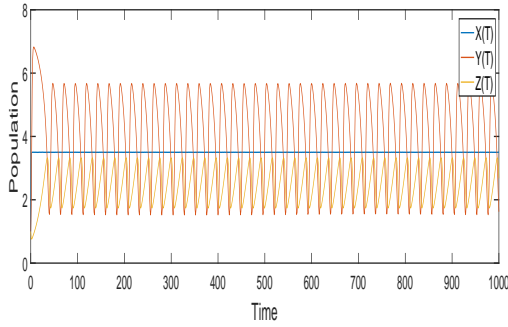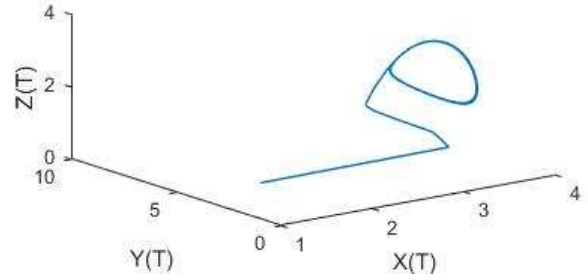
Figure 3.4: Stable state of the system (3.8) around E_3 for $\alpha = 3.5$, $\beta = 1.5$, $\sigma = 1.05$, $\gamma = 0.9$ when $\tau = 1.5$: (a) Time series plot, (b) Phase diagram plot.

Figure 3.5: Chaotic solution of the system (3.8) around E_3 for $\alpha = 3.5$, $\beta = 1.5$, $\sigma = 1.05$, $\gamma = 0.9$ when $\tau = 1.9$: (a) Time series plot, (b) Phase diagram plot.

Figure 3.6: Hopf-bifurcation diagram of the model system (3.8) around E_3 for $\alpha = 3.5$, $\beta = 1.5$, $\sigma = 1.05$, $\gamma = 0.9$ when $\tau = 1.6804$: (a) Time series plot, (b) Phase diagram plot.
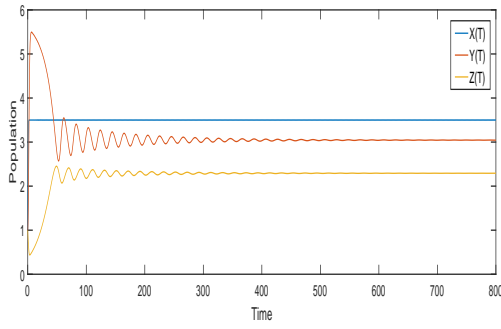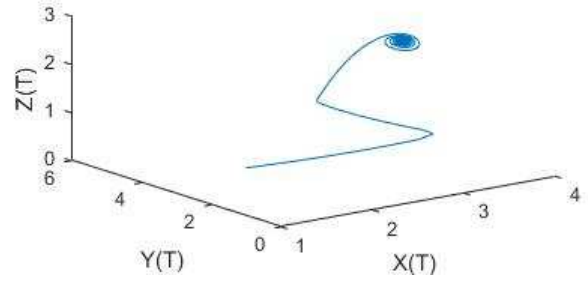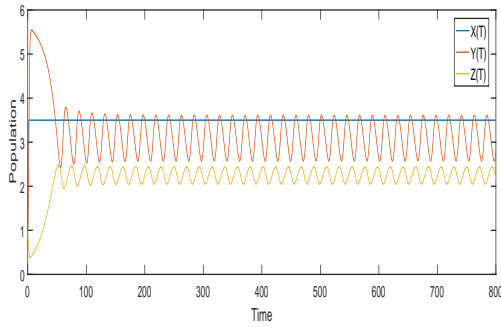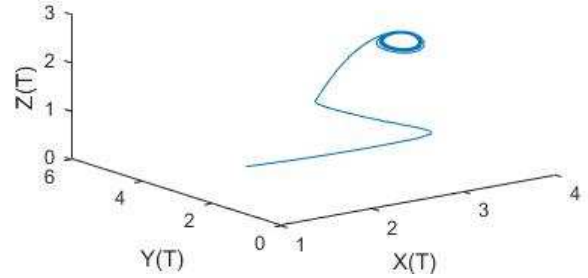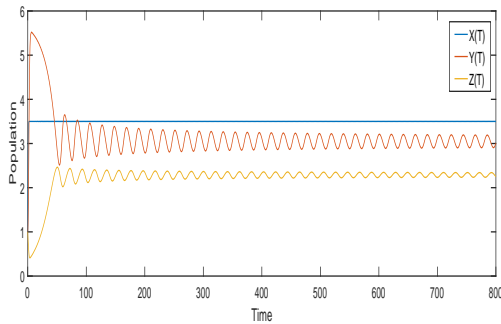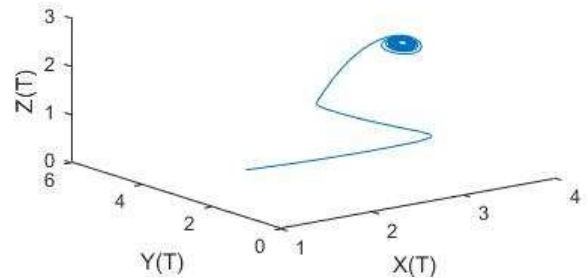
biomass. We also observed that at first the population of micro-organism pool oscillates with small amplitude and the oscillation gradually decreases as the time increases and the prey population attains its steady state value. The same picture is seen for predator population. Thus, through these figures, it is seen that the system (3.2) is globally asymptotically stable which proved the theoretical finding of global stability analysis.

We now select the value of $\gamma = 0.7$ in Figure 3.2. The system's instability is depicted in this figure. In this figure, the detritus maintains its steady state, but the prey and predator populations exhibit a huge amplitude oscillation with increasing time, which results a limit cycle.

We have now fixed the value of γ to 0.79. Figure 3.3 illustrates Hopf-bifurcation with small amplitude periodic oscillation around the interior equilibrium point.

We obtain the values of $\omega^* = 0.3081$ and the critical value of τ, that is, $\hat{\tau}^0 = 1.6804$, for the same set of parameter values. Using $\tau = 1.5$ in Figure 3.4, we have demonstrated that the system is stable when $\tau < \hat{\tau}^0 = 1.6804$.

In Figure 3.5, we take the value of $\tau = 1.9$, and it is seen that the system is unstable for $\tau > \hat{\tau}^0 = 1.6804$ and thus, a limit cycle is formed. We use $\tau = \hat{\tau}^0 = 1.6804$ in Figure 3.6 to demonstrate the existence of small-amplitude Hopf-bifurcating periodic oscillations. The numerical simulation reveals that, out of all the parameters, the system parameter γ and the time-delay τ are the most crucial in illustrating the system dynamics in the Sundarban estuarine ecosystem.

3.10 Conclusions

The main findings of this research align with the widely accepted ecological concepts. It is clear that the mangrove forest's litter biomass is essential to preserving the detritus food chain. This study will contribute an overall idea to understand the dynamics of mangrove

ecosystem in general. We have demonstrated in this study that the functional response is a key factor in determining how the model behaves. In real situation, same sort of functional response can be seen in Sundarban estuary. The Sundarban Estuary's ecology is known to exhibit a variety of stable behaviours throughout time, some of which are constant, oscillatory, reach a fixed point, or exhibit other types of behaviour. The criteria for the presence of the global attractor, the limit cycle, and the Hopf-bifurcation under specific circumstances are derived in this chapter. One may argue that the Sundarban Estuary exhibits the same dynamic activity in real life as well. Thus, the analysis deepens our knowledge of how the functional response of an invertebrate predator shapes the dynamics of this detritus based prey-predator ecosystem. It is also demonstrated here that the ecosystem's dynamics are significantly impacted by the discrete time-delay. When the delay parameter passes its critical value $\hat{\tau}^0$, it even destabilises the stable equilibrium point $E_3(X^*, Y^*, Z^*)$, resulting in Hopf-bifurcating periodic oscillations with little amplitude. A limit cycle forms as a result of the instability.

Chapter 4

Dynamical Complexity of a Detritus-Based Predator-Prey Model with Multiple Time Delays in Sundarban Mangrove Ecosystem, India *

4.1   Introduction

Sundarban mangrove forest has an incredible ecosystem that allows us to study its rich dynamics. Several authors have done their works based on the diverse characteristics of this forest and the adjacent estuary (Das et al., 2015; Mukhopadhyay et al., 2010; Murmu and Sarkar, 2020; Sarkar and Ghosh, 1997; Thakur et al., 2017). Our study proposes a detritus-based predator-prey mathematical model, where mangrove leaves of different species like *Heritiera, Avicennia, Sonneratia,* and *Exocaria* are the prime fount of detritus. The decomposition process forms this detritus with the help of several micro-organisms present in the soil (Bandyopadhyay et al., 2003; Dash, 2001; Sarkar and Ghosh, 1997). The detritus is also created by recycling the dead bodies of various invertebrate predators in the ground. Several insect larvae, especially *chironomidae* and *nematodes*, are seen in the ecosystem as invertebrate predators. The micro-organism pool acts as the prey in this food chain and

---

consumes its nutrients from the detritus. Here, invertebrate predators live on the food taken from the micro-organism pool (Joint, 1978; Sarkar and Ghosh, 1997). Several authors have already worked on detritus-based models on different conditions and prospects. Vetter (1998) studied the detritus-based model in the Southern California Submarine canyon ecosystem. Charles (1993) studied a model in which detritus was formed by two macrophytes such as Cytoseira mediteranca and Posidonia oceanica. Faust and Gulledge (1996) assumed a model where detritus was formed from microalgae. Linley and Adams (1997), Linley (1968), and Ray and Choudhury (1998) examined some models where detritus was mainly formed from the dead bodies of certain insect larvae by the recycling process. Sarkar et al. (1991) studied a model where the primary source of detritus was the plant litter of several mangrove trees in the Sundarban mangrove forest.

In any prey-predator system, the uptake function plays an essential part in building the system dynamics. For an extended period, many researchers have shown their interest in various kinds of response functions like Holling type-I (Li et al., 2021; Seo and DeAngelis, 2003; Seo and Kot, 2008), Holling type-II (Alsakaji et al., 2021; Das and Gazi, 2011; Huang et al., 2018; Molla et al., 2019; Zhou et al., 2019), Holling type-III (Agarwal and Pathak, 2012; Ghosh and Sarkar, 1997; Gonzlez-Olivares, 2011; Huang et al., 2006; Majumdar, 2022), Holling type-IV (Agarwal and Pathak, 2017; Datta et al., 2019; Liu and Huang, 2020), Ivlev type (Kooij and Zegeling, 1996; Liu et al., 2016; Murmu and Sarkar, 2020; Wang et al., 2010), Crowley Martin (Gazi and Das, 2010; Maiti et al., 2019; Panja, 2021; Santra et al., 2020; Thakur et al., 2020), Beddington-Deangelis (Haque, 2012; Pal and Mandal, 2014; Pal et al., 2019; Cantrell and Cosner, 2001; Hwang, 2003), Hassell-Varley (Hsu et al., 2008; Xu and Li, 2015), suitable for their field of research. In our work to sustain invertebrate predators, the Ivlev type response function which is a prey-dependent functional response, is incorporated into the growth equation of invertebrate predators. Another critical factor in any prey-predator dynamical system is the time delay. Some delays usually exist in any

system. Ignoring time delay means ignoring reality. A few time delays, especially maturation, gestation, and hunting, can be seen in any natural ecosystem (Banerjee and Takeuchi, 2017; Dubey et al., 2020; Gazi and Das, 2010; Haque et al., 2011; Hu and Huang, 2010; Kundu and Maitra, 2018; Maiti et al., 2019; Thakur et al., 2020). These delays affect the stability of the system. It transforms any steady ecosystem into an unstable ecosystem by creating a limit cycle, Hopf-bifurcating periodic oscillations. For an ordinary differential equation system, the characteristic equation is linear, whereas, for a delay-induced system of differential equations, the characteristic equation is exponential or quasi-exponential, leading to more complicated dynamics. Hutchinson first applied delay in the logistic differential equation (Hutchinson et al., 1948). Many prosperous works on time lag have been noticed in recent years in many research papers and articles (Banerjee and Takeuchi, 2017; Dubey et al., 2020; Gazi and Das, 2010; Hu and Huang, 2010; Kundu and Maitra, 2018; Maiti et al., 2019; Thakur et al., 2020). In many articles, the delays used in the prey and predator growth equation are supposed to be equal (Xie et al., 2015; Xu and Li, 2015; Yan and Li, 2006; Yan and Zhang, 2008). However, the fact is that these delays may not always be the same. Two different valued discrete time delays have been taken for our model's prey and predator growth equation.

This paper contains the following works sequentially: In section 4.2, model formulation is carried out, assuming some basic assumptions. Section 4.3 consists of the equilibrium points and their feasibility. Section 4.4 describes the system's non-negativity and boundedness. Section 4.5 includes the system's dynamic behavior without time delay. Section 4.6 outlines the delay model, and the consequence of delay on the system has been discussed here. In section 4.7, numerical simulations are accomplished based on some parameter values. Finally, in section 4.8, the outcomes of our study have been explained.

4.2   Model formulation

Here, we construct a deterministic model as follows:

$$
\begin{aligned}
\frac{dx_1}{dt} &= x_1(a - bx_1) - \frac{hx_1y_1}{k + x_1} + k_1 m z_1. \\
\frac{dy_1}{dt} &= y_1\left(c - \frac{dy_1}{bx_1}\right) - qz_1\{1 - e^{-fy_1}\}. \\
\frac{dz_1}{dt} &= z_1\left[-m + q\{1 - e^{-fy_1}\}\right],
\end{aligned}
\tag{4.1}
$$

where

$x_1(0) = x_{10} > 0, y_1(0) = y_{20} > 0$ and $z_1(0) = z_{30} > 0$, and

$x_1 =$ biomass of detritus,

$y_1 =$ biomass of micro-organism,

$z_1 =$ biomass of invertebrate predator,

$a =$ detritus's growth rate,

$c =$ micro-organism pool's growth rate,

$\frac{bc}{d} =$ carrying capacity of micro-organism pool,

$q =$ rate of conversion of food of invertebrate predator,

$m =$ invertebrate predator's normal death rate,

$k_1 m =$ detritus recycle rate after the death of invertebrate predator,

$f =$ hunting success.

Here, the growth of detritus is assumed to follow a logistic type growth equation, and a micro-organism dependent uptake function i.e., Ivlev-type is considered for predator. For simplicity, we convert our system into a non-dimensional system using the following transformations:

$x_1 = kX$, $y_1 = \frac{mkY}{h}$, $z_1 = \frac{km^2 Z}{qh}$, $t = \frac{T}{m}$.

Then (4.1) converted into

$$
\begin{aligned}
\frac{dX}{dT} &= X\left\{(\alpha - \beta X) - \frac{Y}{1+X}\right\} + \gamma Z. \\
\frac{dY}{dT} &= Y\left(\eta - \frac{\xi Y}{X}\right) - Z\{1 - e^{-\sigma Y}\}. \\
\frac{dZ}{dT} &= Z\left[-1 + \phi\{1 - e^{-\sigma Y}\}\right].
\end{aligned}
\tag{4.2}
$$

Here, $\alpha = \frac{a}{m}$, $\beta = \frac{bk}{m}$, $\gamma = k_1 m$, $\eta = \frac{c}{m}$, $\xi = \frac{d}{bh}$, $\phi = \frac{q}{m}$, $\sigma = \frac{fmk}{h}$.

4.3   Equilibria and their stability

There exists three equilibria as follows:

$(i)\, E_1(\frac{\alpha}{\beta}, 0, 0)$,

$(ii)\, E_2(\overline{X_1}, \overline{Y_1}, 0)$, in which

$\overline{X_1} = \frac{(\alpha - \beta) + \sqrt{\xi^2(\alpha-\beta)^2 - 4\xi\beta(\eta - \alpha\xi)}}{2\beta}$, $\overline{Y_1} = \frac{\eta}{\xi}\frac{(\alpha - \beta) + \sqrt{\xi^2(\alpha-\beta)^2 - 4\xi\beta(\eta - \alpha\xi)}}{2\beta}$.

$(iii)\, E_3(X_1{}^*, Y_1{}^*, Z_1{}^*)$, in which

$Y_1{}^* = \frac{1}{\sigma}ln(\frac{\phi}{\phi-1})$.

It is pretty challenging to find the exact value of $X_1{}^*$ and $Z_1{}^*$, but we find a polynomial of X, which is as follows:

$$
\beta\left(1 - exp(-\sigma Y)\right)X^4 + (1 - exp(-\sigma Y))(\beta - \alpha)X^3 - \left\{\alpha\left(1 - exp(-\sigma Y)\right) + \eta\xi Y\right\}X^2
$$
$$
+ \left(\xi\gamma Y^2 - \eta\xi Y\right)X + (1 - exp(-\sigma Y))Y + \xi\gamma Y^2 = 0.
$$

Here, $\alpha > \beta$ and $(1 - exp(-\sigma Y)) > 0$.

So, the coefficient of X^4 is positive and the coefficient of X^3 is negative. So, there exists minimum one positive real root, say $X_1{}^*$. So,

$Z_1{}^* = \frac{1}{(1 - exp(-\sigma Y_1{}^*))}\left\{Y_1{}^*\left(\eta - \frac{\xi Y_1{}^*}{X_1{}^*}\right)\right\}$.

$E_2(\overline{X_1}, \overline{Y_1}, 0)$ is feasible when $\xi > \frac{\eta}{\alpha}$, and $E_3(X_1{}^*, Y_1{}^*, Z_1{}^*)$ exists when

(a) $\phi > 1$, (b) $Y_1{}^* < \frac{\eta}{\xi} X_1{}^*$.

4.4 Non-negativity and boundedness

Let $R_+ =$ positive real numbers' set. From the model system (4.2), the functions of right hand side can be written as $f = (f_1, f_2, f_3)$, where

$f_1 = X\left\{(\alpha - \beta X) - \frac{Y}{1+X}\right\} + \gamma Z,$

$f_2 = Y\left(\eta - \frac{\xi Y}{X}\right) - Z\{1 - exp(-\sigma Y)\},$

$f_3 = Z\big[-1 + \phi\{1 - exp(-\sigma Y)\}\big].$

Here, it is clear that $f \in C^1(R_+^3)$, where $R_+^3 = \big\{(X, Y, Z) \in R^3 : X \in R_+, Y \in R_+, Z \in R_+\big\}.$

So, the function $f : R_+^3 \to R^3$ satisfies the Lipschitz condition on R_+^3. So, the fundamental theorem of existence and uniqueness states that there is a unique solution for the system (4.2).

Now, $\dot{X}|_{X=0} = \gamma Z \geq 0$. So, $X(T) \geq 0 \ \forall \ T \geq 0$. Also, $\dot{Y}|_{Y=0} \geq 0$ and $\dot{Z}|_{Z=0} \geq 0$. So, $Y(T) \geq 0 \ \forall \ T \geq 0$ and $Z(T) \geq 0 \ \forall \ T \geq 0$.

The following lemma gives the proof of boundedness.

Lemma 4.1

The system (4.2) possesses uniformly bounded solutions.

Proof

Suppose $W(T) = X + \phi Y + Z$.

$$\frac{dW}{dT} = \frac{dX}{dT} + \phi \frac{dY}{dT} + \frac{dZ}{dT}$$

$$\leq \alpha X - \beta X^2 + \gamma Z + \phi \eta Y - \frac{\phi \xi Y^2}{X} - Z$$

$$\leq \alpha X - \beta X^2 - (1 - \gamma)Z - \phi \xi \left(\frac{Y}{\sqrt{X}} - \frac{\eta}{\xi}\sqrt{X} \right)^2 + \frac{\phi \eta^2}{\xi} X - \phi \eta Y$$

$$\leq 2\alpha X - \beta X^2 + \frac{\phi \eta^2}{\xi} X - \alpha X - \phi \eta Y - (1 - \gamma)Z$$

$$\leq -m_1 W(T) + 2\alpha X - \beta X^2 + \frac{\phi \eta^2}{\xi} X. \tag{4.3}$$

Let $F(X) = 2\alpha X - \beta X^2 + \frac{\phi \eta^2}{\xi} X$, then F has maximum value $F_{max} = \frac{\alpha}{\beta} \left(2\alpha + \frac{\phi \eta^2}{\xi} \right)$
$- \frac{1}{4\beta} \left(2\alpha + \frac{\phi \eta^2}{\xi} \right)^2 + \frac{\phi \eta^2}{2\xi \beta} \left(2\alpha + \frac{\phi \eta^2}{\xi} \right)$ at $X = \frac{1}{2\beta} \left(2\alpha + \frac{\phi \eta^2}{\xi} \right)$.

Hence, it follows that $\frac{dW}{dT} + m_1 W(T) \leq F_{max}$,

where $m_1 = \min\{\eta, \alpha, (1 - \gamma)\}$,

which implies

$W(T) \leq F_{max} + e^{-m_1 T} W(X(0), Y(0), Z(0))$.

Hence, $\limsup\limits_{T \to \infty} W(T) \leq \frac{F_{max}}{m_1}$.

Hence, the lemma is proved.

4.5 System's dynamical behaviour without time delay

At E_1, the variational matrix has three eigenvalues which are $-\alpha$, η, -1. So in the X and Z directions, E_1 is stable and in the Y direction, it is unstable.

At E_2, the characteristic equation of the variational matrix is

$$\left[-1 + \phi \left(1 - e^{-\sigma \overline{Y_1}} \right) - \lambda \right] \left[\lambda^2 + P_1 \lambda + Q_1 \right] = 0,$$

where

$$P_1 = -\alpha + 2\beta\overline{X_1} + \frac{\overline{Y_1}}{(1 + \overline{X_1})^2} - \eta + \frac{2\xi\overline{Y_1}}{\overline{X_1}},$$

$$Q_1 = \left(\eta - \frac{2\xi\overline{Y_1}}{\overline{X_1}}\right)\left\{\alpha - 2\beta\overline{X_1} - \frac{\overline{Y_1}}{(1 + \overline{X_1})^2}\right\} + \frac{\xi\overline{X_1}^2}{\overline{X_1}(1 + \overline{X_1})}.$$

So, in the XY plane, the equilibrium $E_2(\overline{X_1}, \overline{Y_1}, 0)$ is stable when P_1 and Q_1 are both positive and stable in the the Z-direction when $\overline{Y_1} < {Y_1}^*$.

At E_3, the variational matrix has the characteristic equation as follows:

$$\lambda^3 + A\lambda^2 + B\lambda + C = 0,$$

where

$$A = -\left[\left\{\alpha - 2\beta{X_1}^* - \frac{{Y_1}^*}{(1 + {X_1}^*)^2}\right\} + \left\{\eta - \frac{2\xi{Y_1}^*}{{X_1}^*} - {Z_1}^*\sigma e^{-\sigma{Y_1}^*}\right\}\right],$$

$$B = \left[\left\{\alpha - 2\beta{X_1}^* - \frac{{Y_1}^*}{(1 + {X_1}^*)^2}\right\} + \left\{\eta - \frac{2\xi{Y_1}^*}{{X_1}^*} - {Z_1}^*\sigma e^{-\sigma{Y_1}^*}\right\}\right.$$
$$\left. + \sigma {Z_1}^* e^{-\sigma{Y_1}^*} + \frac{{X_1}^*}{1 + {X_1}^*}\frac{\xi{Y_1}^{*2}}{{X_1}^{*2}}\right],$$

$$C = -\sigma {Z_1}^* e^{-\sigma{Y_1}^*}\left\{\alpha - 2\beta{X_1}^* - \frac{{Y_1}^*}{(1 + {X_1}^*)^2}\right\} - \frac{\gamma\xi{Y_1}^{*2}}{{X_1}^{*2}}\sigma\phi{Z_1}^* e^{-\sigma{Y_1}^*}.$$

Using Routh-Hurwitz Criterion, we can say that if $A > 0$, $C > 0$, and $AB - C > 0$, $E_3({X_1}^*, {Y_1}^*, {Z_1}^*)$ is locally stable.

4.6   Analysis of the model with time delay

Here, two non-negative gestation time delays τ_1, and τ_2 have been introduced into the system (4.1).

Then the system (4.1) turns into a system which is as follows:

$$
\begin{aligned}
\frac{dx_1}{dt} &= x_1(a - bx_1) - \frac{hx_1y_1}{k + x_1} + k_1mz_1. \\
\frac{dy_1}{dt} &= y_1\left(c - \frac{dy_1(t - \tau_1)}{bx_1(t - \tau_1)}\right) - qz_1\left\{1 - e^{-fy_1}\right\}. \\
\frac{dz_1}{dt} &= z_1\left[-m + q\left\{1 - e^{-fy_1(t-\tau_2)}\right\}\right].
\end{aligned}
\tag{4.4}
$$

The non-dimensional model of the system (4.4) becomes as follows:

$$
\begin{aligned}
\frac{dX}{dT} &= X\left\{(\alpha - \beta X) - \frac{Y}{1 + X}\right\} + \gamma Z. \\
\frac{dY}{dT} &= Y\left(\eta - \frac{\xi Y(T - \tau_1)}{X(T - \tau_1)}\right) - Z\left\{1 - e^{-\sigma Y}\right\}. \\
\frac{dZ}{dT} &= Z\left[-1 + \phi\left\{1 - e^{-\sigma Y(T-\tau_2)}\right\}\right],
\end{aligned}
\tag{4.5}
$$

where α, β, γ, η, ξ, σ, ϕ are same as described in section (4.2), and $\tau_1 \geq 0$, $\tau_2 \geq 0$.

To linearize the above system (4.5), let us consider the small perturbations $P \equiv P(T)$, $Q \equiv Q(T)$, and $R \equiv R(T)$ about X_1^*, Y_1^*, and Z_1^* respectively.

Substituting $X = X_1^* + P$, $Y = Y_1^* + Q$ and $Z = Z_1^* + R$ in (4.5), we get

$$
\begin{aligned}
\frac{dP}{dT} &= a_{11}P + a_{12}Q + a_{13}R. \\
\frac{dQ}{dT} &= a_{21}P(T - \tau_1) + a_{22}Q(T - \tau_1) + a_{22'}Q + a_{23}R. \\
\frac{dR}{dT} &= a_{32}Q(T - \tau_2),
\end{aligned}
\tag{4.6}
$$

where

$a_{11} = \alpha - 2\beta X_1^* - \frac{Y_1^*}{(1+X_1^*)^2}$, $a_{12} = -\frac{X_1^*}{1+X_1^*}$, $a_{13} = \gamma$, $a_{21} = \frac{\xi Y_1^{*2}}{X_1^{*2}}$, $a_{22} = -\frac{\xi Y_1^*}{X_1^*}$,

$a_{22'} = -\sigma Z_1^* e^{-\sigma Y_1^*} + \left(\eta - \frac{\xi Y_1^*}{X_1^*}\right)$, $a_{23} = -(1 - e^{-\sigma Y_1^*})$, $a_{32} = \sigma\phi Z_1^* e^{-\sigma Y_1^*}$.

The variational matrix of the system (4.6) has the characteristic equation as follows:

$$\lambda^3 + \lambda^2 \left(\theta + \rho e^{-\lambda \tau_1}\right) + \lambda \left(\psi e^{-\lambda \tau_2} + r e^{-\lambda \tau_1} + \sigma_1\right) + \sigma_2 e^{-\lambda \tau_2} + \sigma_3 e^{-\lambda \tau_1} e^{-\lambda \tau_2} = 0, \quad (4.7)$$

where $\theta = -a_{11} - a_{22'}$, $\rho = -a_{22}$, $\psi = -a_{23} a_{32}$, $r = a_{11} a_{22} - a_{12} a_{21}$, $\sigma_1 = a_{11} a_{22'}$,

$\sigma_2 = a_{11} a_{23} a_{32}$, $\sigma_3 = -a_{13} a_{21} a_{32}$.

Now we consider six cases, assuming that the existence conditions of $E_3(X_1^*, Y_1^*, Z_1^*)$ are satisfied.

Case 1. $\tau_1 = \tau_2 = 0$.

Then the system (4.5) reduces to the system (4.2). In section (4.5), we have already discussed about the system's stability.

Case 2. When τ_1 exists positively and $\tau_2 = 0$.

If $\tau_1 > 0$ and $\tau_2 = 0$, then (4.7) turns into

$$\left(\lambda^3 + \theta \lambda^2 + (\psi + \sigma_1) \lambda + \sigma_2\right) + \left(\rho \lambda^2 + r \lambda + \sigma_3\right) e^{-\lambda \tau_1} = 0. \quad (4.8)$$

Let the equation (4.8) has a root $i\omega_1$, where $\omega_1 > 0$. Thus,

$$-\omega_1^2 \theta - \left(\rho \omega_1^2 - \sigma_3\right) cos\omega_1 \tau_1 + \omega_1 r sin\omega_1 \tau_1 + \sigma_2 = 0,$$

and

$$-\omega_1^3 + \left(\omega_1^2 \rho - \sigma_3\right) sin\omega_1 \tau_1 + \omega_1 (\phi + \sigma_1) + \omega_1 r cos\omega_1 \tau_1 = 0. \quad (4.9)$$

This leads to

$$\omega_1^6 + \omega_1^4 \left[\theta^2 - 2(\psi + \sigma_1) - \rho^2\right] + \omega_1^2 \left[(\psi + \sigma_1)^2 - 2\theta \sigma_2 - r^2 + 2\rho \sigma_3\right] + \sigma_2^2 - \sigma_3^2 = 0. \quad (4.10)$$

Let the equation (4.10) has one positive root, say $\omega_1{}^*$. Now substituting $\omega_1{}^*$ into the equation (4.9), we get

$$\hat{\tau}_1 = \frac{1}{\omega_1{}^*}\arctan\left[\frac{\theta r\omega_1{}^{*3} - \sigma_2\omega_1{}^*r + \left(\rho\omega_1{}^{*2} - \sigma_3\right)\omega_1{}^{*3} - \left(\rho\omega_1{}^{*2} - \sigma_3\right)\omega_1{}^*\left(\psi + \sigma_1\right)}{\omega_1{}^{*4}r - \omega_1{}^{*2}r\left(\psi + \sigma_1\right) - \left(\rho\omega_1{}^{*2} - \sigma_3\right)\omega_1{}^{*2}\theta + \sigma_2\left(\rho\omega_1{}^{*2} - \sigma_3\right)}\right] + \frac{n\pi}{\omega_1{}^*},$$

$n = 0, 1, 2, 3, \ldots.$

If we choose $n = 0$, we get the smallest value of $\hat{\tau}_1$ denoted by $\hat{\tau}_1{}^0$, where

$$\hat{\tau}_1{}^0 = \frac{1}{\omega_1{}^*}\arctan\left[\frac{\theta r\omega_1{}^{*3} - \sigma_2\omega_1{}^*r + \left(\rho\omega_1{}^{*2} - \sigma_3\right)\omega_1{}^{*3} - \left(\rho\omega_1{}^{*2} - \sigma_3\right)\omega_1{}^*\left(\psi + \sigma_1\right)}{\omega_1{}^{*4}r - \omega_1{}^{*2}r\left(\psi + \sigma_1\right) - \left(\rho\omega_1{}^{*2} - \sigma_3\right)\omega_1{}^{*2}\theta + \sigma_2\left(\rho\omega_1{}^{*2} - \sigma_3\right)}\right].$$

Now the equation (4.8) is differentiated with respect to τ_1, and we obtain

$$\left(\frac{d\lambda}{d\tau_1}\right)^{-1} = -\frac{3\lambda^2 + 2\theta\lambda + (\psi + \sigma_1)}{\lambda\left(\lambda^3 + \theta\lambda^2 + (\psi + \sigma_1)\lambda + \sigma_2\right)} + \frac{(2\rho\lambda + r)}{\lambda\left(\rho\lambda^2 + r\lambda + \sigma_3\right)} - \frac{\tau_1}{\lambda}.$$

Thus, we get

$$\left[\frac{d(Re\lambda)}{d\tau_1}\right]^{-1}_{\tau_1 = \hat{\tau}_1{}^0}$$

$$= Re\left(\frac{d\lambda}{d\tau_1}\right)^{-1}_{\tau_1 = \hat{\tau}_1{}^0}$$

$$= Re\left[\frac{+3\omega_1{}^{*2} - 2\theta\omega_1{}^*i - (\psi + \sigma_1)}{i\omega_1{}^*\left\{-\omega_1{}^{*3}i - \theta\omega_1{}^{*2} + (\psi + \sigma_1)\omega_1{}^*i + \sigma_2\right\}} + \frac{2\rho\omega_1{}^*i + r}{i\omega_1{}^*\left(-\rho\omega_1{}^{*2} + r\omega_1{}^*i + \sigma_3\right)} - \frac{\tau_1}{i\omega_1{}^*}\right]$$

$$= \frac{W_1\left(\omega_1{}^*, \psi, \theta, \rho, r, \sigma_1, \sigma_2, \sigma_3\right)}{\left[\left\{\omega^3 - (\psi + \sigma_1)\omega\right\}^2 + \left(\sigma_2 - \theta\omega^2\right)^2\right]},$$

where

$$W_1 \left(\omega_1{}^*, \psi, \theta, \rho, r, \sigma_1, \sigma_2, \sigma_3 \right)$$

$$= \left\{ + 3\omega_1{}^{*2} - (\psi + \sigma_1) \right\} \left\{ \omega_1{}^{*2} - (\psi + \sigma_1) \right\} \left\{ r^2 \omega_1{}^{*2} + \left(\sigma_3 - \rho \omega_1{}^{*2} \right)^2 \right\}$$

$$= -2\theta \left(\sigma_2 - \theta \omega_1{}^{*2} \right) \left\{ r^2 \omega_1{}^{*2} + \left(\sigma_3 - \rho \omega_1{}^{*2} \right)^2 \right\} + \left\{ -r^2 + 2\rho \left(\sigma_3 - \rho \omega_1{}^{*2} \right) \right\}$$

$$= \left[\left\{ \omega_1{}^{*3} - (\psi + \sigma_1) \omega_1{}^* \right\}^2 + \left(\sigma_2 - \theta \omega_1{}^{*2} \right)^2 \right].$$

Since,

$$\text{Sign} \left[\frac{d(Re\lambda)}{d\tau_1} \right]_{\tau_1 = \hat{\tau}_1{}^0} = \text{Sign} \left[\frac{d(Re\lambda)}{d\tau_1} \right]_{\tau_1 = \hat{\tau}_1{}^0}^{-1}$$

$$= \text{Sign} \left\{ W_1 \left(\omega_1{}^*, \psi, \theta, \rho, r, \sigma_1, \sigma_2, \sigma_3 \right) \right\},$$

so, $\text{Sign} \left[\frac{d(Re\lambda)}{d\tau_1} \right]_{\tau_1 = \hat{\tau}_1{}^0} \neq 0$, as $W_1 \left(\omega_1{}^*, \psi, \theta, \rho, r, \sigma_1, \sigma_2, \sigma_3 \right) \neq 0$.

So, the transversality condition of (4.8) is satisfied. Thus, the following theorem can be obtained.

Theorem 4.1

Let $E_3 \left(X_1{}^*, Y_1{}^*, Z_1{}^* \right)$ be feasible and locally asymptotically stable without time delay. In the system (4.5), when among two delay parameters τ_1 and τ_2, only τ_1 exists positively and τ_2 does not exist, then $\exists \, \tau_1 = \hat{\tau}_1{}^0$, such that $E_3 \left(X_1{}^*, Y_1{}^*, Z_1{}^* \right)$ is locally asymptotically stable or unstable for $\tau_1 < \hat{\tau}_1{}^0$ or $\tau_1 > \hat{\tau}_1{}^0$ respectively. At $\tau_1 = \hat{\tau}_1{}^0$, There exists a Hopf-bifurcation, provided $W_1 \left(\omega_1{}^*, \psi, \theta, \rho, r, \sigma_1, \sigma_2, \sigma_3 \right) \neq 0$.

Case 3. $\tau_1 = 0$, $\tau_2 > 0$.

In this case, from (4.7) we get

$$\lambda^3 + (\theta + \rho)\lambda^2 + (r + \sigma_1)\lambda + (\psi\lambda + \sigma_2 + \sigma_3)e^{-\lambda\tau_2} = 0. \tag{4.11}$$

Let us consider the equation (4.11) has a root $i\omega_2$, where ω_2 is positive. Then we have

$$\omega_2{}^2\psi^2 sin^2\omega_2\tau_2 + (\sigma_2 + \sigma_3)^2 cos^2\omega_2\tau_2 + 2\omega_2\psi(\sigma_2 + \sigma_3)cos\omega_2\tau_2 sin\omega_2\tau_2 = \omega_2{}^4(\theta + \rho)^2, \tag{4.12}$$

and

$$\omega_2{}^2\psi^2 cos^2\omega_2\tau_2 + (\sigma_2 + \sigma_3)^2 sin^2\omega_2\tau_2 - 2\omega_2\psi(\sigma_2 + \sigma_3)sin\omega_2\tau_2 cos\omega_2\tau_2$$
$$= \omega_2{}^6 + (r + \sigma_1)^2\omega_2{}^2 - 2\omega_2{}^4(r + \sigma_1). \tag{4.13}$$

From (4.12) and (4.13), eliminating $sin(\omega_2\tau_2)$ and $cos(\omega_2\tau_2)$, we have

$$\omega_2{}^6 + \omega_2{}^4\left[(\theta + \rho))^2 - 2(r + \sigma_1)\right] + \omega_2{}^2\left[(r + \sigma_1)^2 - \psi^2\right] - (\sigma_2 + \sigma_3)^2 = 0. \tag{4.14}$$

Let $\omega_2{}^2 = \Omega_2$. Then we have

$$\Omega_2{}^3 + \Omega_2{}^2\left[(\theta + \rho)^2 - 2(r + \sigma_1)\right] + \Omega_2\left[(r + \sigma_1)^2 - \psi^2\right] - (\sigma_2 + \sigma_3)^2 = 0. \tag{4.15}$$

From the Routh-Hurtz criterion, we can conclude that the Equation (4.15) has always at least one positive root, say $\omega_2{}^*$.

Thus, we get

$$\hat{\tau}_2 = \frac{1}{\omega_2{}^*} \arctan\left[\frac{\omega_2{}^{*2}\psi(\theta + \rho) - \omega_2{}^{*2}(\sigma_2 + \sigma_3) + (r + \sigma_1)(\sigma_2 + \sigma_3)}{\omega_2{}^{*3}\psi - (r + \sigma_1)\omega_2{}^*\psi + \omega_2{}^*(\theta + \rho)(\sigma_2 + \sigma_3)}\right] + \frac{n\pi}{\omega_2{}^*}, n = 0, 1, 2, 3, ...$$

Choosing $n = 0$, we get the smallest value of $\hat{\tau}_2$ denoted by $\hat{\tau}_2{}^0$, where

$$\hat{\tau}_2{}^0 = \frac{1}{\omega_2{}^*} \arctan \left[\frac{\omega_2{}^{*2}\psi(\theta+\rho) - \omega_2{}^{*2}(\sigma_2+\sigma_3) + (r+\sigma_1)(\sigma_2+\sigma_3)}{\omega_2{}^{*3}\psi - (r+\sigma_1)\omega_2{}^*\psi + \omega_2{}^*(\theta+\rho)(\sigma_2+\sigma_3)} \right].$$

Now

$$\left(\frac{d\lambda}{d\tau_2}\right)^{-1} = -\frac{3\lambda^2 + 2(\theta+\rho)\lambda + (r+\sigma_1)}{\lambda\{\lambda^3 + (\theta+\rho)\lambda^2 + (r+\sigma_1)\lambda\}} + \frac{\psi}{\lambda(\psi\lambda + \sigma_2 + \sigma_3)} - \frac{\tau_2}{\lambda}.$$

Thus, finally we get

$$\left[\frac{d(Re\lambda)}{d\tau_2}\right]^{-1}_{\tau_2 = \hat{\tau}_2{}^0}$$

$$= Re \left(\frac{d\lambda}{d\tau_2}\right)^{-1}_{\tau_2 = \hat{\tau}_2{}^0}$$

$$= Re \left[-\frac{-3\omega_2{}^{*2} + 2(\theta+\rho)\omega_2{}^*i + (r+\sigma_1)}{i\omega_2{}^*\{-\omega_2{}^{*3}i - (\theta+\rho)\omega_2{}^{*2} + (r+\sigma_1)\omega_2{}^*i\}} + \frac{\psi}{i\omega_2{}^*(\psi\omega_2{}^*i + \sigma_2 + \sigma_3)} - \frac{\tau_2}{i\omega_2{}^*} \right]$$

$$= \frac{W_2(\omega_2{}^*, \psi, \theta, \rho, r, \sigma_1, \sigma_2, \sigma_3)}{\omega_2{}^{*2}\left[\{\omega_2{}^{*2} - (r+\sigma_1)\}^2 + (\theta+\rho)^2\omega_2{}^{*2}\right]\{\psi^2\omega_2{}^{*2} + (\sigma_2+\sigma_3)^2\}},$$

where

$$W_2(\omega_2{}^*, \psi\theta, \rho, r, \sigma_1, \sigma_2, \sigma_3) = 2\psi^2\omega_2{}^{*6} + \omega_2{}^{*4}\left[3(\sigma_2+\sigma_3)^2 - 2(r+\sigma_1)\psi^2 + (\theta+\rho)^2\psi^2\right]$$

$$+ \omega_2{}^{*2}\left[-4(r+\sigma_1)(\sigma_2+\sigma_3)^2 + 2(\theta+\rho)^2(\sigma_2+\sigma_3)^2\right] + (r+\sigma_1)^2(\sigma_2+\sigma_3)^2.$$

Since

$$\text{Sign}\left[\frac{d(Re\lambda)}{d\tau_2}\right]_{\tau_2 = \hat{\tau}_2{}^0} = \text{Sign}\left[\frac{d(Re\lambda)}{d\tau_2}\right]^{-1}_{\tau_2 = \hat{\tau}_2{}^0}$$

$$= \text{Sign}\{W_2(\omega_2{}^*, \psi, \theta, \rho, r, \sigma_1, \sigma_2, \sigma_3)\},$$

so, if $\{W_2(\omega_2{}^*, \psi, \theta, \rho, r, \sigma_1, \sigma_2, \sigma_3)\} \neq 0$, then $\text{Sign}\left[\frac{d(Re\lambda)}{d\tau_2}\right]_{\tau_2 = \hat{\tau}_2{}^0} \neq 0$,

which satisfies the transversality condition of (4.11).

The above discussions generate the following theorem.

Theorem 4.2

Let $E_3\left(X_1{}^*, Y_1{}^*, Z_1{}^*\right)$ be locally asymptotically stable when the feasibility conditions of the existence of $E_3\left(X_1{}^*, Y_1{}^*, Z_1{}^*\right)$ are satisfied and the delay parameters $\tau_1 = 0$ and $\tau_2 = 0$. In the system (4.5), when among two delay parameters τ_1 and τ_2, only τ_2 exists positively and τ_1 does not exist, then $\exists\ \tau_2 = \hat{\tau}_2{}^0$, such that $E_3\left(X_1{}^*, Y_1{}^*, Z_1{}^*\right)$ is locally asymptotically stable (or unstable) for $\tau_2 < \hat{\tau}_2{}^0$ (or $\tau_2 > \hat{\tau}_2{}^0$), and there exists a Hopf-bifurcation at $\tau_2 = \hat{\tau}_2{}^0$, provided $W_2\left(\omega_1{}^*, \psi, \theta, \rho, r, \sigma_1, \sigma_2, \sigma_3\right) \neq 0$.

Case 4. $\tau_1 = \tau_2 = \tau \neq 0$.

In this situation, the equation (4.7) becomes

$$\lambda^3 + \left(\theta + \rho e^{-\lambda\tau}\right)\lambda^2 + \left(\psi e^{-\lambda\tau} + r e^{-\lambda\tau} + \sigma_1\right)\lambda + \sigma_2 e^{-\lambda\tau} + \sigma_3 e^{-2\lambda\tau} = 0. \tag{4.16}$$

Multiplying by $e^{\lambda\tau}$, (4.16) becomes

$$e^{\lambda\tau}\lambda^3 + \left[\rho\lambda^2 + (\psi + r)\lambda + \sigma_2\right] + e^{-\lambda\tau}\sigma_3 + e^{\lambda\tau}\lambda\left(\lambda\theta + \sigma_1\right) = 0. \tag{4.17}$$

Putting $\lambda = i\omega_3\ (\omega_3 > 0)$, we get

$$sin\omega_3\tau\left(\omega_3{}^3 - \omega_3\sigma_1\right) + cos\omega_3\tau\left(\sigma_3 - \omega_3{}^2\theta\right) = \rho\omega_3{}^2 - \sigma_2,$$

and

$$-sin\omega_3\tau\left(\sigma_3 + \omega_3{}^2\theta\right) - cos\omega_3\tau\left(\omega_3{}^3 - \omega_3\sigma_1\right) = -\left(\phi + r\right)\omega_3, \tag{4.18}$$

which leads to

$$\omega_3{}^{12} + A_1\omega_3{}^{10} + B_1\omega_3{}^8 + C_1\omega_3{}^6 + D_1\omega_3{}^4 + E_1\omega_3{}^2 + F_1 = 0, \tag{4.19}$$

where

$A_1 = (-4\sigma_1 + 2\theta^2 - \rho^2),$

$B_1 = 6\sigma_1^2 + \theta^4 - 4\theta^2\sigma_1 + 2\rho^2\sigma_1 + 2\rho\sigma_2 - \rho^2\theta^2 - (\psi + r)^2,$

$C_1 = -2\sigma_3^2 + \sigma_1^2(2\theta^2 - \rho^2 - 4\sigma_1) - \sigma_2^2 - 4\rho\sigma_1\sigma_2 + (\psi + r)^2(2\sigma_1 - \theta^2)$
$\quad + 2\rho\theta(\sigma_2\theta - \rho\sigma_3) + 6\rho\sigma_3(\psi + r),$

$D_1 = \sigma_1^2(\sigma_1^2 + 2\rho\sigma_2) + \sigma_3^2(4\sigma_1 - 2\theta^2 - \rho^2) + \sigma_2^2(2\sigma_1 - \theta^2) - 4\sigma_3(\psi + r)(\rho\sigma_1 + \sigma_2)$
$\quad + 4\rho\sigma_2\sigma_3\theta + (\psi + r)^2(2\sigma_3\theta - \sigma_1^2),$

$E_1 = -2\sigma_1^2\sigma_3^2 - \sigma_1^2\sigma_2^2 - (\psi + r)^2\sigma_3^2 + 4\sigma_1\sigma_2\sigma_3(\psi + r) + 2\rho\sigma_2\sigma_3^2 - 2\sigma_2^2\sigma_3\theta,$

$F_1 = -\sigma_2^2\sigma_3^2 + \sigma_3^4.$

Let $\omega_3^2 = \Omega_3$. Then (4.19) becomes

$$\Omega_3^6 + A_1\Omega_3^5 + B_1\Omega_3^4 + C_1\Omega_3^3 + D_1\omega_3^2 + E_1\Omega_3 + F_1 = 0. \qquad (4.20)$$

The equation (4.20) possesses minimum one positive root if $F_1 < 0$. Let the root be ω_3^*.
Substituting ω_3^* into (4.18), we get

$$\hat{\tau}_3 = \frac{1}{\omega_3^*}\arccos\left[\frac{\left(\rho\omega_3^{*2} - \sigma_2\right)\left(\sigma_3 + \omega_3^{*2}\theta\right) - (\psi + r)\omega_3^{*2}\left(\omega_3^{*2} - \sigma_1\right)}{\left(\sigma_3 - \omega_3^{*2}\theta\right)\left(\sigma_3 + \omega_3^{*2}\theta\right) - \left(\omega_3^{*3} - \omega_3^*\sigma_1\right)^2}\right] + \frac{2n_1\pi}{\omega_3^*},$$

$\quad n_1 = 0, 1, 2, 3, ...$

If $n_1 = 0$, we get the smallest value of $\hat{\tau}_3$ denoted by $\hat{\tau}_3^{\,0}$, where

$$\hat{\tau}_3^{\,0} = \frac{1}{\omega_3^*}\arccos\left[\frac{\left(\rho\omega_3^{*2} - \sigma_2\right)\left(\sigma_3 + \omega_3^{*2}\theta\right) - (\psi + r)\omega_3^{*2}\left(\omega_3^{*2} - \sigma_1\right)}{\left(\sigma_3 - \omega_3^{*2}\theta\right)\left(\sigma_3 + \omega_3^{*2}\theta\right) - \left(\omega_3^{*3} - \omega_3^*\sigma_1\right)^2}\right].$$

Putting $\lambda = \mu_1 + iv_1$ in (4.16), we get

$$e^{\mu_1 \tau} cos v_1 \tau \left(\mu_1{}^3 - 3\mu_1 v_1{}^2\right) - e^{\mu_1 \tau} sin v_1 \tau \left(3\mu_1{}^2 v_1 - v_1{}^3\right) + \rho \left(\mu_1{}^2 - v_1{}^2\right) + \left(\psi + r\right) \mu_1$$

$$+\sigma_2 + e^{-\mu_1 \tau} \sigma_3 cos v_1 \tau + \left(\mu_1 e^{\mu_1 \tau} cos v_1 \tau - v_1 e^{\mu_1 \tau} sin v_1 \tau\right) \left(\mu_1 \theta + \sigma_1\right)$$

$$- \left(\mu_1 e^{\mu_1 \tau} sin v_1 \tau + v_1 e^{\mu_1 \tau} cos v_1 \tau\right) v_1 \theta = 0, \tag{4.21}$$

and

$$e^{\mu_1 \tau} cos v_1 \tau \left(3\mu_1{}^2 v_1 - v_1{}^3\right) + e^{\mu_1 \tau} sin v_1 \tau \left(\mu_1{}^3 - 3\mu_1 v_1{}^2\right) + 2\rho\mu_1 v_1 + \left(\psi + r\right) v_1$$

$$-e^{-\mu_1 \tau} \sigma_3 sin v_1 \tau + \left(\mu_1 e^{\mu_1 \tau} sin v_1 \tau + v_1 e^{\mu_1 \tau} cos v_1 \tau\right) \left(\mu_1 \theta + \sigma_1\right)$$

$$+ \left(\mu_1 e^{\mu_1 \tau} cos v_1 \tau - v_1 e^{\mu_1 \tau} sin v_1 \tau\right) v_1 \theta = 0. \tag{4.22}$$

When $\tau = \hat{\tau}_3{}^0$, $\mu_1(\hat{\tau}_3{}^0) = 0$ and $v_1 \neq 0$, from (4.21) and (4.22), we get

$$P_0 \left[\frac{d\mu_1}{d\tau}\right]_{\tau = \hat{\tau}_3{}^0} + Q_0 \left[\frac{dv_1}{d\tau}\right]_{\tau = \hat{\tau}_3} = R_0,$$

$$-Q_0 \left[\frac{d\mu_1}{d\tau}\right]_{\tau = \hat{\tau}_3{}^0} + P_0 \left[\frac{dv_1}{d\tau}\right]_{\tau = \hat{\tau}_3} = S_0, \tag{4.23}$$

where

$P_0 = -3v_1{}^2 cos v_1 \hat{\tau}_3{}^0 + v_1{}^3 \tau sin v_1 \hat{\tau}_3{}^0 + \left(\psi + r\right) - \sigma_3 \tau cos v_1 \hat{\tau}_3{}^0 - v_1 \theta sin v_1 \hat{\tau}_3{}^0$

$\qquad + \sigma_1 cos v_1 \hat{\tau}_3{}^0 - \sigma_1 v_1 \tau sin v_1 \hat{\tau}_3{}^0 - v_1 \theta sin v_1 \hat{\tau}_3{}^0 - v_1{}^2 \theta \tau cos v_1 \hat{\tau}_3{}^0,$

$Q_0 = 3v_1{}^2 sin v_1 \hat{\tau}_3{}^0 + v_1{}^3 \hat{\tau}_3{}^0 cos v_1 \hat{\tau}_3{}^0 - 2\rho v_1 - \sigma_3 \hat{\tau}_3{}^0 sin v_1 \hat{\tau}_3{}^0 - \sigma_1 v_1 \hat{\tau}_3{}^0 cos v_1 \hat{\tau}_3{}^0$

$\qquad - \sigma_1 sin v_1 \hat{\tau}_3{}^0 + v_1{}^2 \theta \hat{\tau}_3{}^0 sin v_1 \hat{\tau}_3{}^0 - 2v_1 \theta cos v_1 \hat{\tau}_3{}^0,$

$R_0 = -v_1{}^4 cos v_1 \hat{\tau}_3{}^0 + \sigma_3 v_1 sin v_1 \hat{\tau}_3{}^0 + \sigma_1 v_1{}^2 cos v_1 \hat{\tau}_3{}^0 - v_1{}^3 \theta sin v_1 \hat{\tau}_3{}^0,$

$S_0 = \sigma_3 v_1 cos v_1 \hat{\tau}_3{}^0 + \sigma_1 v_1{}^2 sin v_1 \hat{\tau}_3{}^0 + v_1{}^3 \theta cos v_1 \hat{\tau}_3{}^0 - v_1{}^4 sin v_1 \hat{\tau}_3{}^0.$

From (4.23), we get

$\left[\frac{d\mu_1}{d\tau}\right]_{\tau = \hat{\tau}_3{}^0} = \frac{P_0 R_0 - Q_0 S_0}{P_0{}^2 + Q_0{}^2}.$

Now if $P_0 R_0 - Q_0 S_0 \neq 0$, $\left[\frac{d\mu_1}{d\tau}\right]_{\tau=\hat{\tau}_3{}^0} \neq 0$, which is the required transversality condition of (4.16).

Thus, we can obtain the following theorem.

Theorem 4.3

Let $E_3\left(X_1{}^*, Y_1{}^*, Z_1{}^*\right)$ be locally asymptotically stable when the feasibility conditions of the existence of $E_3\left(X_1{}^*, Y_1{}^*, Z_1{}^*\right)$ are satisfied and the delay parameters $\tau_1 = 0$ and $\tau_2 = 0$. Then in the system (4.5), when both the delay parameters τ_1 and τ_2 exist positively and are equal such that $\tau_1 = \tau_2 = \tau$, then $\exists\, \tau = \hat{\tau}_3{}^0$, such that $E_3\left(X_1{}^*, Y_1{}^*, Z_1{}^*\right)$ is locally asymptotically stable (or unstable) for $\tau \in \left(0, \hat{\tau}_3{}^0\right)$ (or $\tau > \hat{\tau}_3{}^0$). Also, there exists a Hopf-bifurcation at $\tau = \hat{\tau}_3{}^0$, provided $P_0 R_0 - Q_0 S_0 \neq 0$.

Case 5. $\tau_1 > 0, \tau_2 \in \left[0, \hat{\tau}_2{}^0\right)$, and $\tau_1 \neq \tau_2$.

In this case, the characteristic equation (4.7) becomes

$$\lambda^3 + \theta\lambda^2 + \left(\psi e^{-\lambda\tau_2} + \sigma_1\right)\lambda + \sigma_2 e^{-\lambda\tau_2} + \left(\rho\lambda^2 + r\lambda + \sigma_3 e^{-\lambda\tau_2}\right) e^{-\lambda\tau_1} = 0. \tag{4.24}$$

Putting $\lambda = i\omega_4$ $(\omega_4 > 0)$ into (4.24), we get

$$sin\omega_4\tau_1\left(\omega_4 r - \sigma_3 sin\omega_4\tau_2\right) + cos\omega_4\tau_1\left(-\rho\omega_4{}^2 + \sigma_3 cos\omega_4\tau_2\right)$$
$$= \omega_4{}^2\theta - \sigma_2 cos\omega_4\tau_2 - \psi\omega_4 sin\omega_4\tau_2, \tag{4.25}$$

and

$$-sin\omega_4\tau_1\left(-\rho\omega_4{}^2 + \sigma_3 cos\omega_4\tau_2\right) + cos\omega_4\tau_1\left(\omega_4 r - \sigma_3 sin\omega_4\tau_2\right)$$
$$= \omega_4{}^3 - \omega_4\sigma_1 - \omega_4\psi cos\omega_4\tau_2 + \sigma_2 sin\omega_4\tau_2, \tag{4.26}$$

which leads to

$$\omega_4{}^6 + \omega_4{}^4 \left(\theta^2 - 2\sigma_1 - 2\psi cos\omega_4\tau_2 - \rho^2\right) + \omega_4{}^3 \left(-2\psi\theta sin\omega_4\tau_2 + 2\sigma_2 sin\omega_4\tau_2\right)$$

$$+\omega_4{}^2 \left(\psi^2 - 2\sigma_2\theta cos\omega_4\tau_2 + \sigma_1{}^2 + 2\sigma_1\psi cos\omega_4\tau_2 + 2\rho\sigma_3 cos\omega_4\tau_2 - r^2\right)$$

$$+\omega_4 \left(-2\sigma_1\sigma_2 sin\omega_4\tau_2 + 2\sigma_3 r sin\omega_4\tau_2\right) + \left(\sigma_2{}^2 - \sigma_3{}^2\right) = 0. \tag{4.27}$$

Without loss of generality, let the equation (4.27) has a positive solution for ω_4, say $\omega_4{}^*$.
Thus, we get

$$\overline{\tau_1} = \frac{1}{\omega_4{}^*} arctan \left[\frac{U_1}{V_1}\right] + \frac{n\pi}{\omega_4{}^*}, n = 0, 1, 2, 3, ...,$$

where

$$U_1 = \left(\omega_4{}^* r - \sigma_3 sin\omega_4{}^*\tau_2\right) \left(\omega_4{}^{*2}\theta - \sigma_2 cos\omega_4{}^*\tau_2 - \psi\omega_4{}^* sin\omega_4{}^*\tau_2\right) - \left(-\rho\omega_4{}^{*2} + \sigma_3 cos\omega_4{}^*\tau_2\right)$$

$$\left(\omega_4{}^{*3} - \omega_4{}^*\sigma_1 - \omega_4{}^*\psi cos\omega_4{}^*\tau_2 + \sigma_2 sin\omega_4{}^*\tau_2\right),$$

$$V_1 = \left(\omega_4{}^* r - \sigma_3 sin\omega_4{}^*\tau_2\right) \left(\omega_4{}^{*3} - \omega_4{}^*\sigma_1 - \omega_4{}^*\psi cos\omega_4{}^*\tau_2 + \sigma_2 sin\omega_4{}^*\tau_2\right)$$

$$+ \left(-\rho\omega_4{}^{*2} + \sigma_2 cos\omega_4{}^*\tau_2\right) \left(\omega_4{}^{*2}\theta - \sigma_2 cos\omega_4{}^*\tau_2 - \psi\omega_4{}^* sin\omega_4{}^*\tau_2\right).$$

Putting $n = 0$, we get the smallest value of $\overline{\tau_1}$, denoted by $\overline{\tau_1}^0$.
So,

$$\overline{\tau_1}^0 = \frac{1}{\omega_4{}^*} arctan \left[\frac{U_1}{V_1}\right].$$

Now putting $\lambda = \mu + iv$ into (4.24), we get

$$\mu^3 - 3\mu v^2 + \theta \left(\mu^2 - v^2\right) + \mu\psi e^{-\mu\tau_2} cos v\tau_2 + v\psi e^{-\mu\tau_2} sin v\tau_2 + \sigma_1\mu$$

$$+\sigma_2 e^{-\mu\tau_2} cos v\tau_2 + e^{-\mu\tau_1} cos v\tau_1 \left[\rho \left(\mu^2 - v^2\right) + r\mu + \sigma_3 e^{-\mu\tau_2} cos v\tau_2\right]$$

$$+e^{-\mu\tau_1} sin v\tau_1 \left[2\rho\mu v + rv - \sigma_3 e^{-\mu\tau_2} sin v\tau_2\right] = 0, \tag{4.28}$$

and

$$-v^3 + 3\mu^2 v + 2\theta\mu v + v\psi e^{-\mu\tau_2}cosv\tau_2 - \mu\psi e^{-\mu\tau_2}sinv\tau_2 + \sigma_1 v$$

$$-\sigma_2 e^{-\mu\tau_2}sinv\tau_2 - e^{-\mu\tau_1}sinv\tau_1\left[\rho\left(\mu^2 - v^2\right) + r\mu + \sigma_3 e^{-\mu\tau_2}cosv\tau_2\right]$$

$$+e^{-\mu\tau_1}cosv\tau_1\left[2\rho\mu v + rv - \sigma_3 e^{-\mu\tau_2}sinv\tau_2\right] = 0. \qquad (4.29)$$

Now differentiating (4.28) and (4.29) with respect to τ_1, and then putting $\tau_1 = \overline{\tau_1}^0$, $\mu(\overline{\tau_1}^0) = 0$, and $v \neq 0$, we get

$$P_2\left[\frac{d\mu}{d\tau_1}\right]_{\tau_1=\overline{\tau_1}^0} + Q_2\left[\frac{dv}{d\tau_1}\right]_{\tau_1=\overline{\tau_1}^0} = R_2,$$

$$-Q_2\left[\frac{d\mu}{d\tau_1}\right]_{\tau_1=\overline{\tau_1}^0} + P_2\left[\frac{dv}{d\tau_1}\right]_{\tau_1=\overline{\tau_1}^0} = S_2, \qquad (4.30)$$

where

$P_2 = -3v^2 + \psi cosv\tau_2 - \tau_2 v\psi sinv\tau_2 + \sigma_1 - \sigma_2\tau_2 cosv\tau_2 + rcosv\overline{\tau_1}^0 - \sigma_3\tau_2 cosv(\overline{\tau_1}^0 + \tau_2)$

$\qquad + \overline{\tau_1}^0\rho v^2 cosv\overline{\tau_1}^0 - \sigma_3\overline{\tau_1}^0 cosv(\overline{\tau_1}^0 + \tau_2) + 2\rho v sinv\overline{\tau_1}^0 - \overline{\tau_1}^0 rv sinv\overline{\tau_1}^0,$

$Q_2 = -2\theta v + \psi v\tau_2 cosv\tau_2 + psi sinv\tau_2 - \sigma_2\tau_2 sinv\tau_2 - 2\rho v cosv\overline{\tau_1}^0 - \sigma_3\tau_2 sinv(\overline{\tau_1}^0 + \tau_2)$

$\qquad + \overline{\tau_1}^0\rho v^2 sinv\overline{\tau_1}^0 + rsinv\overline{\tau_1}^0 + \overline{\tau_1}^0 rv cosv\overline{\tau_1}^0 - \sigma_3\overline{\tau_1}^0 sinv(\overline{\tau_1}^0 + \tau_2),$

$R_2 = vsinv\overline{\tau_1}^0\left(-\rho v^2 + \sigma_3 cosv\tau_2\right) - vcosv\overline{\tau_1}^0\left(rv - \sigma_3 sinv\tau_2\right),$

$S_2 = vcosv\overline{\tau_1}^0\left(-\rho v^2 + \sigma_3 cosv\tau_2\right) + vsinv\overline{\tau_1}^0\left(rv - \sigma_3 sinv\tau_2\right).$

From (4.30), we get

$\left[\frac{d\mu}{d\tau_1}\right]_{\tau_1=\overline{\tau_1}^0} = \frac{P_2 R_2 - Q_2 S_2}{P_2{}^2 + Q_2{}^2}.$

Now $\left[\frac{d\mu}{d\tau_1}\right]_{\tau_1=\overline{\tau_1}^0} \neq 0$, assuming $P_2 R_2 - Q_2 S_2 \neq 0$.

Therefore, we can obtain the following theorem.

Theorem 4.4

Let $E_3\left(X_1{}^*, Y_1{}^*, Z_1{}^*\right)$ be locally asymptotically stable when the feasibility conditions of the existence of $E_3\left(X_1{}^*, Y_1{}^*, Z_1{}^*\right)$ are satisfied and the delay parameters $\tau_1 = 0$ and $\tau_2 = 0$. In the system (4.5), when the delay parameter τ_1 exists positively and if we take τ_2 from the range in which τ_2 is stable i.e., $\tau_2 \in \left[0, \hat{\tau}_2{}^0\right)$, then $\exists\ \tau_1 = \overline{\tau}_1{}^0$, such that $E_3\left(X_1{}^*, Y_1{}^*, Z_1{}^*\right)$ is locally asymptotically stable (or unstable) when $\tau_1 < \overline{\tau}_1{}^0$ (or $\tau_1 > \overline{\tau}_1{}^0$). Also, there exists Hopf-bifurcation at $\tau_1 = \overline{\tau}_1{}^0$ around E_3, provided $P_2 R_2 - Q_2 S_2 \neq 0$.

Case 6. $\tau_2 > 0, \tau_1 \in \left[0, \hat{\tau}_1{}^0\right)$, and $\tau_1 \neq \tau_2$.

In this situation, the characteristic equation (4.7) becomes

$$\lambda^3 + \left(\theta + \rho e^{-\lambda \tau_1}\right)\lambda^2 + \left(re^{-\lambda \tau_1} + \sigma_1\right)\lambda + \left(\psi\lambda + \sigma_2 + \sigma_3 e^{-\lambda \tau_1}\right)e^{-\lambda \tau_2} = 0. \tag{4.31}$$

Putting $\lambda = i\omega_5\ (\omega_5 > 0)$, we get

$$sin\omega_5 \tau_2 \left(\omega_5 \psi - \sigma_3 sin\omega_5 \tau_1\right) + cos\omega_5 \tau_2 \left(\sigma_2 + \sigma_3 cos\omega_5 \tau_1\right)$$
$$= -\omega_5 r sin\omega_5 \tau_1 + \rho\omega_5{}^2 cos\omega_5 \tau_1 + \omega_5{}^2 \theta, \tag{4.32}$$

and

$$-sin\omega_5 \tau_2 \left(\sigma_2 + \sigma_3 cos\omega_5 \tau_1\right) + cos\omega_5 \tau_2 \left(\omega_5 \psi - \sigma_3 sin\omega_5 \tau_1\right)$$
$$= -\omega_5 r cos\omega_5 \tau_1 - \rho\omega_5{}^2 sin\omega_5 \tau_1 + \omega_5{}^3 - \omega_5 \sigma_1, \tag{4.33}$$

which leads to

$$\omega_5{}^6 + \omega_5{}^5\left(-2\rho sin\omega_5\tau_1\right) + \omega_5{}^4\left(\rho^2 + \theta^2 + 2\rho\theta cos\omega_5\tau_1 - 2\sigma_1 - 2rcos\omega_5\tau_1\right)$$

$$+\omega_5{}^3\left(2\rho\sigma_1 sin\omega_5\tau_1 - 2r\theta sin\omega_5\tau_1\right) + \omega_5{}^2\left(r^2 + \sigma_1{}^2 + 2\sigma_1 rcos\omega_5\tau_1 - \psi^2\right)$$

$$+\omega_5\left(2\sigma_3\psi sin\omega_5\tau_1\right) - \sigma_3{}^2 - \sigma_2{}^2 - 2\sigma_2\sigma_3 cos\omega_5\tau_1 = 0. \tag{4.34}$$

Without loss of generality, let the equation (4.34) has a positive solution for ω_5, say $\omega_5{}^*$. Thus, we get

$$\overline{\tau}_2 = \frac{1}{\omega_5{}^*}\arccos\left[\frac{U_2}{V_2}\right] + \frac{2n\pi}{\omega_4{}^*}, n = 0, 1, 2, 3, ...,$$

where

$$U_2 = \left(-\omega_5 r sin\omega_5\tau_1 + \rho\omega_5{}^2 cos\omega_5\tau_1 + \omega_5{}^2\theta\right)\left(\sigma_2 + \sigma_3 cos\omega_5\tau_1\right)$$

$$+ \left(-\omega_5 r cos\omega_5\tau_1 - \rho\omega_5{}^2 sin\omega_5\tau_1 + \omega_5{}^3 - \omega_5\sigma_1\right)\left(\omega_5\psi - \sigma_3 sin\omega_5\tau_1\right),$$

$$V_2 = \left(\sigma_2 + \sigma_3 cos\omega_5\tau_1\right)^2 + \left(\omega_5\psi - \sigma_3 sin\omega_5\tau_1\right)^2.$$

Putting $n = 0$, we get the smallest value of $\overline{\tau}_2$, say $\overline{\tau}_2{}^0$.

So,

$$\overline{\tau}_2{}^0 = \frac{1}{\omega_5{}^*}\arccos\left[\frac{U_2}{V_2}\right].$$

Now putting $\lambda = \mu_2 + iv_2$ into (4.31), and after some calculations, we can prove that

$$\left[\frac{d\mu}{d\tau_2}\right]_{\tau_2=\overline{\tau}_2{}^0} = \frac{P_3 R_3 - Q_3 S_3}{P_3{}^2 + Q_3{}^2}.$$

Now $\left[\frac{d\mu}{d\tau_2}\right]_{\tau_2=\overline{\tau}_2{}^0} \neq 0$ if $P_3 R_3 - Q_3 S_3 \neq 0$,

where

$$P_3 = -3v_2^2 + \psi cosv_2\overline{\tau}_2{}^0 - v_2\psi\overline{\tau}_2{}^0 sinv_2\overline{\tau}_2{}^0 + \sigma_1 - \sigma_2\overline{\tau}_2{}^0 cosv_2\overline{\tau}_2{}^0 + rcosv_2\tau_1 - \sigma_3\overline{\tau}_2{}^0 cosv_2(\tau_1 + \overline{\tau}_2{}^0)$$

$$+ \rho v_2{}^2\tau_1 cosv_2\tau_1 - \sigma_3\tau_1 cosv_2(\tau_1 + \overline{\tau}_2{}^0) + 2\rho v_2 sinv_2\tau_1 - rv_2\tau_1 sinv_2\tau_1,$$

$$Q_3 = -2\theta v_2 + \psi v_2\overline{\tau}_2{}^0 cosv_2\overline{\tau}_2{}^0 + \psi sinv_2\overline{\tau}_2{}^0 - \sigma_2\overline{\tau}_2{}^0 sinv_2\overline{\tau}_2{}^0 - 2\rho v_2 cosv_2\tau_1 - \sigma_3\overline{\tau}_2{}^0 sinv_2(\tau_1 + \overline{\tau}_2{}^0)$$

$$+ \rho v_2{}^2\tau_1 sinv_2\tau_1 - \sigma_3\tau_1 sinv_2(\tau_1 + \overline{\tau}_2{}^0) + rsinv_2\tau_1 + rv_2\tau_1 cosv_2\tau_1,$$

$$R_3 = -\psi v_2{}^2 cosv_2\overline{\tau}_2{}^0 + \sigma_2 v_2 sinv_2\overline{\tau}_2{}^0 + \sigma_3 v_2 sinv_2(\tau_1 + \overline{\tau}_2{}^0),$$

$$S_3 = v_2{}^2 \psi sinv_2 \overline{\tau_2}^0 + \sigma_2 v_2 cosv_2 \overline{\tau_2}^0 + \sigma_3 v_2 cosv_2(\tau_1 + \overline{\tau_2}^0).$$

Therefore, we can have the theorem stated below.

Theorem 4.5

Let $E_3\left(X_1{}^*, Y_1{}^*, Z_1{}^*\right)$ be locally asymptotically stable when the feasibility conditions of the existence of $E_3\left(X_1{}^*, Y_1{}^*, Z_1{}^*\right)$ are satisfied and the delay parameters $\tau_1 = 0$ and $\tau_2 = 0$. In the system (4.5), when the delay parameter τ_2 exists positively, and if we take τ_1 from the range in which τ_1 is stable i.e., $\tau_1 \in \left[0, \hat{\tau_1}^0\right)$, then $\exists \ \tau_2 = \overline{\tau_2}^0$, such that $E_3\left(X_1{}^*, Y_1{}^*, Z_1{}^*\right)$ is locally asymptotically stable (or unstable) when $\tau_2 < \overline{\tau_2}^0$ (or $\tau_2 > \overline{\tau_2}^0$). Also, there exists a Hopf-bifurcation at $\tau_2 = \overline{\tau_2}^0$, provided $P_3 R_3 - Q_3 S_3 \neq 0$.

4.7 Simulation results

This section carries some numerical simulations using MATLAB-R $2016a$ to establish our theoretical findings. Here, we take the parameters values as follows: $\alpha = 5, \eta = 0.4, \xi = 0.92$, $\beta = 0.2$, $\phi = 1.005$, $\gamma = 0.3$, $\sigma = 1$. Then we get a locally asymptotically stable system around $E_3(24.0051, 5.3033, 1.0486)$ without time lag, as all the conditions of the Routh Hurtz Criterion are satisfied. Figures 4.1 and 4.2 show the same.

For case 2, we have got the values of $\omega_1{}^* = 0.1318$ and $\hat{\tau_1}^0 = 3.4082$, when $\tau_1 > 0$ and $\tau_2 = 0$. It is seen that, $E_3(24.0051, 5.3033, 1.0486)$ is locally stable or unstable according to the conditions $\tau_1 < \hat{\tau_1}^0$ or $\tau_1 > \hat{\tau_1}^0$. Also, at $\tau_1 = \hat{\tau_1}^0$, a Hopf-bifurcation is noticed around $E_3(24.0051, 5.3033, 1.0486)$. Figures 4.3 and 4.4 show that, the system (4.5) is stable for $\tau_1 = 3.2(< \hat{\tau_1}^0 = 3.4082)$ and $\tau_2 = 0$. Figures 4.5 and 4.6 portray that, the system (4.5) is unstable when $\tau_1 = 3.6(> \hat{\tau_1}^0 = 3.4082)$ and $\tau_2 = 0$, whereas, Figures 4.7 and 4.8 show a clear picture of the existence of Hopf-bifurcation at $\tau_1 = \hat{\tau_1}^0 = 3.4082$ and $\tau_2 = 0$.
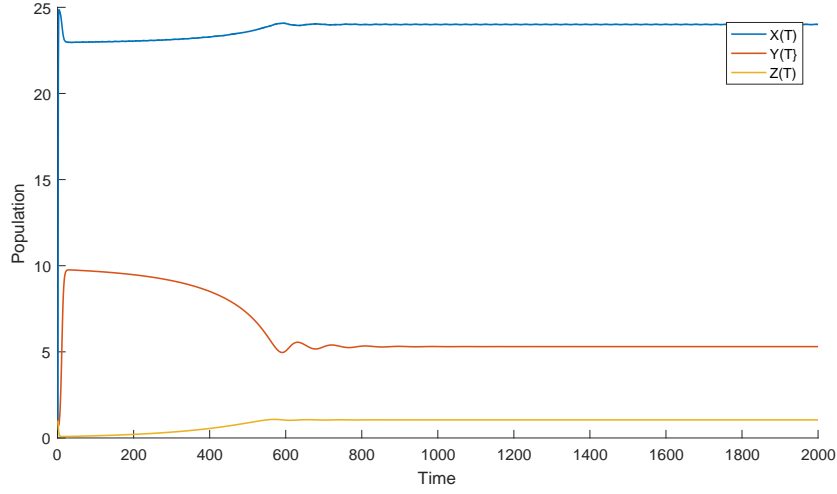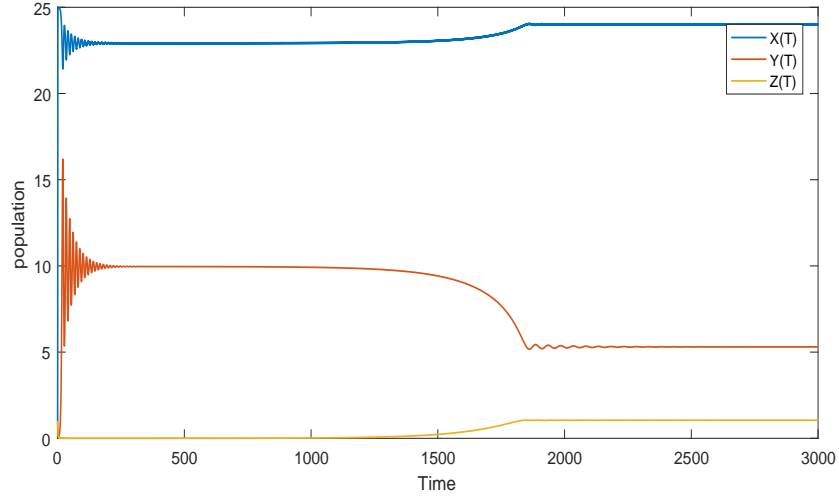
Figure 4.1: Time evolution of the system (4.5), when $\alpha = 5$, $\eta = 0.4$, $\xi = 0.92$, $\beta = 0.2$, $\phi = 1.005$, $\sigma = 1$, $\gamma = 0.3$, $\tau_1 = 0$, and $\tau_2 = 0$.
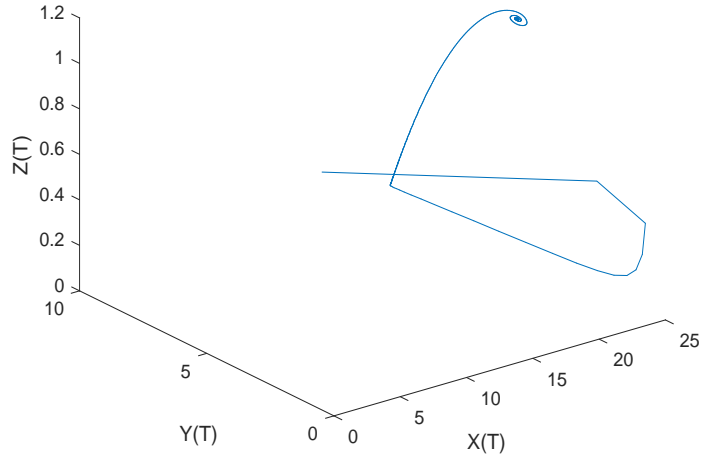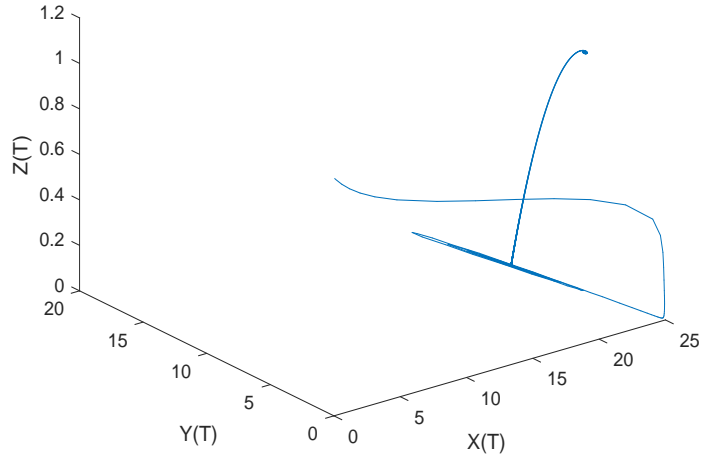

Figure 4.2: Trajectory of the system (4.5) in the phase plane for $\alpha = 5$, $\eta = 0.4$, $\xi = 0.92$, $\beta = 0.2$, $\phi = 1.005$, $\gamma = 0.3$, $\sigma = 1$, $\tau_1 = 0$, and $\tau_2 = 0$.

For case 3, we calculate $\omega_2^* = 0.0707$ and $\hat{\tau}_2^0 = 4.1152$ when $\tau_1 = 0$ and $\tau_2 > 0$. From Figures 4.9, 4.10, 4.11, and 4.12, it is seen that, $E_3(24.0051, 5.3033, 1.0486)$ is asymptotically stable when $\tau_2 = 3.8 (< \hat{\tau}_2^0 = 4.1152)$, and unstable when $\tau_2 = 4.4 (> \hat{\tau}_2^0 = 4.1152)$. Figures 4.13 and 4.14 illustrate about the Hopf-bifurcation at $\tau_2 = \hat{\tau}_2^0 = 4.1152$.
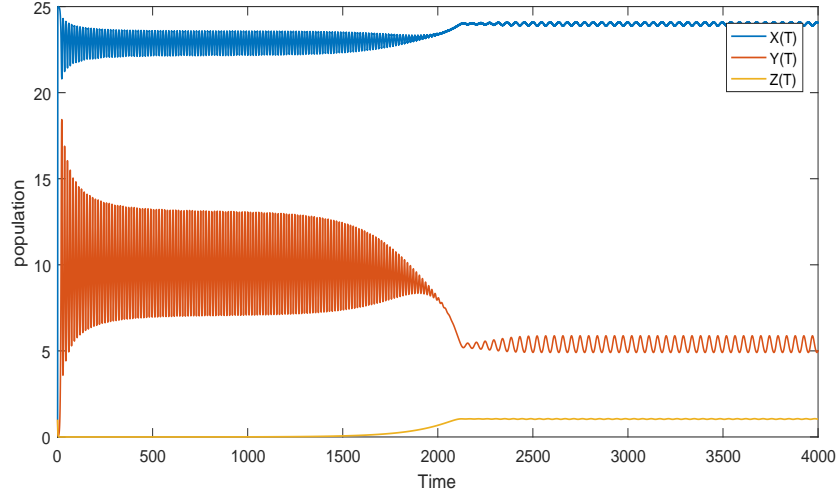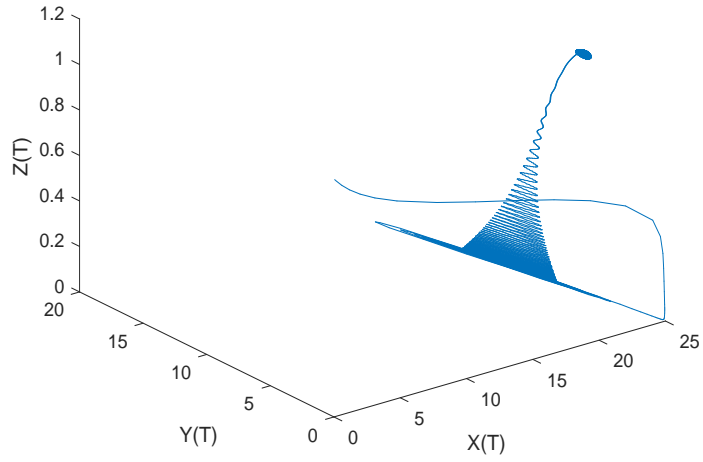
Figure 4.3: Time evolution of the system (4.5) for $\alpha = 5$, $\eta = 0.4$, $\xi = 0.92$, $\beta = 0.2$, $\phi = 1.005$, $\gamma = 0.3$, $\sigma = 1$, $\tau_1 = 3.2(< \hat{\tau}_1{}^0 = 3.4082)$, and $\tau_2 = 0$.

Figure 4.4: Trajectory of the system (4.5) in the phase plane for $\alpha = 5$, $\eta = 0.4$, $\xi = 0.92$, $\beta = 0.2$, $\phi = 1.005$, $\gamma = 0.3$, $\sigma = 1$, $\tau_1 = 3.2(< \hat{\tau}_1{}^0 = 3.4082)$, and $\tau_2 = 0$.

For case 4, when $\tau_1 \neq 0$, $\tau_2 \neq 0$, and $\tau_1 = \tau_2 = \tau$, we find the value of $\omega_3{}^* = 0.1049$ and $\hat{\tau}_3{}^0 = 2.5880$. From Figures 4.15, 4.16, 4.17, 4.18, 4.19, and 4.20, it has been depicted that, the system (4.5) is stable if $\tau = 2.3(< \hat{\tau}_3{}^0 = 2.5880)$, unstable if $\tau = 2.9(> \hat{\tau}_3{}^0 = 2.5880)$, and undergoes a Hopf-bifurcation when $\tau = \hat{\tau}_3{}^0 = 2.5880$ respectively.
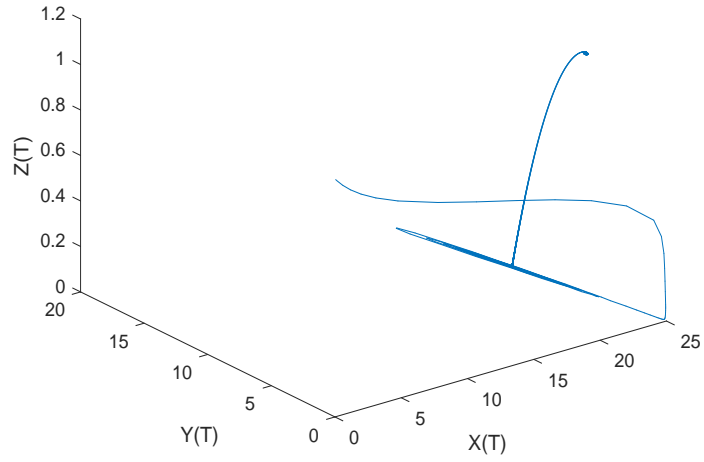
Figure 4.5: Time evolution of the system (4.5) for $\alpha = 5$, $\eta = 0.4$, $\xi = 0.92$, $\beta = 0.2$, $\phi = 1.005$, $\gamma = 0.3$, $\sigma = 1$, $\tau_1 = 3.6(> \hat{\tau_1}^0 = 3.4082)$, and $\tau_2 = 0$.
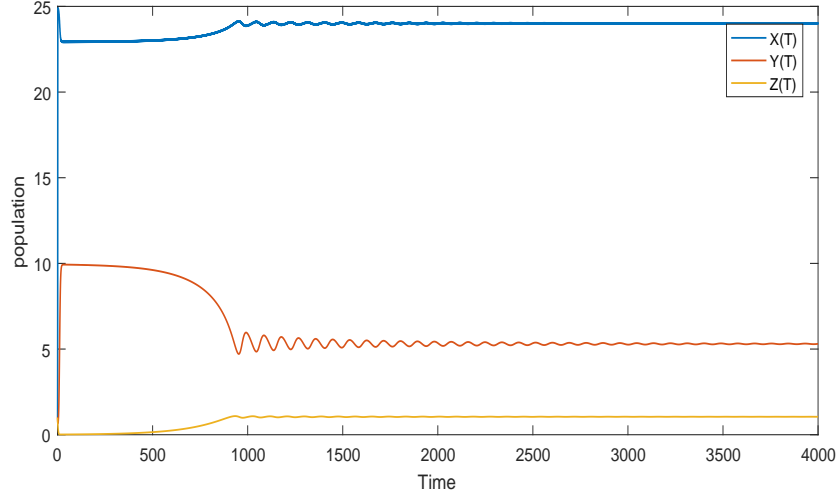

Figure 4.6: Trajectory of the system (4.5) in the phase plane for $\alpha = 5$, $\eta = 0.4$, $\xi = 0.92$, $\beta = 0.2$, $\phi = 1.005$, $\gamma = 0.3$, $\sigma = 1$, $\tau_1 = 3.6(> \hat{\tau_1}^0 = 3.4082)$, and $\tau_2 = 0$.
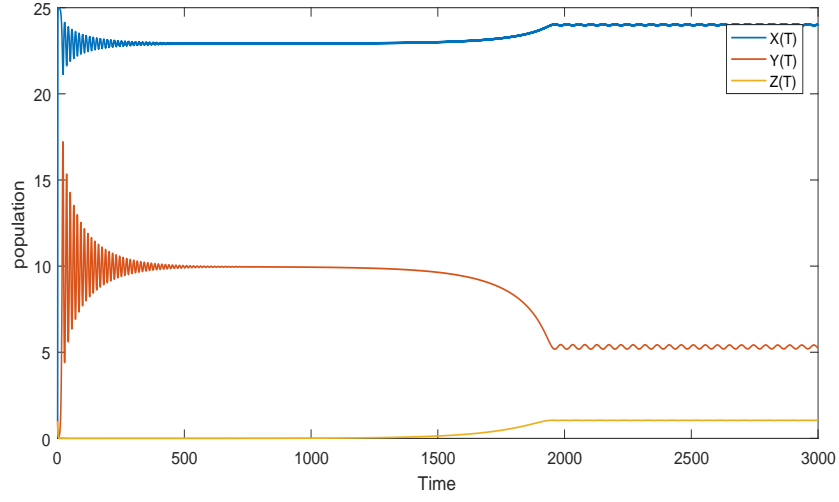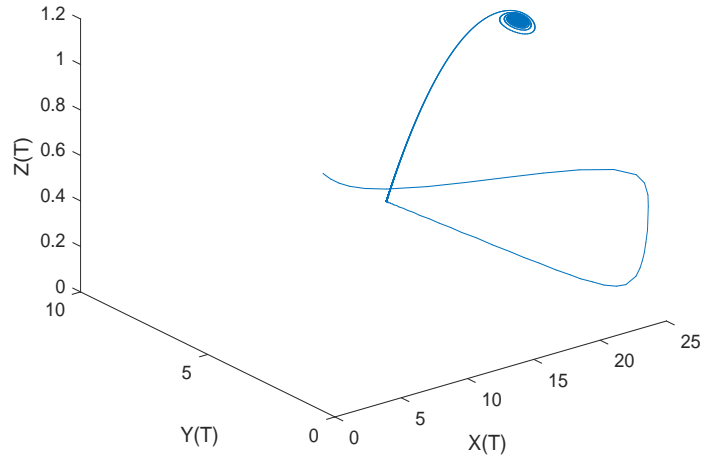
Figure 4.7: Time evolution of the system (4.5) for $\alpha = 5$, $\eta = 0.4$, $\xi = 0.92$, $\beta = 0.2$, $\phi = 1.005$, $\gamma = 0.3$, $\sigma = 1$, $\tau_1 = \hat{\tau}_1{}^0 = 3.4082$, and $\tau_2 = 0$.

Figure 4.8: Trajectory of the system (4.5) in the phase plane for $\alpha = 5$, $\eta = 0.4$, $\xi = 0.92$, $\beta = 0.2$, $\phi = 1.005$, $\gamma = 0.3$, $\sigma = 1$, $\tau_1 = \hat{\tau}_1{}^0 = 3.4082$, and $\tau_2 = 0$.
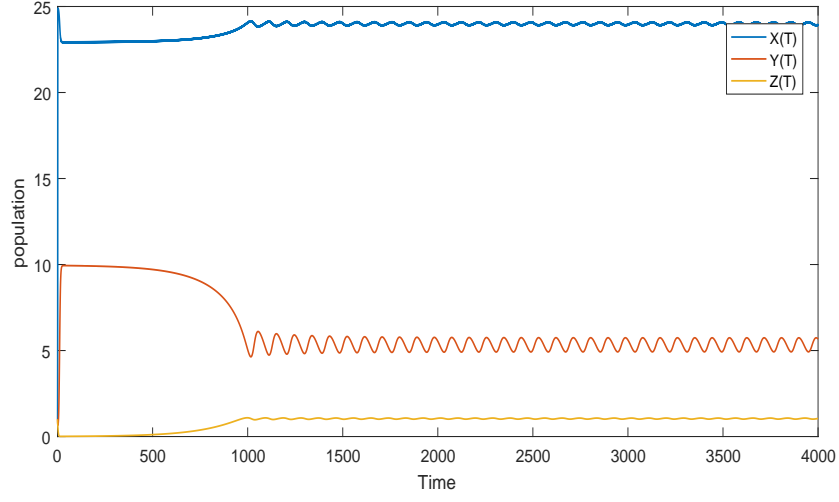
Figure 4.9: Time evolution of the system (4.5) for $\alpha = 5$, $\eta = 0.4$, $\xi = 0.92$, $\beta = 0.2$, $\phi = 1.005$, $\gamma = 0.3$, $\sigma = 1$, $\tau_2 = 3.8(< \hat{\tau}_2{}^0 = 4.1152)$, and $\tau_1 = 0$.

Figure 4.10: Trajectory of the system (4.5) in the phase plane $\alpha = 5$, $\eta = 0.4$, $\xi = 0.92$, $\beta = 0.2$, $\phi = 1.005$, $\gamma = 0.3$, $\sigma = 1$, $\tau_2 = 3.8(< \hat{\tau}_2{}^0 = 4.1152)$, and $\tau_1 = 0$.
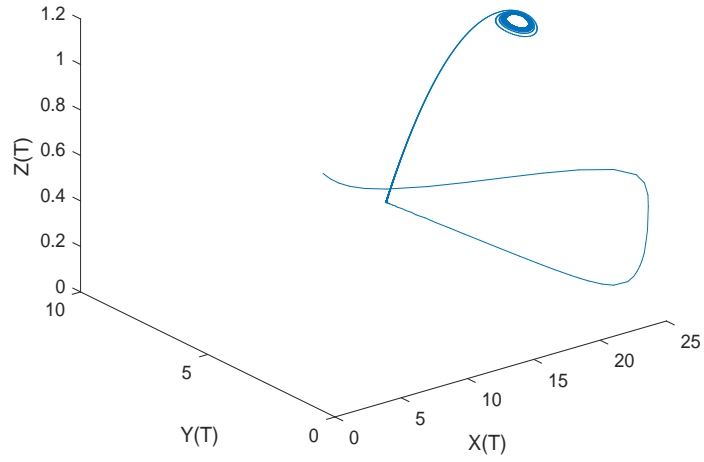
Figure 4.11: Time evolution of the system (4.5) for $\alpha = 5$, $\eta = 0.4$, $\xi = 0.92$, $\beta = 0.2$, $\phi = 1.005$, $\gamma = 0.3$, $\sigma = 1$, $\tau_2 = 4.4 (> \hat{\tau}_2^{\ 0} = 4.1152)$, and $\tau_1 = 0$.
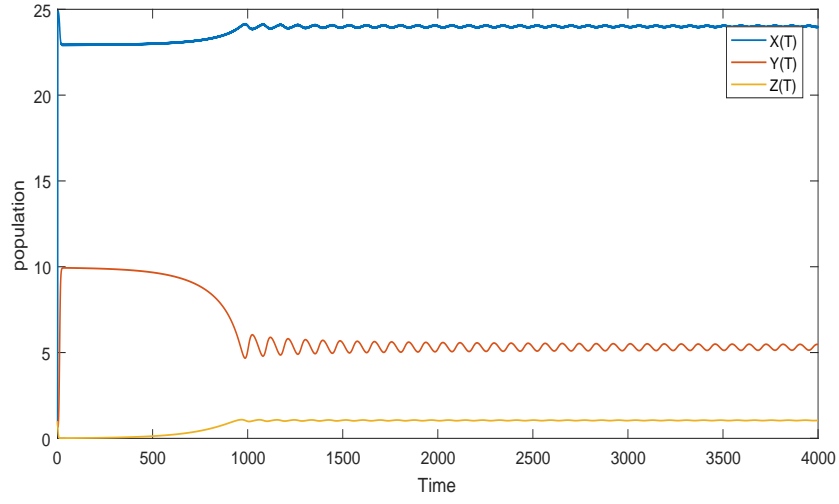

Figure 4.12: Trajectory of the system (4.5) in the phase plane for $\alpha = 5$, $\eta = 0.4$, $\xi = 0.92$, $\beta = 0.2$, $\phi = 1.005$, $\gamma = 0.3$, $\sigma = 1$, $\tau_2 = 4.4 (> \hat{\tau}_2^{\ 0} = 4.1152)$, and $\tau_1 = 0$.

Figure 4.13: Time evolution of the system (4.5) for $\alpha = 5$, $\eta = 0.4$, $\xi = 0.92$, $\beta = 0.2$, $\phi = 1.005$, $\gamma = 0.3$, $\sigma = 1$, $\tau_2 = \hat{\tau}_2{}^0 = 4.1152$, and $\tau_1 = 0$.

Figure 4.14: Trajectory of the system (4.5) in the phase plane for $\alpha = 5$, $\eta = 0.4$, $\xi = 0.92$, $\beta = 0.2$, $\phi = 1.005$, $\gamma = 0.3$, $\sigma = 1$, $\tau_2 = \hat{\tau}_2{}^0 = 4.1152$, and $\tau_1 = 0$.
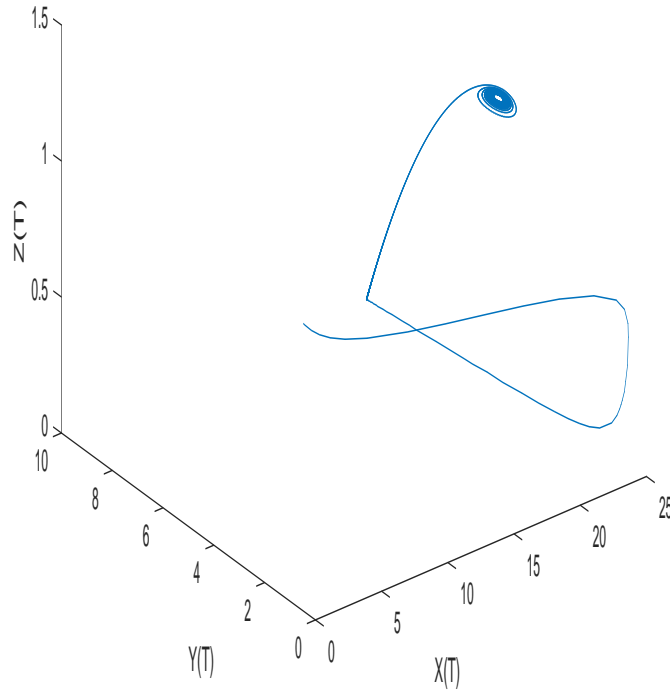
Figure 4.15: Time evolution of the system (4.5) for $\alpha = 5$, $\eta = 0.4$, $\xi = 0.92$, $\beta = 0.2$, $\phi = 1.005$, $\gamma = 0.3$, $\sigma = 1$, and $\tau_1 = \tau_2 = \tau = 2.3 (< \hat{\tau_3}^0 = 2.5880)$.

Figure 4.16: Trajectory of the system (4.5) in the phase plane for $\alpha = 5$, $\eta = 0.4$, $\xi = 0.92$, $\beta = 0.2$, $\phi = 1.005$, $\gamma = 0.3$, $\sigma = 1$, and $\tau_1 = \tau_2 = \tau = 2.3 (< \hat{\tau_3}^0 = 2.5880)$.

84
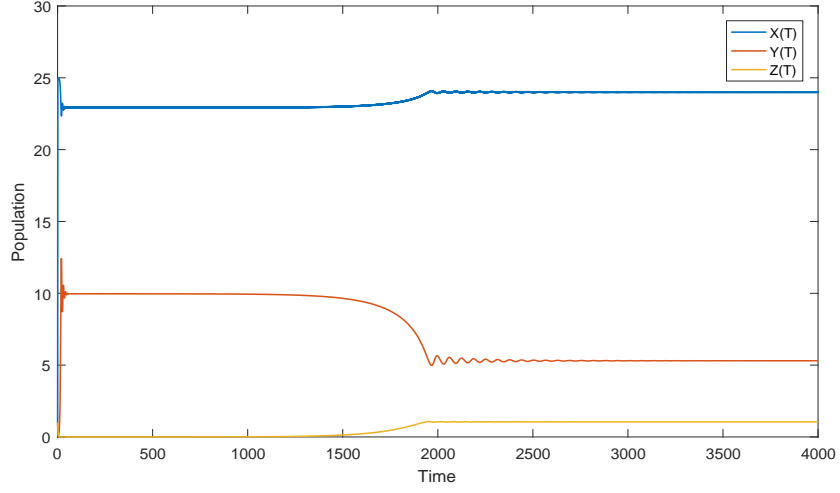
Figure 4.17: Time evolution of the system (4.5) for $\alpha = 5$, $\eta = 0.4$, $\xi = 0.92$, $\beta = 0.2$, $\phi = 1.005$, $\gamma = 0.3$, $\sigma = 1$, and $\tau_1 = \tau_2 = \tau = 2.9 (> \hat{\tau_3}^0 = 2.5880)$.
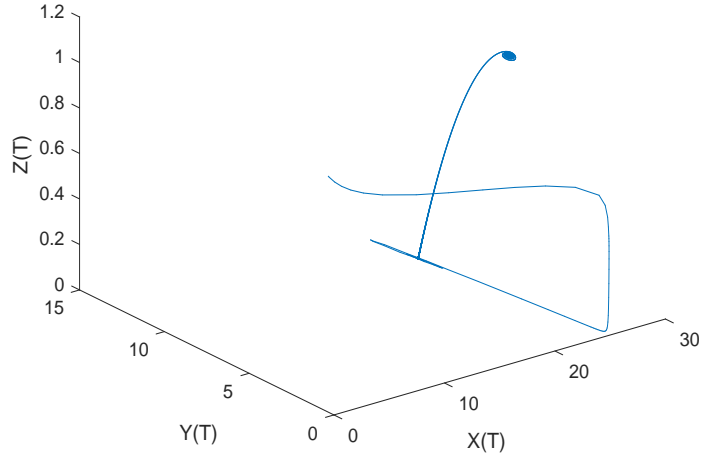

Figure 4.18: Trajectory of the system (4.5) in the phase plane for $\alpha = 5$, $\eta = 0.4$, $\xi = 0.92$, $\beta = 0.2$, $\phi = 1.005$, $\gamma = 0.3$, $\sigma = 1$, and $\tau_1 = \tau_2 = \tau = 2.9 (> \hat{\tau_3}^0 = 2.5880)$.
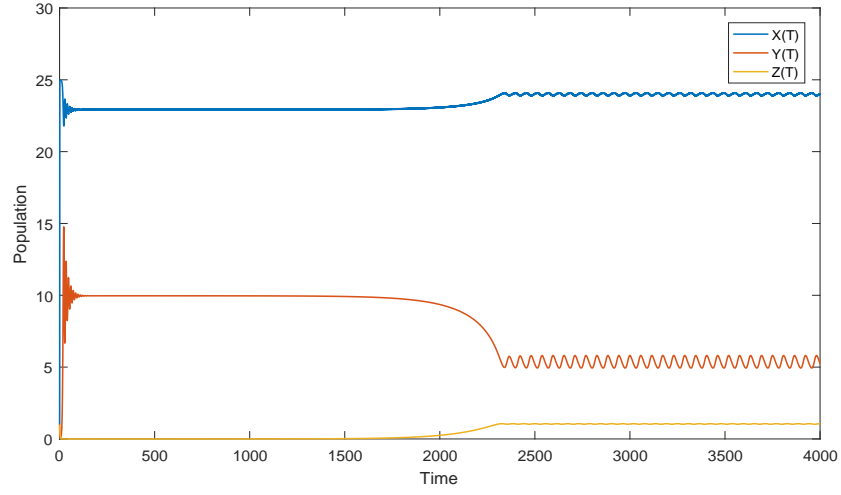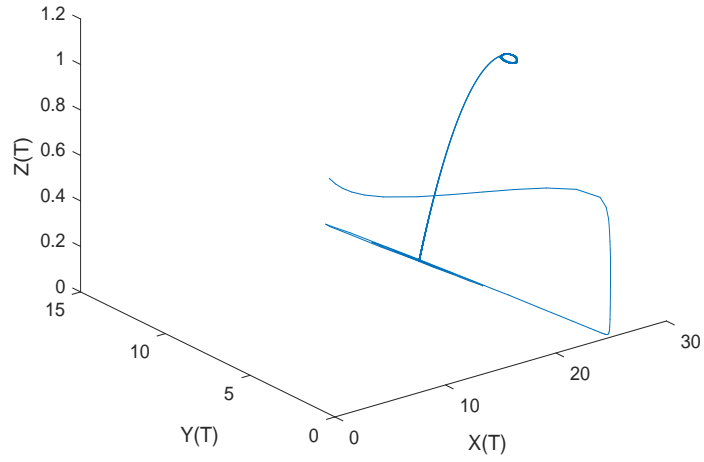
85

Figure 4.19: Time evolution of the system (4.5) for $\alpha = 5$, $\eta = 0.4$, $\xi = 0.92$, $\beta = 0.2$, $\phi = 1.005$, $\gamma = 0.3$, $\sigma = 1$, and $\tau_1 = \tau_2 = \tau = \hat{\tau}_3{}^0 = 2.5880$.

Figure 4.20: Trajectory of the system (4.5) in the phase plane for $\alpha = 5$, $\eta = 0.4$, $\xi = 0.92$, $\beta = 0.2$, $\phi = 1.005$, $\gamma = 0.3$, $\sigma = 1$, and $\tau_1 = \tau_2 = \tau = \hat{\tau}_3{}^0 = 2.5880$.

For case 5, when $\tau_1 \neq \tau_2 \neq 0$, we vary τ_1 and keep the value of τ_2 in its stable range $(0, 4.1152)$. We take $\tau_2 = 1.5$ and get the value of $\omega_4{}^* = 0.1177$ and $\overline{\tau}_1{}^0 = 3.3087$. From Figures 4.21, 4.22, 4.23, 4.24, 4.25, and 4.26, it has been verified that the system (4.5)

is stable when $\tau_1 = 2.9 (< \bar{\tau}_1{}^0 = 3.3087)$, unstable when $\tau_1 = 3.6 (> \bar{\tau}_1{}^0 = 3.3087)$, and experience a Hopf-bifurcation at $\tau_1 = \bar{\tau}_1{}^0 = 3.3087$.

Similarly, for case 6, we vary τ_2, and take the value of τ_1 in its stable range $(0, 3.4082)$. We

Figure 4.21: Time evolution of the system (4.5) for $\alpha = 5$, $\eta = 0.4$, $\xi = 0.92$, $\beta = 0.2$, $\phi = 1.005$, $\gamma = 0.3$, $\sigma = 1$, $\tau_1 = 2.9 (< \bar{\tau}_1{}^0 = 3.3087)$, and $\tau_2 = 1.5$.
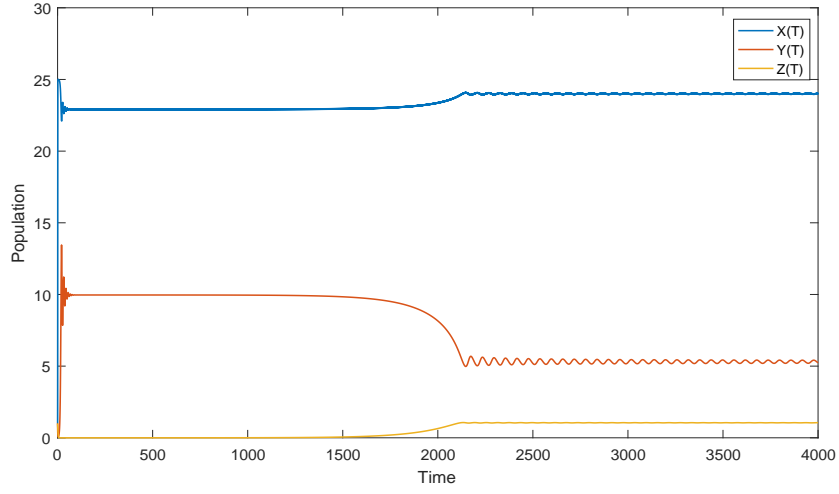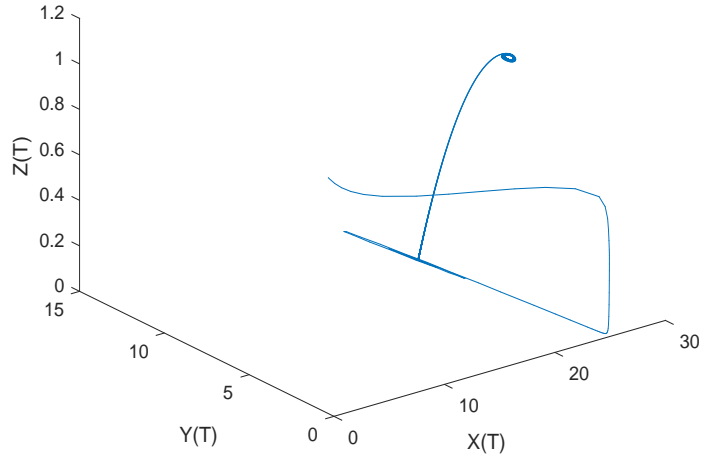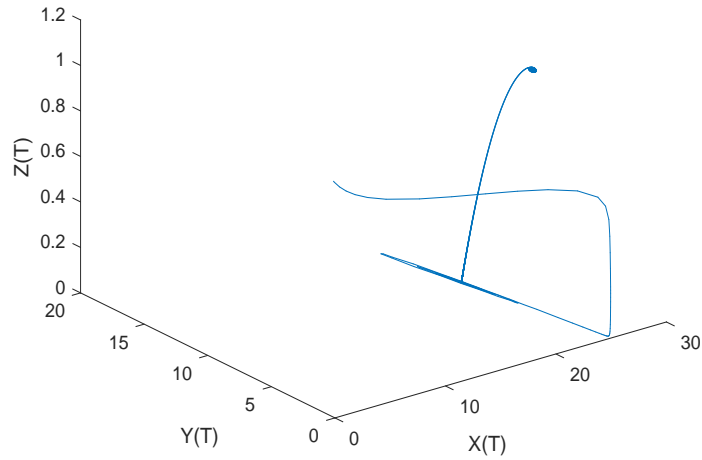

Figure 4.22: Trajectory of the system (4.5) in the phase plane for $\alpha = 5$, $\eta = 0.4$, $\xi = 0.92$, $\beta = 0.2$, $\phi = 1.005$, $\gamma = 0.3$, $\sigma = 1$, $\tau_1 = 2.9 (< \bar{\tau}_1{}^0 = 3.3087)$, and $\tau_2 = 1.5$.
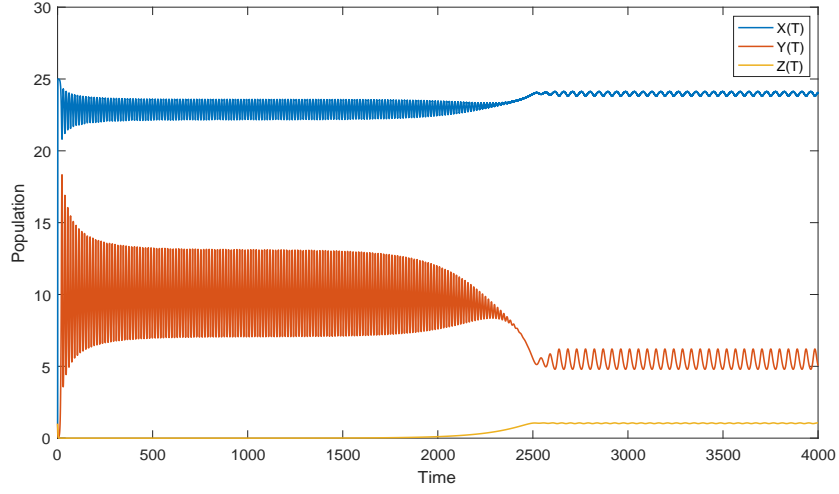
Figure 4.23: Time evolution of the system (4.5) for $\alpha = 5$, $\eta = 0.4$, $\xi = 0.92$, $\beta = 0.2$, $\phi = 1.005$, $\gamma = 0.3$, $\sigma = 1$, $\tau_1 = 3.6(> \overline{\tau_1}^0 = 3.3087)$, and $\tau_2 = 1.5$.

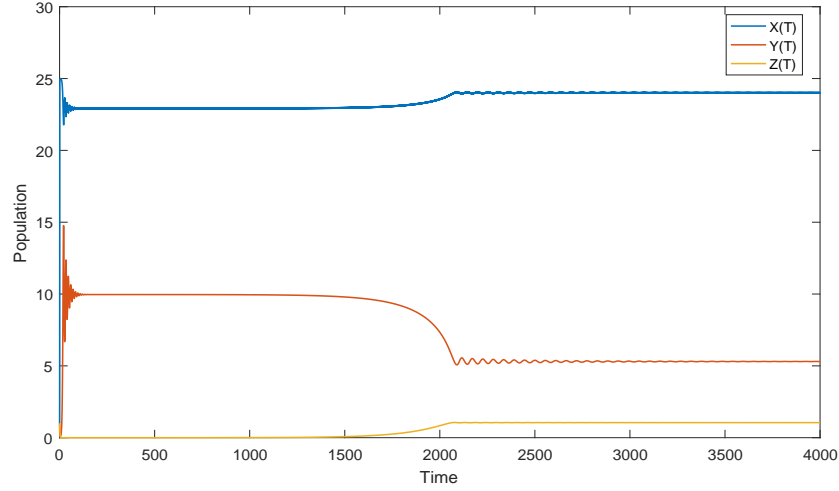**Figure 4.24:** Trajectory of the system (4.5) in the phase plane for $\alpha = 5$, $\eta = 0.4$, $\xi = 0.92$, $\beta = 0.2$, $\phi = 1.005$, $\gamma = 0.3$, $\sigma = 1$, $\tau_1 = 3.6(> \overline{\tau_1}^0 = 3.3087)$, and $\tau_2 = 1.5$.

assume $\tau_1 = 1$, and get $\omega_5{}^* = 0.0794$ and $\overline{\tau_2}^0 = 3.9264$. Figures 4.27, 4.28, 4.29, 4.30, 4.31, and 4.32 show that the system (4.5) is stable if $\tau_2 = 3.6(< \overline{\tau_2}^0 = 3.9264)$, possesses oscillatory behavior if $\tau_2 = 4.3(> \overline{\tau_2}^0 = 3.9264)$, and have Hopf-bifurcation at $\tau_2 = \overline{\tau_2}^0 = 3.9264$.

Figure 4.25: Time evolution of the system (4.5) for $\alpha = 5$, $\eta = 0.4$, $\xi = 0.92$, $\beta = 0.2$, $\phi = 1.005$, $\gamma = 0.3$, $\sigma = 1$, $\tau_1 = \overline{\tau_1}^0 = 3.3087$, and $\tau_2 = 1.5$.

Figure 4.26: Trajectory of the system (4.5) in the phase plane for $\alpha = 5$, $\eta = 0.4$, $\xi = 0.92$, $\beta = 0.2$, $\phi = 1.005$, $\gamma = 0.3$, $\sigma = 1$, $\tau_1 = \overline{\tau_1}^0 = 3.3087$, and $\tau_2 = 1.5$.

89
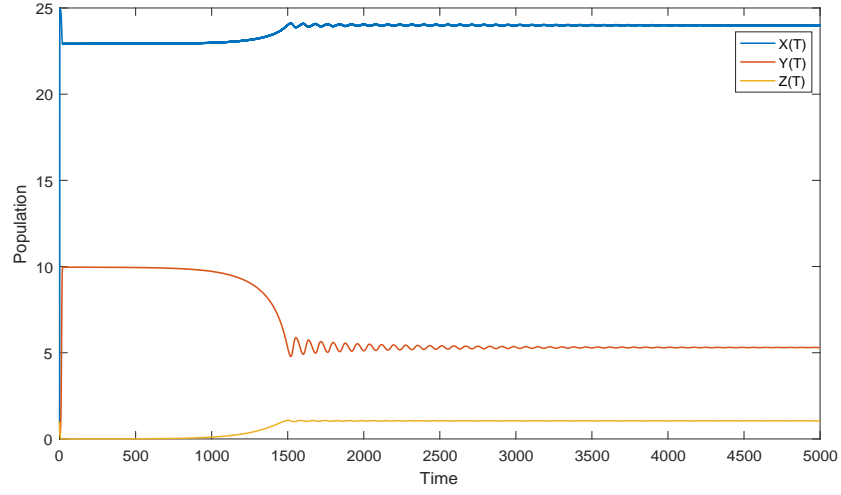
Figure 4.27: Time evolution of the system (4.5) for $\alpha = 5$, $\eta = 0.4$, $\xi = 0.92$, $\beta = 0.2$, $\phi = 1.005$, $\gamma = 0.3$, $\sigma = 1$, $\tau_2 = 3.6 (< \overline{\tau_2}^0 = 3.9264)$, and $\tau_1 = 1$.
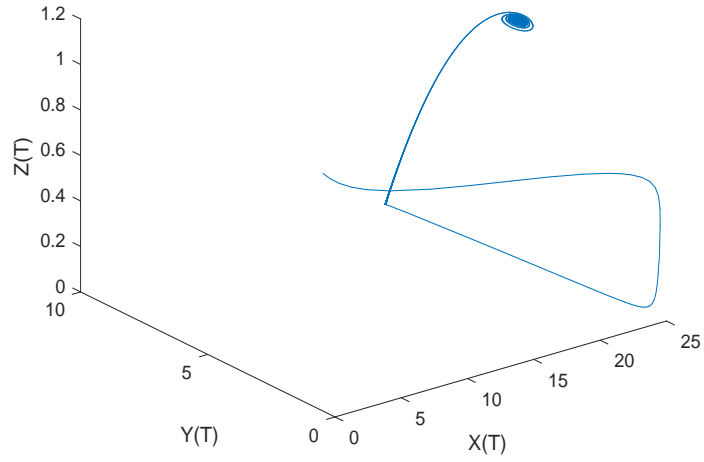
Figure 4.28: Trajectory of the system (4.5) in the phase plane for $\alpha = 5$, $\eta = 0.4$, $\xi = 0.92$, $\beta = 0.2$, $\phi = 1.005$, $\gamma = 0.3$, $\sigma = 1$, $\tau_2 = 3.6 (< \overline{\tau_2}^0 = 3.9264)$, and $\tau_1 = 1$.
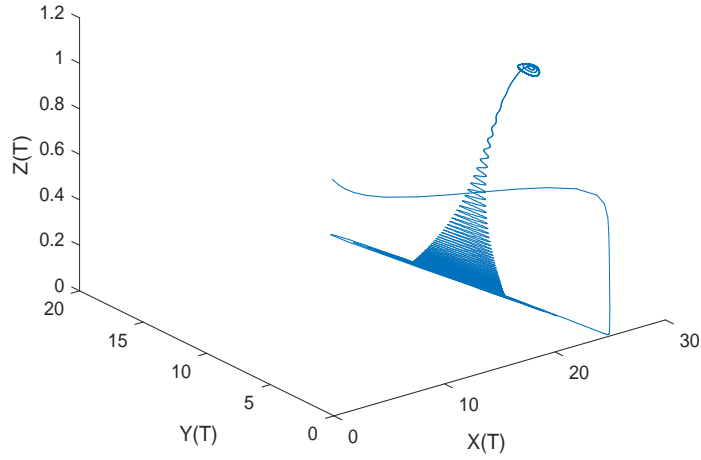
90
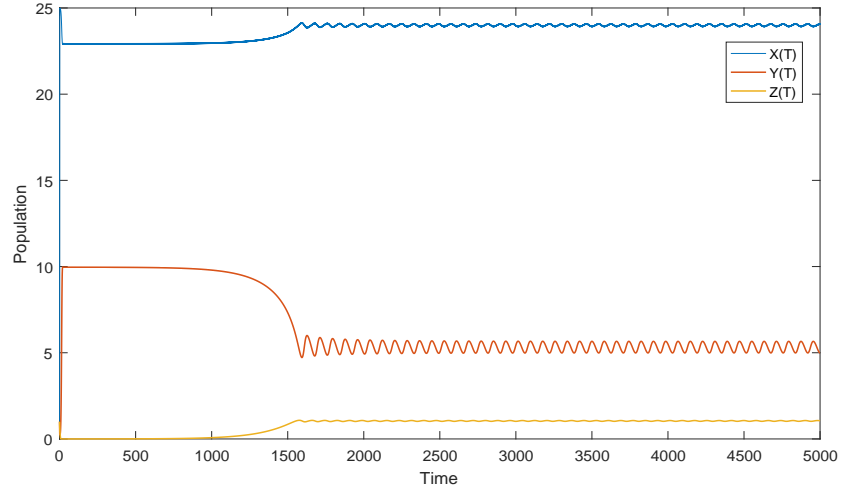
Figure 4.29: Time evolution of the system (4.5) for $\alpha = 5$, $\eta = 0.4$, $\xi = 0.92$, $\beta = 0.2$, $\phi = 1.005$, $\gamma = 0.3$, $\sigma = 1$, $\tau_2 = 4.3(> \overline{\tau_2}^0 = 3.9264)$, and $\tau_1 = 1$.

Figure 4.30: Trajectory of the system (4.5) in the phase plane for $\alpha = 5$, $\eta = 0.4$, $\xi = 0.92$, $\beta = 0.2$, $\phi = 1.005$, $\gamma = 0.3$, $\sigma = 1$, $\tau_2 = 4.3(> \overline{\tau_2}^0 = 3.9264)$, and $\tau_1 = 1$.
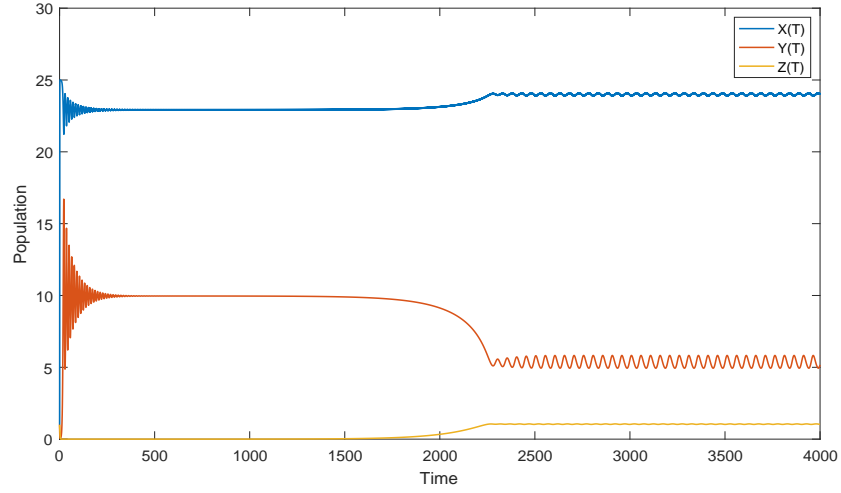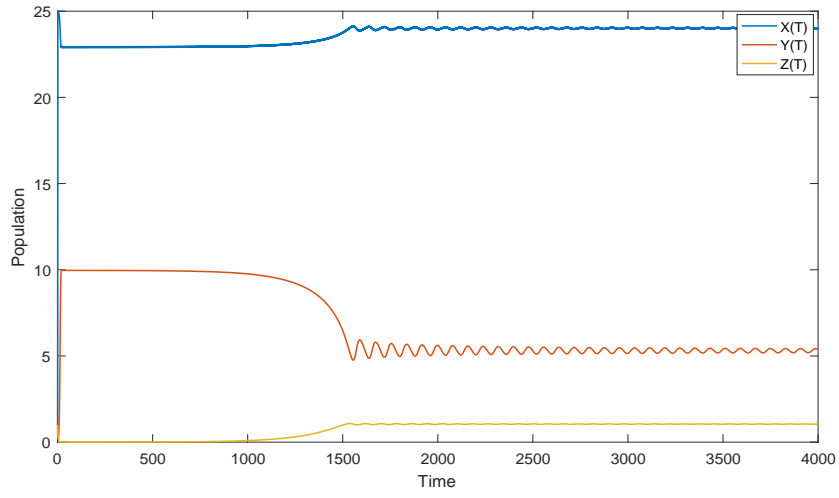
Figure 4.31: Time evolution of the system (4.5) for $\alpha = 5$, $\eta = 0.4$, $\xi = 0.92$, $\beta = 0.2$, $\phi = 1.005$, $\gamma = 0.3$, $\sigma = 1$, $\tau_2 = \overline{\tau_2}^0 = 3.9264$, and $\tau_1 = 1$.
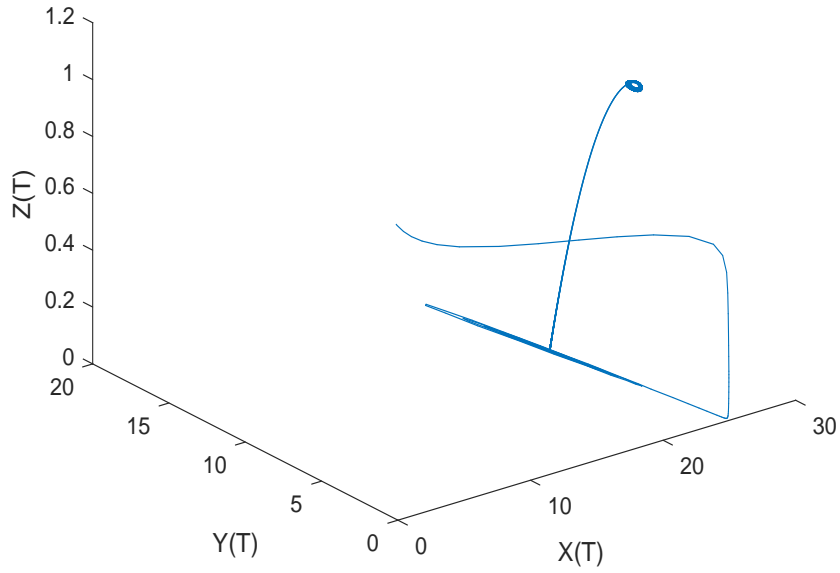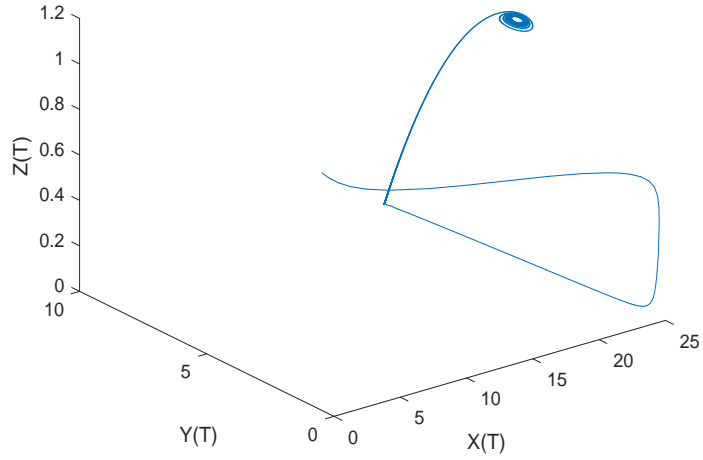

Figure 4.32: Trajectory of the system (4.5) in the phase plane for $\alpha = 5$, $\eta = 0.4$, $\xi = 0.92$, $\beta = 0.2$, $\phi = 1.005$, $\gamma = 0.3$, $\sigma = 1$, $\tau_2 = \overline{\tau_2}^0 = 3.9264$, and $\tau_1 = 1$.

4.8 Conclusions
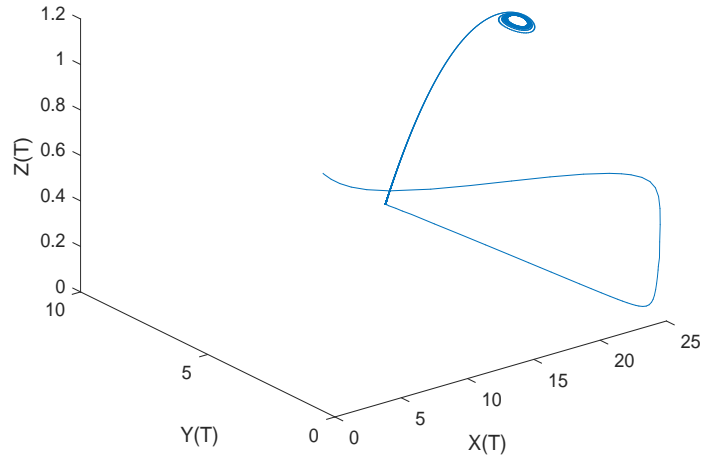
The relationship between prey and predator plays a crucial role in structuring the ecological community. Realizing the tropic connections is vital for preserving functional ecological relationships. Thus, this chapter, which proposes a detritus-based predator-prey model, is very significant in understanding the dynamics of the Sundarban mangrove ecosystem. To maintain the stability of the ecosystem, neither prey nor predator should be extinct. Throughout the chapter, we have derived the stability criterion, which makes the system stable for both the delayed and non-delayed systems.

The present work is an extension of the earlier work of Sarkar et al. (1991), where a simple detritus-based predator-prey model was studied without time delay. In their paper, they considered the Holling type-II functional response as the uptake function of invertebrate predators. In our work, the Ivlev-type response function has been taken in place of the Holling type-II functional response as the uptake function of invertebrate predators. Also, we have assumed that, though the leading source of detritus is the plant litter of mangrove forest, a small amount of detritus is also formed from the dead bodies of invertebrate predators by the recycling process. The beauty of this study is that we have incorporated two different valued discrete time delays for the gestation of prey (micro-organism pool) and predator (invertebrate predator). Due to the time lag, our proposed model possesses more complicated dynamics than the ordinary differential equations system. Indeed, no particular model can fully describe the dynamic behavior of any natural ecosystem like the detritus-based predator-prey model. So, modification and extension of existing models are always encouraged to better understand any ecosystem's dynamics. That is the beauty of the mathematical modeling of natural ecosystems.

This detritus-based prey-predator model has huge applications in ecology. As our model describes the conditions which ensure the stability of the ecosystem of Sundarban mangrove

forest, this helps to maintain the balance between different animal species. Also, this prey-predator interaction is essential to maintain the diversity of organisms. This interaction can change the stability of the food chain, and elimination of any part of the chain can have a extreme effect on the ecological community.

We have made a thorough theoretical and numerical investigation without time delay and with time delay throughout the chapter. From the analysis of our model, some engrossing and functional outcomes have been obtained. From the biological aspect, the most salient fact we got from our study is that, the time lag plays a leading role in shaping the dynamics of our proposed model. Without delays, the system is locally asymptotically stable under some circumstances. These delays demolish the dynamical ecosystem's stability and give rise to periodic oscillations. It has been observed that for both delays, under the critical values of the delay parameters, the dynamical system is stable. The dynamical system becomes unstable when the delay parameter crosses its critical magnitude. A periodic oscillation is found with increasing delay, which leads to a complex dynamical system. A Hopf-bifurcation with small amplitude occurs at the critical values for both the delay parameters. Numerical illustrations also ensure our theoretical observations that the dynamics of our model are widely influenced by taking distinct values of delay parameters.

Chapter 5

Approximate Analytical Solution of a Fractional Order Detritus-Based Predator-Prey Model Using Homotopy Perturbation Method *

5.1 Introduction

In recent times, fractional calculus has received much recognition and popularity. It provides some particular descriptions of various linear and non-linear systems. In the past few years, it has been extensively used in various fields of science like mathematics, physics, biology, engineering, etc. (Das, 2007; Hifer, 2000; Kilbas, 2006; Kumar, 2006; Magin, 2004; Podlubny, 1999; Rivero et al., 2011; Ross, 1993; Sabatier et al., 2007; Wang, 2009). In 1695, Leibniz first introduced fractional order derivatives in calculus for differentiation and integration. In most of the cases of real physical problems, the behavior of a non-linear system depends on the instant time as well as the previous time of interval, which may be acquired by a fractional derivative. A differential equation with fractional order is a special case of a differential equation with integer order. Fractional order differential equation can be derived by changing the order of the differential equation from integer to fraction. The key advantage of the system with fractional order is that it permits higher degrees of freedom compared to

the differential equations with integer order. In population dynamics, generally, differential equations with integer order are applied to formulate a model, but many authors have already worked on fractional order differential equations in population dynamics and ecology in the past few years (Dubey et al., 2020; Khan et al., 2019; Sunil Kumar et al., 2003; Ogunmiloro et al., 2021). In maximum cases, finding the accurate analytical solution of fractional order differential equations is quite challenging (Golmankhaneh et al., 2011; Jiang, 2006; Rida et al., 2008; Wang and Xu, 2009). As a result, some analytical approximation methods are developed to find the approximate analytical solutions close to the exact analytical solutions. Numerous methods are present for solving fractional differential equations. Among them, some convenient methods are the Adomian Decomposition Method (ADM) (Biazar, 2006; Shawagfeh, 1996), Variational Iteration Method (VIM) (Batiha et al., 2007; Rafei et al., 2007), Homotopy Perturbation Method (HPM) (Das and Gupta, 2011; Rafei et al., 2007), Homotopy Analysis Method (HAM) (Arqub and El-Ajou, 2013; Awawdeh et al., 2009), etc. All these methods are based on some numerical and analytical aspects. The HPM is a very efficacious and appropriate approximation method. This method is not only applicable to linear equations but also suitable for non-linear equations. The HPM was first introduced by HE in 1999 (He, 1999, 2005) for solving both non-linear and linear differential and integral equations. Later, the applications of HPM were widely spread. Several authors have applied this method in different areas of mathematics like Volterra's integrow-differential equation (Jayaprakasha, 2020; Sayevand K et al., 2013), delay-differential equations (Mishra et al., 2020; Yzbasi et al., 2017), boundary value problems (Noor et al., 2008; Saadatmandi et al., 2009), non-linear wave equations (Chun et al., 2009; He and Ji-Huan, 2005), fractional order quadratic Riccati differential equation (Odibat and Shawagfeh, 2007) and so many others. This is a perturbation method by which any differential and integral equations with fractional order can be solved analytically easily by constructing a homotopy. The main benefit of this method is that it has no limitation of having any small parameter for getting an

approximate solution, while the other perturbation methods generally require small parameters. This small parameter has a profound impact on the solution of the system. This is a very rapid convergence method requiring few iterations to get an accurate solution.

The main focus of our study is to enhance the implementation of the HPM to our proposed detritus-based prey-predator model to get an approximate analytical solution. In this work, a deterministic model is formulated, where detritus is the primary source of energy level, the micro-organism pool acts as the prey, and the predator is the invertebrate predator in the Sundarban mangrove forest in India. The orders of the derivatives used in the model are considered fractions of different values. Here, the uptake rate of the micro-organism pool due to the predation of the invertebrate predator is taken as the Ivlev-type response function.

In this paper, all the sections are arranged in the following manner. Section 5.2 contains model formulation. In section 5.3, some preliminaries are discussed, which are used throughout the paper to find the solution to our model. In section 5.4, different steps of HPM are discussed. In section 5.4, we have found the approximate solution of our model using the HPM. Numerical simulations are done in 5.5 to illustrate our analytical solutions.

5.2   Model formulation

In this Section, a deterministic detritus-based predator-prey mathematical model is considered as follows:

$$
\begin{aligned}
\frac{dx}{dt} &= x(b_1 - ax) - \frac{fxy}{k_1 + x} \\
\frac{dy}{dt} &= y\left(b_2 - \frac{dy}{ax}\right) - hz\{1 - exp(-gy)\}. \\
\frac{dz}{dt} &= z\big[-m + h\{1 - exp(-gy)\}\big],
\end{aligned}
\tag{5.1}
$$

where

x, y, and z are biomass of detritus, micro-organism pool, and invertebrate predator, respectively at time t, and all are positive at $t = 0$. Here, b_1 is detritus's growth rate, b_2 is the micro-organism pool's growth rate, h is the food conversion efficiency rate of the invertebrate predator, m is the normal rate of mortality of invertebrate predator, and g represents the hunting success. Here, the uptake function of invertebrate predator is considered as the Ivlev-type response function. For mathematical simplicity, we convert our system into a non-dimensional system using the following transformations:

$x = k_1 P$, $y = \frac{mk_1 Q}{f}$, $z = \frac{k_1 m^2 R}{fh}$, $t = \frac{T_1}{m}$.

Then, the model system (5.1) is reduced to

$$\begin{aligned} \frac{dP}{dT_1} &= P\left\{(\alpha - \eta P) - \frac{Q}{1+P}\right\}. \\ \frac{dQ}{dT_1} &= Q\left(\beta - \frac{\gamma Q}{P}\right) - R\{1 - exp(-\phi Q)\}. \\ \frac{dR}{dT_1} &= R\big[-1 + \sigma\{1 - exp(-\phi Q)\}\big], \end{aligned} \qquad (5.2)$$

where $\alpha = \frac{b_1}{m}$, $\eta = \frac{ak_1}{m}$, $\beta = \frac{b_2}{m}$, $\gamma = \frac{d}{af}$, $\sigma = \frac{h}{m}$, $\phi = \frac{gmk_1}{f}$.

Now we consider the fractional derivatives and considering $0 < m_1 \le 1$, $0 < n_1 \le 1$, $0 < n_2 \le 1$, we get the following model:

$$\begin{aligned} D_{T_1}^{m_1} P &= P\left\{(\alpha - \eta P) - \frac{Q}{1+P}\right\}. \\ D_{T_1}^{n_1} Q &= Q\left(\beta - \frac{\gamma Q}{P}\right) - R\{1 - exp(-\phi Q)\}. \\ D_{T_1}^{n_2} R &= R\big[-1 + \sigma\{1 - exp(-\phi Q)\}\big], \end{aligned} \qquad (5.3)$$

where the initial conditions of P, Q, and R are assumed as $P_0 = \delta_1 > 0$, $Q_0 = \delta_2 > 0$, and $R_0 = \delta_3 > 0$. Also, all the parameters α, η, β, γ, σ, and ϕ are positive.

5.3　Some Preliminaries

In this section, for finding the approximate solution of our system using HPM, some preliminaries of fractional calculus have been provided.

5.3.1　Definition 5.1:

A function $f_1 : (0, \infty) \to \mathbb{R}$ belongs to the space $C_\alpha, \alpha \in \mathbb{R}$ if $\exists$ a number $\beta_1 > \alpha (\alpha \in \mathbb{R})$ such that $f_1(t) = t^{\beta_1} f_2(t)$, where $f_2 : (0, \infty) \to \mathbb{R}$ and the function f_2 belongs to the space $C_\alpha{}^{\beta_2}$ iff $f_3(\beta_2) \in C_\alpha$, $\beta_2 \in \mathbb{N}$, where $f_3 : (0, \infty) \to \mathbb{R}$ is a function.

5.3.2　Definition 5.2:

Let $f_1(t) : \mathbb{R}^+ \longrightarrow \mathbb{R}$ be a function. Then the fractional integral of order w of the function $f_1(t)$ is given by

$$J_t{}^w f_1(t) = \frac{1}{\Gamma(w)} \int_0^t (t - \xi)^{w-1} f_1(\xi) d\xi,$$

where $\frac{1}{\Gamma(w)} \int_0^t (t-\xi)^{w-1} f_1(\xi) d\xi$ is point wise continuous on $\mathbb{R}^+$ and $w \geq 0$. Also, $\Gamma(w)$ denotes the gamma function.

5.3.3　Definition 5.3:

Let $g(t) : \mathbb{R}^+ \longrightarrow \mathbb{R}$ is a continuous function. Then the Caputo derivative of order $s > 0$ of $g(t)$ is defined as follows:

$$D_t{}^s g(t) = \frac{1}{\Gamma(z_1 - s)} \int_0^t \frac{g^{(z_1)}(\phi)}{(t - \phi)^{s-z_1+1}} d\phi,$$

where $z_1 \in \mathbb{Z}(\mathbb{Z} = \text{set of integers}), s \in \mathbb{R}(\mathbb{R} = \text{set of real numbers})$ and $z_1 - 1 \leq s < z_1$.

Here, we mention some basic properties of the integral operator $J_t{}^w$ and the differential

operator $D_t{}^s$, which are as follows:

(i) $J^\mu J^\eta f(t) = J^{\mu+\eta} f(t) = J^\eta J^\mu f(t),$

(ii) $J^\mu t^\psi = \frac{\Gamma(\psi+1)}{\Gamma(\mu+\psi+1)} t^{\mu+\psi},$

(iii) $D^\mu J^\eta f(t) = J^{\eta-\mu} f(t),$

where $f(t) \in C_\alpha, \alpha \geq -1, \mu, \eta \geq 0,$ and $\psi > -1.$

5.4   Analysis of HPM

To understand the method easily, first we will discuss a review of HPM. Then we will come to our problem.

For this, a non-linear differential equation is considered as follows:

$$L_1(v) + N_1(v) = f_1(u), u \in \Omega_1, \tag{5.4}$$

satisfying the following boundary conditions

$$\mathbf{B_1}\left(v, \frac{\nabla v}{\nabla n_3}\right) = 0, u \in \Gamma, \tag{5.5}$$

where L_1, N_1, and $\mathbf{B_1}$ represent the linear, non-linear and boundary operator respectively. Also, Γ represents the boundary of the region Ω_1, and $f_1(u)$ is an analytic function that is known.

According to He's HPM (He, 1999, 2005), at first a homotopy is formed as follows:

$$w(u, p_1) : \Omega_1 \times [0, 1] \longrightarrow \mathbb{R},$$

satisfying

$$H_1(w, p_1) = (1 - p_1)[L_1(w) - L_1(v_0)] + p_1[L_1(w) + N_1(w) - f_1(u)] = 0, \qquad (5.6)$$

or

$$H_1(w, p_1) = [L_1(w) - L_1(v_0)] + p_1 L_1(v_0) + p_1[N_1(w) - f_1(u)] = 0, \qquad (5.7)$$

where p_1 represents the embedding parameter and $p_1 \in [0, 1]$, $u \in \Omega_1$ and v_0 is assumed as the approximation of initial value satisfying the boundary conditions.

Using (5.6) and (5.7), we obtain

$$H_1(w, 0) = L_1(w) - L_1(v_0) = 0, \qquad (5.8)$$

$$H_1(w, 1) = L_1(w) + N_1(w) - f_1(u) = 0. \qquad (5.9)$$

Here, the values of p_1 changes from 0 to 1, which means $w(u, p_1)$ changes from v_0 to $v(u)$. In topological terms, this is called deformation.

Here, $L_1(w) - L_1(v_0)$ and $L_1(w) + N_1(w) - f_1(u)$ are named homotopic.

Here, p_1 acts as a "small embedding parameter." Thus the equations (5.6) and (5.7) have the solution which is as follows:

$$w = \sum_{n_3=0}^{\infty} p_1^{n_3} w_{n_3}(t) = w_0(t) + p_1 w_1(t) + p_1^2 w_2(t) + p_1^3 w_3(t) + \dots, \qquad (5.10)$$

which is a power series of p_1 of the equation (5.4).

Setting $p_1 \to 1$, we get

$$v = \lim_{p_1 \to 1} w = \lim_{p_1 \to 1} \sum_{n_3=0}^{\infty} p_1^{n_3} w_{n_3}(t) = w_0(t) + w_1(t) + w_2(t) + w_3(t) + \dots, \qquad (5.11)$$

which is the approximate solution of the equation (5.4).

In most of the cases, the series in (5.11) is convergent, which has been proved in He's works (He, 1999, 2005).

5.5 Solution of our problem by using HPM

In this section, for system (5.3), we will find the approximate solution using HPM. We have already considered the initial conditions as follows:

$$P_0(T_1) = \delta_1, Q_0(T_1) = \delta_2, R_0(T_1) = \delta_3.$$

Here, for the system (5.2), we set up the homotopy, which is as follows:

$$
\begin{aligned}
D_{T_1}^{m_1} P &= p_1 P \left\{ (\alpha - \eta P) - \frac{Q}{1+P} \right\}. \\
D_{T_1}^{n_1} Q &= p_1 Q \left(\beta - \frac{\gamma Q}{P} \right) - R\{1 - exp(-\phi Q)\}. \\
D_{T_1}^{n_2} R &= p_1 R \left[-1 + \sigma\{1 - exp(-\phi Q)\} \right],
\end{aligned}
\tag{5.12}
$$

where the orders of the derivatives i.e., $m_1, n_1, n_2 \in [0, 1]$, and the homotopy parameter $p_1 \in [0, 1]$.

If $p_1 = 0$, then the system (5.12) will be transformed into a system of homogeneous fractional differential equations. Using fractional approach (Podlubny, 1999; Ross, 1993), this transformed system can be solved.

The solutions of (5.12) can be written as:

$$P(T_1) = \sum_{n=0}^{\infty} p_1{}^n P_n(T_1) = P_0(T_1) + p_1 P_1(T_1) + p_1{}^2 P_2(T_1) + p_1{}^3 P_3(T_1) + ..., \tag{5.13}$$

$$Q(T_1) = \sum_{n=0}^{\infty} p_1{}^n Q_n(T_1) = Q_0(T_1) + p_1 Q_1(T_1) + p_1{}^2 Q_2(T_1) + p_1{}^3 Q_3(T_1) + \ldots\ldots, \quad (5.14)$$

$$R(T_1) = \sum_{n=0}^{\infty} p_1{}^n R_n(T_1) = R_0(T_1) + p_1 R_1(T_1) + p_1{}^2 R_2(T_1) + p_1{}^3 R_3(T_1) + \ldots\ldots \quad (5.15)$$

Setting $p_1 \to 1$, we get the solution of the equation (5.12), which is close to the accurate solution. The estimated solution is as follows:

$$P(T_1) = \lim_{p_1 \to 1} \sum_{n=0}^{\infty} p_1{}^n P_n(T_1) = P_0(T_1) + P_1(T_1) + P_2(T_1) + P_3(T_1) + \ldots\ldots, \quad (5.16)$$

$$Q(T_1) = \lim_{p_1 \to 1} \sum_{n=0}^{\infty} p_1{}^n Q_n(T_1) = Q_0(T_1) + Q_1(T_1) + Q_2(T_1) + Q_3(T_1) + \ldots\ldots, \quad (5.17)$$

$$R(T_1) = \lim_{p_1 \to 1} \sum_{n=0}^{\infty} p_1{}^n R_n(T_1) = R_0(T_1) + R_1(T_1) + R_2(T_1) + R_3(T_1) + \ldots\ldots \quad (5.18)$$

Now we have substituted the equations (5.13), (5.14), (5.15) in (5.12) and then equating the powers of p_1 from both sides, we get

$$p_1{}^0 : D^{m_1} P_0(T_1) = 0,$$

$$D^{n_1} Q_0(T_1) = 0,$$

$$D^{n_2} R_0(T_1) = 0,$$

$$p_1{}^1 : D^{m_1} P_1(T_1) = P_0 \left(\alpha - \eta P_0 - Q_0 + P_0 Q_0 - P_0{}^2 Q_0 + P_0{}^3 Q_0 \right),$$

$$D^{n_1} Q_1(T_1) = Q_0 \left(\beta - \tfrac{\gamma Q_0}{P_0} \right) - R_0 \left(\phi Q_0 - \tfrac{\phi^2 Q_0{}^2}{2!} + \tfrac{\phi^3 Q_0{}^3}{3!} \right),$$

$$D^{n_2} R_1(T_1) = R_0 \left(-1 + \sigma \phi Q_0 - \tfrac{\sigma \phi^2 Q_0{}^2}{2!} + \tfrac{\sigma \phi^3 Q_0{}^3}{3!} \right),$$

$$p_1{}^2 : D^{m_1} P_2(T_1) = P_0 \left(-\eta P_1 - Q_1 + P_1 Q_0 + P_0 Q_1 - 2 P_0 P_1 Q_0 - P_0{}^2 Q_1 + 3 P_0{}^2 P_1 Q_0 + P_0{}^3 Q_1 \right)$$
$$+ P_1 \left(\alpha - \eta P_0 - Q_0 + P_0 Q_0 - P_0{}^2 Q_0 + P_0{}^3 Q_0 \right),$$

$$D^{n_1} Q_2(T_1) = Q_0 \left\{ -\tfrac{P_1}{P_0} \left(\beta - \tfrac{\gamma Q_0}{P_0} \right) - \tfrac{\gamma Q_1}{P_0} \right\} + Q_1 \left(\beta - \tfrac{\gamma Q_0}{P_0} \right) - R_0 \left(\phi Q_1 - \phi^2 Q_0 Q_1 \right.$$
$$\left. + \tfrac{\phi^3 Q_0{}^2 Q_1}{2} \right) - R_1 \left(\phi Q_0 - \tfrac{\phi^2 Q_0{}^2}{2!} + \tfrac{\phi^3 Q_0{}^3}{3!} \right),$$

$$D^{n_2} R_2(T_1) = R_0 \left(\sigma\phi Q_1 - \phi^2 \sigma Q_0 Q_1 + \frac{\phi^3 \sigma Q_0^2 Q_1}{2} \right) + R_1 \left(-1 + \sigma\phi Q_0 - \frac{\phi^2 \sigma Q_0^2}{2!} + \frac{\phi^3 \sigma Q_0^3}{3!} \right),$$

$$p_1{}^3 : D^{m_1} P_3(T_1) = P_0 \big(-\eta P_2 - Q_2 + P_2 Q_0 + P_1 Q_1 + P_0 Q_2 - P_1{}^2 Q_0 - 2P_0 P_2 Q_0$$
$$- 2P_0 P_1 Q_1 - P_0{}^2 Q_2 + 3P_0 P_1{}^2 Q_0 + 3P_0{}^2 P_2 Q_0 + 3P_0{}^2 P_1 Q_1 + P_0{}^3 Q_2 \big)$$
$$+ P_1 \big(-\eta P_1 - Q_1 + P_1 Q_0 + P_0 Q_1 - 2P_0 P_1 Q_0 - P_0{}^2 Q_1 + 3P_0{}^2 P_1 Q_0$$
$$+ P_0{}^3 Q_1 \big) + P_2 \big(\alpha - \eta P_0 - Q_0 + P_0 Q_0 - P_0{}^2 Q_0 + P_0{}^3 Q_0 \big),$$

$$D^{n_1} Q_3(T_1) = Q_0 \left\{ \left(\beta - \frac{\gamma Q_0}{P_0} \right) \left(-\frac{P_2}{P_0} + \frac{P_1{}^2}{P_0{}^2} \right) + \frac{\gamma P_1 Q_1}{P_0{}^2} - \frac{\gamma Q_2}{P_0} \right\} + Q_1 \left\{ -\frac{P_1}{P_0} \right.$$
$$\left(\beta - \frac{\gamma Q_0}{P_0} \right) - \frac{\gamma Q_1}{P_0} \right\} + Q_2 \left(\beta - \frac{\gamma Q_0}{P_0} \right) - R_0 \left\{ \phi Q_2 - \frac{\phi^2}{2!} (Q_1{}^2 + 2Q_0 Q_2) \right.$$
$$\left. + \frac{\phi^3}{3!} (3Q_0 Q_1{}^2 + 3Q_0{}^2 Q_2) \right\} - R_1 \left(\phi Q_1 - \phi^2 Q_0 Q_1 + \frac{\phi^3 Q_0{}^2 Q_1}{2} \right)$$
$$- R_2 \left(\phi Q_0 - \frac{\phi^2 Q_0{}^2}{2!} + \frac{\phi^3 Q_0{}^3}{3!} \right),$$

$$D^{n_2} R_3(T_1) = R_0 \left\{ \sigma\phi Q_2 - \frac{\phi^2 \sigma}{2!} (Q_1{}^2 + 2Q_0 Q_2) + \frac{\phi^3 \sigma}{3!} (3Q_0 Q_1{}^2 + 3Q_0{}^2 Q_2) \right\} + R_1 \left(\sigma\phi Q_1 \right.$$
$$\left. - \phi^2 \sigma Q_0 Q_1 + \frac{\phi^3 \sigma Q_0{}^2 Q_1}{2} \right) + R_2 \left(-1 + \sigma\phi Q_0 - \frac{\phi^2 \sigma Q_0{}^2}{2!} + \frac{\phi^3 \sigma Q_0{}^3}{3!} \right),$$

$$(5.19)$$

and so on.

Now we have applied $J_{T_1}^{m_1}$, $J_{T_1}^{n_1}$, $J_{T_1}^{n_2}$ on the set of equations (5.19), and we get

$$P_0(T_1) = \delta_1,$$

$$Q_0(T_1) = \delta_2,$$

$$R_0(T_1) = \delta_3,$$

$$P_1(T_1) = \left\{ \alpha\delta_1 - \eta\delta_1{}^2 - \delta_1\delta_2 \left(1 - \delta_1 + \delta_1{}^2 - \delta_1{}^3 \right) \right\} \frac{T_1{}^{m_1}}{\Gamma(m_1+1)},$$

$$Q_1(T_1) = \left\{ \delta_2\left(\beta - \frac{\gamma\delta_2}{\delta_1}\right) - \delta_3\left(\phi\delta_2 - \frac{\phi^2\delta_2{}^2}{2!} + \frac{\phi^3\delta_2{}^3}{3!}\right) \right\} \frac{T_1{}^{n_1}}{\Gamma(n_1+1)},$$

$$R_1(T_1) = \left\{ -\delta_3 + \sigma\delta_3\left(\phi\delta_2 - \frac{\phi^2\delta_2{}^2}{2!} + \frac{\phi^3\delta_2{}^3}{3!}\right) \right\} \frac{T_1{}^{n_2}}{\Gamma(n_2+1)},$$

$$P_2(T_1) = \left\{ (\alpha - 2\eta\delta_1) - \delta_1\delta_2\left(-1 + 2\delta_1 - 3\delta_1{}^2\right) - \delta_2\left(1 - \delta_1 + \delta_1{}^2 - \delta_1{}^3\right) \right\}$$
$$\left\{ \alpha\delta_1 - \eta\delta_1{}^2 - \delta_1\delta_2\left(1 - \delta_1 + \delta_1{}^2 - \delta_1{}^3\right) \right\} \frac{T_1{}^{2m_1}}{\Gamma(2m_1 + 1)} - \delta_1\left(1 - \delta_1 + \delta_1{}^2 - \delta_1{}^3\right)$$
$$\left\{ \delta_2\left(\beta - \frac{\gamma\delta_2}{\delta_1}\right) - \delta_3\left(\phi\delta_2 - \frac{\phi^2\delta_2{}^2}{2!} + \frac{\phi^3\delta_2{}^3}{3!}\right) \right\} \frac{T_1{}^{m_1+n_1}}{\Gamma(m_1 + n_1 + 1)},$$

$$Q_2(T_1) = -\frac{\delta_2}{\delta_1}\left(\beta - \frac{\gamma\delta_2}{\delta_1}\right)\left\{ \alpha\delta_1 - \eta\delta_1{}^2 - \delta_1\delta_2\left(1 - \delta_1 + \delta_1{}^2 - \delta_1{}^3\right) \right\} \frac{T_1{}^{m_1+n_1}}{\Gamma(m_1 + n_1 + 1)}$$
$$+ \left\{ -\frac{2\gamma\delta_2}{\delta_1} + \beta - \delta_3\left(\phi - \phi^2\delta_2 + \frac{\phi^3\delta_2{}^2}{2}\right) \right\}\left\{ \delta_2\left(\beta - \frac{\gamma\delta_2}{\delta_1}\right) - \delta_3\left(\phi\delta_2 - \frac{\phi^2\delta_2{}^2}{2!}\right.\right.$$
$$\left.\left. + \frac{\phi^3\delta_2{}^3}{3!}\right) \right\} \frac{T_1{}^{2n_1}}{\Gamma(2n_1 + 1)} - \left(\phi\delta_2 - \frac{\phi^2\delta_2{}^2}{2!} + \frac{\phi^3\delta_2{}^3}{3!}\right)\left\{ -\delta_3 + \sigma\delta_3\left(\phi\delta_2 - \frac{\phi^2\delta_2{}^2}{2!}\right.\right.$$
$$\left.\left. + \frac{\phi^3\delta_2{}^3}{3!}\right) \right\} \frac{T_1{}^{n_1+n_2}}{\Gamma(n_1 + n_2 + 1)},$$

$$R_2(T_1) = \sigma\delta_3\left(\phi - \phi^2\delta_2 + \frac{\phi^3\delta_2^2}{2}\right)\left\{ \delta_2\left(\beta - \frac{\gamma\delta_2}{\delta_1}\right) - \delta_3\left(\phi\delta_2 - \frac{\phi^2\delta_2{}^2}{2!} + \frac{\phi^3\delta_2{}^3}{3!}\right) \right\}$$
$$\frac{T_1{}^{n_1+n_2}}{\Gamma(n_1 + n_2 + 1)} + \left\{ -1 + \sigma\left(\phi\delta_2 - \frac{\phi^2\delta_2{}^2}{2!} + \frac{\phi^3\delta_2{}^3}{3!}\right) \right\}$$
$$\left\{ -\delta_3 + \sigma\delta_3\left(\phi\delta_2 - \frac{\phi^2\delta_2{}^2}{2!} + \frac{\phi^3\delta_2{}^3}{3!}\right) \right\} \frac{T_1{}^{2n_2}}{\Gamma(2n_2 + 1)},$$

$$
\begin{aligned}
P_3(T_1) =& \left\{ \alpha - 2\eta\delta_1 - \delta_1\delta_2\left(-1 + 2\delta_1 - 3\delta_1{}^2\right) - \delta_2\left(1 - \delta_1 + \delta_1{}^2 - \delta_1{}^3\right) \right\} \Bigg[\left\{ (\alpha - 2\eta\delta_1) \right. \\
& - \delta_1\delta_2\left(-1 + 2\delta_1 - 3\delta_1{}^2\right) - \delta_2\left(1 - \delta_1 + \delta_1{}^2 - \delta_1{}^3\right) \Bigg\} \left\{ \alpha\delta_1 - \eta\delta_1{}^2 - \delta_1\delta_2 \right. \\
& \left. \left(1 - \delta_1 + \delta_1{}^2 - \delta_1{}^3\right) \right\} \frac{T_1{}^{3m_1}}{\Gamma(3m_1 + 1)} - \delta_1\left(1 - \delta_1 + \delta_1{}^2 - \delta_1{}^3\right) \left\{ \delta_2\left(\beta - \frac{\gamma\delta_2}{\delta_1}\right) \right. \\
& \left. - \delta_3\left(\phi\delta_2 - \frac{\phi^2\delta_2{}^2}{2!} + \frac{\phi^3\delta_2{}^3}{3!}\right) \right\} \frac{T_1{}^{2m_1+n_1}}{\Gamma(2m_1 + n_1 + 1)} \Bigg] + \Bigg\{ -\eta - \delta_1\delta_2\left(1 - 3\delta_1\right) \\
& - \delta_2\left(-1 + 2\delta_1 - 3\delta_1{}^2\right) \Bigg\} \left\{ \alpha\delta_1 - \eta\delta_1{}^2 - \delta_1\delta_2\left(1 - \delta_1 + \delta_1{}^2 - \delta_1{}^3\right) \right\}^2 \frac{\Gamma(2m_1 + 1)}{\Gamma(m_1 + 1)^2} \\
& \frac{T_1{}^{3m_1}}{\Gamma(3m_1 + 1)} + \Bigg\{ -\delta_1\left(-1 + 2\delta_1 - 3\delta_1{}^2\right) - \left(1 - \delta_1 + \delta_1{}^2 - \delta_1{}^3\right) \Bigg\} \left\{ \alpha\delta_1 - \eta\delta_1{}^2 \right. \\
& \left. - \delta_1\delta_2\left(1 - \delta_1 + \delta_1{}^2 - \delta_1{}^3\right) \right\} \left\{ \delta_2\left(\beta - \frac{\gamma\delta_2}{\delta_1}\right) - \delta_3\left(\phi\delta_2 - \frac{\phi^2\delta_2{}^2}{2!} + \frac{\phi^3\delta_2{}^3}{3!}\right) \right\} \\
& \frac{1}{\Gamma(m_1 + 1)} \frac{1}{\Gamma(n_1 + 1)} \frac{\Gamma(m_1 + n_1 + 1)}{\Gamma(2m_1 + n_1 + 1)} T_1{}^{2m_1+n_1} - \delta_1\left(1 - \delta_1 + \delta_1{}^2 - \delta_1{}^3\right) \\
& \left[-\frac{\delta_2}{\delta_1}\left(\beta - \frac{\gamma\delta_2}{\delta_1}\right) \left\{ \alpha\delta_1 - \eta\delta_1{}^2 - \delta_1\delta_2\left(1 - \delta_1 + \delta_1{}^2 - \delta_1{}^3\right) \right\} \frac{T_1{}^{2m_1+n_1}}{\Gamma(2m_1 + n_1 + 1)} \right. \\
& + \left\{ -\frac{2\gamma\delta_2}{\delta_1} + \beta - \delta_3\left(\phi - \phi^2\delta_2 + \frac{\phi^3\delta_2{}^2}{2}\right) \right\} \left\{ \delta_2\left(\beta - \frac{\gamma\delta_2}{\delta_1}\right) \right. \\
& \left. - \delta_3\left(\phi\delta_2 - \frac{\phi^2\delta_2{}^2}{2!} + \frac{\phi^3\delta_2{}^3}{3!}\right) \right\} \frac{T_1{}^{m_1+2n_1}}{\Gamma(m_1 + 2n_1 + 1)} - \left(\phi\delta_2 - \frac{\phi^2\delta_2{}^2}{2!} + \frac{\phi^3\delta_2{}^3}{3!}\right) \\
& \left. \left\{ -\delta_3 + \sigma\delta_3\left(\phi\delta_2 - \frac{\phi^2\delta_2{}^2}{2!} + \frac{\phi^3\delta_2{}^3}{3!}\right) \right\} \frac{T_1{}^{m_1+n_1+n_2}}{\Gamma(m_1 + n_1 + n_2 + 1)} \right],
\end{aligned}
$$

$$Q_3(T_1) = -\frac{\delta_2}{\delta_1}\left(\beta - \frac{\gamma\delta_2}{\delta_1}\right)\left[\left\{\left(\alpha - 2\eta\delta_1\right) - \delta_1\delta_2\left(-1 + 2\delta_1 - 3\delta_1{}^2\right) - \delta_2\left(1 - \delta_1 + \delta_1{}^2 - \delta_1{}^3\right)\right\}\right.$$

$$\left\{\alpha\delta_1 - \eta\delta_1{}^2 - \delta_1\delta_2\left(1 - \delta_1 + \delta_1{}^2 - \delta_1{}^3\right)\right\}\frac{T_1{}^{2m_1+n_1}}{\Gamma(2m_1 + n_1 + 1)} - \delta_1\left(1 - \delta_1 + \delta_1{}^2 - \delta_1{}^3\right)$$

$$\left\{\delta_2\left(\beta - \frac{\gamma\delta_2}{\delta_1}\right) - \delta_3\left(\phi\delta_2 - \frac{\phi^2\delta_2{}^2}{2!} + \frac{\phi^3\delta_2{}^3}{3!}\right)\right\}\frac{T_1{}^{m_1+2n_1}}{\Gamma(m_1 + 2n_1 + 1)}\right] + \frac{\delta_2}{\delta_1{}^2}\left(\beta - \frac{\gamma\delta_2}{\delta_1}\right)$$

$$\left\{\alpha\delta_1 - \eta\delta_1{}^2 - \delta_1\delta_2\left(1 - \delta_1 + \delta_1{}^2 - \delta_1{}^3\right)\right\}^2 \frac{1}{\Gamma(m_1 + 1)^2}\frac{\Gamma(2m_1 + 1)}{\Gamma(2m_1 + n_1 + 1)}T_1{}^{2m_1+n_1}$$

$$+ \left\{\frac{\gamma\delta_2}{\delta_1{}^2} - \frac{1}{\delta_1}\left(\beta - \frac{\gamma\delta_2}{\delta_1}\right)\right\}\left\{\alpha\delta_1 - \eta\delta_1{}^2 - \delta_1\delta_2\left(1 - \delta_1 + \delta_1{}^2 - \delta_1{}^3\right)\right\}\left\{\delta_2\left(\beta - \frac{\gamma\delta_2}{\delta_1}\right)\right.$$

$$\left.- \delta_3\left(\phi\delta_2 - \frac{\phi^2\delta_2{}^2}{2!} + \frac{\phi^3\delta_2{}^3}{3!}\right)\right\}\frac{1}{\Gamma(m_1 + 1)}\frac{1}{\Gamma(n_1 + 1)}\frac{\Gamma(m_1 + n_1 + 1)}{\Gamma(m_1 + 2n_1 + 1)}T_1{}^{m_1+2n_1}$$

$$+ \left\{\beta - \frac{2\gamma\delta_2}{\delta_1} - \delta_3\left(\phi - \phi^2\delta_2 + \frac{\phi^3\delta_2{}^2}{2}\right)\right\}\left[-\frac{\delta_2}{\delta_1}\left(\beta - \frac{\gamma\delta_2}{\delta_1}\right)\left\{\alpha\delta_1 - \eta\delta_1{}^2 - \delta_1\delta_2\right.\right.$$

$$\left.\left(1 - \delta_1 + \delta_1{}^2 - \delta_1{}^3\right)\right\}\frac{T_1{}^{m_1+2n_1}}{\Gamma(m_1 + 2n_1 + 1)} + \left\{-\frac{2\gamma\delta_2}{\delta_1} + \beta - \delta_3\left(\phi - \phi^2\delta_2 + \frac{\phi^3\delta_2{}^2}{2}\right)\right\}$$

$$\left\{\delta_2\left(\beta - \frac{\gamma\delta_2}{\delta_1}\right) - \delta_3\left(\phi\delta_2 - \frac{\phi^2\delta_2{}^2}{2!} + \frac{\phi^3\delta_2{}^3}{3!}\right)\right\}\frac{T_1{}^{3n_1}}{\Gamma(3n_1 + 1)} + \left(\phi\delta_2 - \frac{\phi^2\delta_2{}^2}{2!} + \frac{\phi^3\delta_2{}^3}{3!}\right)$$

$$\left.\left\{-\delta_3 + \sigma\delta_3\left(\phi\delta_2 - \frac{\phi^2\delta_2{}^2}{2!} + \frac{\phi^3\delta_2{}^3}{3!}\right)\right\}\frac{T_1{}^{2n_1+n_2}}{\Gamma(2n_1 + n_2 + 1)}\right] + \left\{-\frac{\gamma}{\delta_1} - \delta_3\left(-\frac{\phi^2}{2} + \frac{\phi^3\delta_2}{2}\right)\right\}$$

$$\left\{\delta_2\left(\beta - \frac{\gamma\delta_2}{\delta_1}\right) - \delta_3\left(\phi\delta_2 - \frac{\phi^2\delta_2{}^2}{2!} + \frac{\phi^3\delta_2{}^3}{3!}\right)\right\}^2\frac{1}{\Gamma(n_1 + 1)^2}\frac{\Gamma(2n_1 + 1)}{\Gamma(3n_1 + 1)}T_1{}^{3n_1}$$

$$- \left(\phi - \phi^2\delta_2 + \frac{\phi^3\delta_2{}^2}{2}\right)\left\{\delta_2\left(\beta - \frac{\gamma\delta_2}{\delta_1}\right) - \delta_3\left(\phi\delta_2 - \frac{\phi^2\delta_2{}^2}{2!} + \frac{\phi^3\delta_2{}^3}{3!}\right)\right\}$$

$$\left\{-\delta_3 + \sigma\delta_3\left(\phi\delta_2 - \frac{\phi^2\delta_2{}^2}{2!} + \frac{\phi^3\delta_2{}^3}{3!}\right)\right\}\frac{1}{\Gamma(n_1 + 1)}\frac{1}{\Gamma(n_2 + 1)}\frac{\Gamma(n_1 + n_2 + 1)}{\Gamma(2n_1 + n_2 + 1)}T_1{}^{2n_1+n_2}$$

$$- \left(\phi\delta_2 - \frac{\phi^2\delta_2{}^2}{2!} + \frac{\phi^3\delta_2{}^3}{3!}\right)\left[\sigma\delta_3\left(\phi - \phi^2\delta_2 + \frac{\phi^3\delta_2^2}{2}\right)\left\{\delta_2\left(\beta - \frac{\gamma\delta_2}{\delta_1}\right)\right.\right.$$

$$\left.- \delta_3\left(\phi\delta_2 - \frac{\phi^2\delta_2{}^2}{2!} + \frac{\phi^3\delta_2{}^3}{3!}\right)\right\}\frac{T_1{}^{2n_1+n_2}}{\Gamma(2n_1 + n_2 + 1)} + \left\{-1 + \sigma\left(\phi\delta_2 - \frac{\phi^2\delta_2{}^2}{2!} + \frac{\phi^3\delta_2{}^3}{3!}\right)\right\}$$

$$\left.\left\{-\delta_3 + \sigma\delta_3\left(\phi\delta_2 - \frac{\phi^2\delta_2{}^2}{2!} + \frac{\phi^3\delta_2{}^3}{3!}\right)\right\}\frac{T_1{}^{n_1+2n_2}}{\Gamma(n_1 + 2n_2 + 1)}\right],$$

$$R_3(T_1) = \left\{ -1 + \sigma\left(\phi\delta_2 - \frac{\phi^2\delta_2{}^2}{2!} + \frac{\phi^3\delta_2{}^3}{3!}\right)\right\}\left[\sigma\delta_3\left(\phi - \phi^2\delta_2 + \frac{\phi^3\delta_2^2}{2}\right)\left\{\delta_2\left(\beta - \frac{\gamma\delta_2}{\delta_1}\right)\right.\right.$$

$$- \delta_3\left(\phi\delta_2 - \frac{\phi^2\delta_2{}^2}{2!} + \frac{\phi^3\delta_2{}^3}{3!}\right)\right\}\frac{T_1{}^{n_1+2n_2}}{\Gamma(n_1+2n_2+1)} + \left\{-1 + \sigma\left(\phi\delta_2 - \frac{\phi^2\delta_2{}^2}{2!}\right.\right.$$

$$\left.\left.+ \frac{\phi^3\delta_2{}^3}{3!}\right)\right\}\left\{-\delta_3 + \sigma\delta_3\left(\phi\delta_2 - \frac{\phi^2\delta_2{}^2}{2!} + \frac{\phi^3\delta_2{}^3}{3!}\right)\right\}\frac{T_1{}^{3n_2}}{\Gamma(3n_2+1)}\right] + \sigma\delta_3$$

$$\left(\phi - \phi^2\delta_2 + \frac{\phi^3\delta_2^2}{2}\right)\left[-\frac{\delta_2}{\delta_1}\left(\beta - \frac{\gamma\delta_2}{\delta_1}\right)\left\{\alpha\delta_1 - \eta\delta_1{}^2 - \delta_1\delta_2\left(1 - \delta_1 + \delta_1{}^2 - \delta_1{}^3\right)\right\}\right.$$

$$\frac{T_1{}^{m_1+n_1+n_2}}{\Gamma(m_1+n_1+n_2+1)} + \left\{-\frac{2\gamma\delta_2}{\delta_1} + \beta - \delta_3\left(\phi - \phi^2\delta_2 + \frac{\phi^3\delta_2{}^2}{2}\right)\right\}\left\{\delta_2\left(\beta - \frac{\gamma\delta_2}{\delta_1}\right)\right.$$

$$\left.- \delta_3\left(\phi\delta_2 - \frac{\phi^2\delta_2{}^2}{2!} + \frac{\phi^3\delta_2{}^3}{3!}\right)\right\}\frac{T_1{}^{2n_1+n_2}}{\Gamma(2n_1+n_2+1)} - \left(\phi\delta_2 - \frac{\phi^2\delta_2{}^2}{2!} + \frac{\phi^3\delta_2{}^3}{3!}\right)$$

$$\left.\left\{-\delta_3 + \sigma\delta_3\left(\phi\delta_2 - \frac{\phi^2\delta_2{}^2}{2!} + \frac{\phi^3\delta_2{}^3}{3!}\right)\right\}\frac{T_1{}^{n_1+2n_2}}{\Gamma(n_1+2n_2+1)}\right] + \sigma\delta_3\left(-\frac{\phi^2}{2!} + \frac{\phi^3\delta_2}{2}\right)$$

$$\left\{\delta_2\left(\beta - \frac{\gamma\delta_2}{\delta_1}\right) - \delta_3\left(\phi\delta_2 - \frac{\phi^2\delta_2{}^2}{2!} + \frac{\phi^3\delta_2{}^3}{3!}\right)\right\}^2\frac{1}{\Gamma(n_1+1)^2}\frac{\Gamma(2n_1+1)}{\Gamma(2n_1+n_2+1)}$$

$$T_1{}^{2n_1+n_2} + \sigma\left(\phi - \phi^2\delta_2 + \frac{\phi^3\delta_2{}^2}{2}\right)\left\{\delta_2\left(\beta - \frac{\gamma\delta_2}{\delta_1}\right) - \delta_3\left(\phi\delta_2 - \frac{\phi^2\delta_2{}^2}{2!} + \frac{\phi^3\delta_2{}^3}{3!}\right)\right\}$$

$$\left\{-\delta_3 + \sigma\delta_3\left(\phi\delta_2 - \frac{\phi^2\delta_2{}^2}{2!} + \frac{\phi^3\delta_2{}^3}{3!}\right)\right\}\frac{1}{\Gamma(n_1+1)}\frac{1}{\Gamma(n_2+1)}$$

$$\frac{\Gamma(n_1+n_2+1)}{\Gamma(n_1+2n_2+1)}T_1{}^{n_1+2n_2}.$$

Therefore, we have got the approximate solution of order 3, which is as follows:

$$P(T_1) = \sum_{n=0}^{3} P_n(T_1) = P_0(T_1) + P_1(T_1) + P_2(T_1) + P_3(T_1), \tag{5.20}$$

$$Q(T_1) = \sum_{n=0}^{3} Q_n(T_1) = Q_0(T_1) + Q_1(T_1) + Q_2(T_1) + Q_3(T_1), \tag{5.21}$$

$$R(T_1) = \sum_{n=0}^{3} R_n(T_1) = R_0(T_1) + R_1(T_1) + R_2(T_1) + R_3(T_1). \tag{5.22}$$

One may also take more terms in the same manner to get a more suitable solution close to the exact solution.

5.6 Numerical simulation results

In this section, we have executed a numerical simulation to find the graphs of the approximate solution of the system (5.3). In this simulation process, we used the series' first four terms to get the approximate solution. Throughout the numerical illustration, we have used a set of parameter values as follows: $\alpha = 0.8$, $\eta = 0.3$, $\beta = 1.2$, $\gamma = 0.94$, $\phi = 1.1$, $\sigma = 2.006$, and the initial values of three populations are assumed as $P_0 = 0.3$, $Q_0 = 0.3$, $R_0 = 0.3$. We have carried out the simulation for different valued fractional orders as well as for standard order 1.

Figure 5.1a shows the graph of solution of $P(T_1)$ with respect to time T_1 for different values of m_1 i.e., for $m_1 = 1/3, 1/2, 2/3, 1$, $n_1 = 1$ and $n_2 = 1$. In this figure, it has been shown that initially, the population density of detritus increases more rapidly with decreasing fractional order m_1 but after a certain period of time, the population density increases more rapidly with increasing fractional order m_1. But for the standard order 1, the population density of detritus initially increases with increasing time, reaches its highest value, and then decreases. Figure 5.1b describe the solution graph of $P(T_1)$ with respect to time T_1 for $m_1 = n_1 = n_2 = 1/3, 1/2, 2/3, 1$. Figures 5.1a and 5.1b show the same kind of solution graphs.

Figure 5.2a represents the solution graph of the population $Q(T_1)$ with respect to time T_1 for $n_1 = 1/3, 1/2, 2/3, 1$, and keeping the values of m_1 and n_2 fixed to 1. In Figure 5.2a, it has been shown that when the value of order n_1 decreases, initially, the population density of the micro-organism pool increases more rapidly with increasing time, but after a certain period of time, the population density decreases more rapidly with increasing time. A similar type of picture is observed in Figure 5.2b, when we plot the solution graph of the population $Q(T_1)$ with respect to time T_1 for $m_1 = n_1 = n_2 = 1/3, 1/2, 2/3, 1$. Figure 5.3a presents the solution graph of $R(T_1)$ with respect to time T_1 for $m_1 = n_1 = 1$ and $n_2 = 1/3, 1/2, 2/3, 1$. This graph shows the rapid decrement of population density with decreasing order n_2 initially but
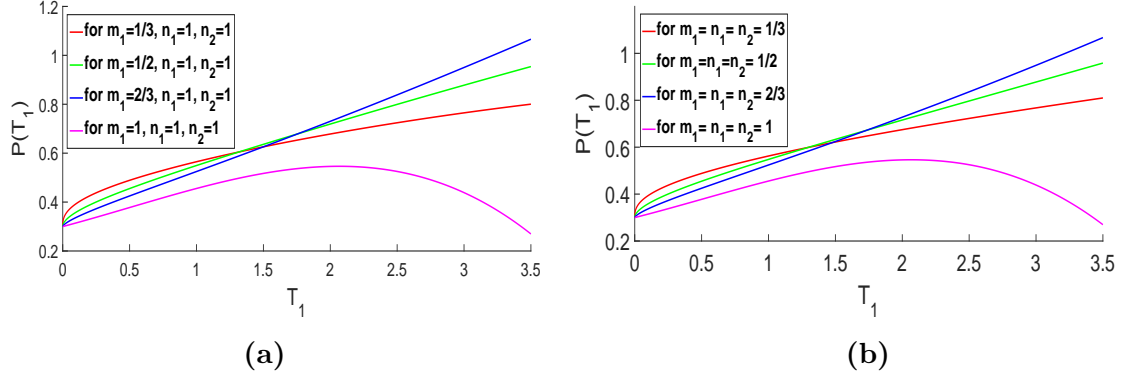
Figure 5.1: Approximate solutions of $P(T_1)$ of the system (5.3) for fractional orders: (a) $m_1 = 1/3, 1/2, 2/3, 1$, $n_1 = 1$ and $n_2 = 1$, (b) $m_1 = n_1 = n_2 = 1/3, 1/2, 2/3, 1$.
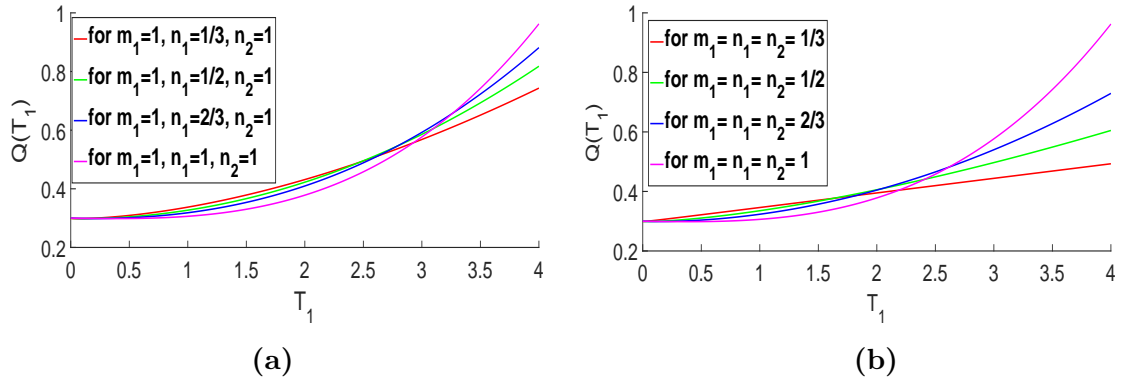
Figure 5.2: Approximate solutions of $Q(T_1)$, of the system (5.3) for fractional orders: (a) $m_1 = 1$, $n_1 = 1/3, 1/2, 2/3, 1$ and $n_2 = 1$, (b) $m_1 = n_1 = n_2 = 1/3, 1/2, 2/3, 1$.

Figure 5.3: Approximate solutions of $R(T_1)$, of the system (5.3) for fractional orders: (a) $m_1 = 1$, $n_1 = 1$ and $n_2 = 1/3, 1/2, 2/3, 1$, (b) $m_1 = n_1 = n_2 = 1/3, 1/2, 2/3, 1$.

after a certain period of time, a rapid increment of population density of $R(T_1)$ is observed with decreasing order n_2. Figures 5.3b describe the solution graph of $R(T_1)$ with respect to time T_1 for $m_1 = n_1 = n_2 = 1/3, 1/2, 2/3, 1$. Figures 5.3a and 5.3b show the same type of solution graph. L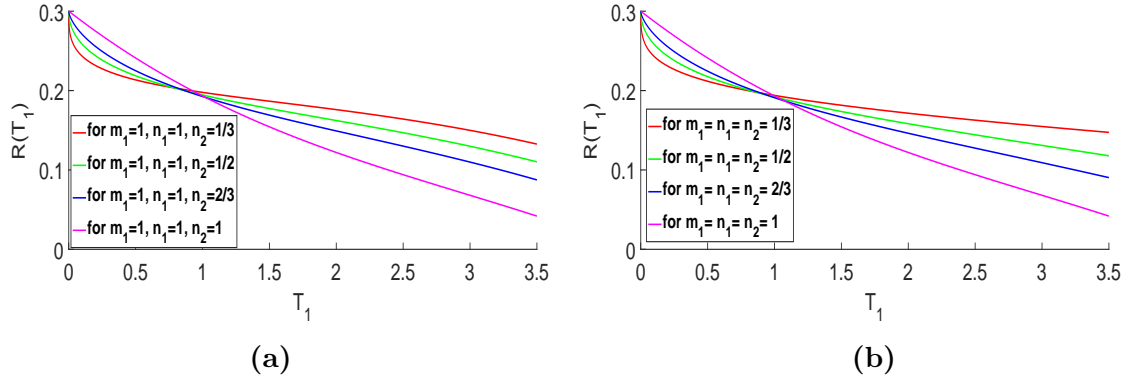astly, Figure 5.4 shows the 3-dimensional phase portrait of solutions of $P(T_1)$, $Q(T_1)$, and $R(T_1)$ for $m_1 = n_1 = n_2 = 1/3, 1/2, 2/3, 1$.
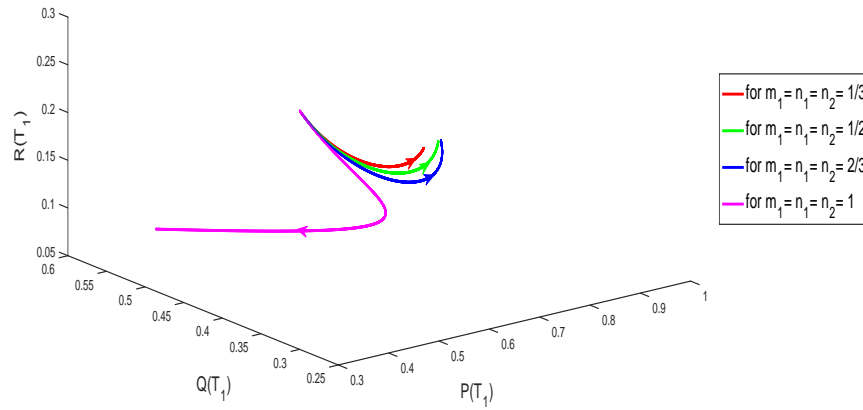
Figure 5.4: 3-dimensional phase portrait of solutions of $P(T_1)$, $Q(T_1)$ and $R(T_1)$ for $m_1 = n_1 = n_2 = 1/3, 1/2, 2/3, 1$.

111

5.7 Conclusions

Integer-order differential equations are commonly used to describe the prey-predator model. Nowadays, fractional order differential equations attract researchers a lot, so they have applied it in different fields of science, including biology, ecology, etc. Many authors have used the HPM to get an approximate solution of the fractional order prey-predator model. But in most of the cases, the models they considered in the papers are two-dimensional. In our study, we have extended the HPM to a three-dimensional prey-predator model, where the three components are detritus, micro-organism pool, and invertebrate predator. Here, we have derived the approximate analytical solution of our model applying the HPM, which is better than other perturbation methods generally used in fractional calculus. In our model, the detritus grows logistically, and loss of detritus due to the micro-organism pool follows Holling type-II response function. Here, we have considered the Ivlev-type response function as the uptake function of the invertebrate predator. This Ivlev-type response function is rarely used in the fractional-order prey-predator models by other researchers. This can be a motivation for solving a much more complicated form of the prey-predator model in the future.

Chapter 6

Effect of Prey Refuge on a Fractional Order Detritus-Based Predator-Prey Model in Presence of Toxicity *

6.1 Introduction

The process of extending differentiation and integration to any non-integer order is referred to as fractional calculus. These days, researchers are very interested in fractional calculus. Over the years, fractional calculus has been widely employed in numerous domains, including fluid dynamics, medicine, biology, ecology, and more (Cole, 1993; El-Sayed et al. , 2007; Fedri, 2012; Machado , 2010; Machado and Galhano, 2012). The application of fractional calculus has been spread massively, and it is very realistic compared to the integer-order calculus for any living system for its memory property. Due to the memory effect, for any prey-predator model, the preceding state has an influence on the present dynamics. There are different types of fractional derivatives. One of the commonly used fractional derivatives in any prey-predator model is the Caputo derivative, which was first introduced by Caputo (Caputo, 1967) and later used by several authors (Balci, 2023; Choi et al., 2014; Isik and Kangalgil, 2024; Owolabi, 2017).

The functional response significantly impacts the behavioral patterns of any prey-predator model. A predator's functional response refers to the quantity of prey it consumes within

---
*Chapter based on the paper submitted in Journal of Mathematical Biology for publication

a specific time frame. Several kinds of functional responses exist, such as Holling type-I (Li et al., 2021; Seo and DeAngelis, 2003; Seo and Kot, 2008), Holling type-II (Alsakaji et al., 2021; Molla et al., 2019; Zhou et al., 2019), Holling type-III (Agarwal and Pathak, 2012; Huang et al., 2006; Majumdar, 2022), Holling type-IV (Agarwal and Pathak, 2017; Datta et al., 2019; Liu and Huang, 2020), Crowley Martin (Gazi and Das, 2010; Panja, 2021; Santra et al., 2020), Beddington-Deangelis (Hwang, 2003; Pal and Mandal, 2014; Pal et al., 2019), Hassell-Varley (Hsu et al., 2008; Xu and Li, 2015), and so on. Nevertheless, Holling type-II is more suitable for the invertebrate predator than other functional responses. A novel functional response was created by Ivlev (1961) that can be used against both vertebrate and invertebrate predators. Ivlev-type functional response has been employed by numerous authors in their prey-predator models (Kooij and Zegeling, 1996; Liu et al., 2016; Wang et al., 2010).

Prey refuge is an additional factor in a prey-predator model that might influence its dynamic behaviour. Several authors have established the influence of prey refuge in the prey-predator paradigm (Balci, 2023; Collings, 1995; Freedman, 1980; Gonzalez-Olivares and Ramos-Jiliberto, 2003; Kar, 2005; Yan and Zhang, 2008; Zhao and Shao, 2008). Li et al. (2017), Chauhan et al. (2024) examined the impact of prey refuge in a fractional-order prey-predator system.

Nowadays, environmental pollution is increasing day by day in such a way that any prey-predator model in an ecosystem is affected if toxicant is present in that ecosystem. The toxic materials that are present in the environment cause damage to the stability of an ecosystem. Numerous researchers have already studied the impact of toxicity on a prey-predator model (Assila et al., 2024; Das et al., 2023, 2009; Freedman and Shukla, 1990; Jana et al., 2016; Moussaoui A. et al., 2010; Samanta, 2010).

A fractional-order mathematical model of prey and predator based on detritus in the Sundarban mangrove forest and the nearby estuary has been reported in our work. In our model,

the micro-organism pool is considered as prey, and the invertebrate is taken as predator. In mangrove estuary, tidal waves come twice a day, and due to tidal influence, some amount of micro-organisms of the adjacent estuary always washed out, and as a result of this type of prey refuge, an amount of micro-organism is protected from predation. This prey refuge enhances the prey-predator coexistence and prevents the micro-organism from extinction. It is known that the industries always release a huge amount of toxic substances into marine water. Due to the tidal influence of the adjacent Bay of Bengal, a huge amount of marine water enters the estuary. The growth of micro-organism pools and invertebrate predators are affected because of this toxicity. Throughout the work, we have discussed how the dynamic is affected by the toxicity and prey-refuge.

The current investigation has been carried out in the following order: Section 6.2 describes the model using certain fundamental presumptions. Section 6.3 comprises preliminary information, such as pre-existing definitions, theorems, and lemmas that are utilized throughout the study. The system's non-negativity is explained in section 6.4. Section 6.5 explains the model system's boundedness, while Section 6.6 demonstrates that the system has a unique solution. The various equilibria and their corresponding feasibility criteria are given in Section 6.7. The system's dynamic behavior is discussed in section 6.8, where the local stability analysis is mainly explained. Numerical simulations for various parameter values are shown in section 6.9. The report culminates in a conclusion included in section 6.10, which provides an explanation of the summary of our study's findings.

6.2 Model formulation

Here, we have constructed a deterministic model as follows:

$$
\begin{aligned}
{}^{c}_{t_0}D^p_t x_1(t) &= x_1(r_1 - ax_1) + kmx_3. \\
{}^{c}_{t_0}D^p_t x_2(t) &= x_2\left(r_2 - \frac{bx_2}{ax_1}\right) - fx_3\{1 - e^{-g(1-\delta)x_2}\} - \alpha x_2{}^2. \\
{}^{c}_{t_0}D^p_t x_3(t) &= x_3\left[-m + f\{1 - e^{-g(1-\delta)x_2}\}\right] - \beta x_3,
\end{aligned}
\tag{6.1}
$$

where

$x_1(0) > 0, x_2(0) > 0, x_3(0) > 0$, and

x_1 = biomass of detritus,

x_2 = biomass of micro-organism,

x_3 = biomass of invertebrate predator,

r_1 = detritus's growth rate,

r_2 = micro-organism pool's growth rate,

$\frac{ar_2}{b}$ = carrying capacity of micro-organism pool,

f = rate of conversion of food of invertebrate predator,

m = invertebrate predator's normal death rate,

km = detritus recycle rate after the death of invertebrate predator,

g = hunting success,

δ = prey refuge rate,

α = coefficient of toxicity to the prey species,

β = coefficient of toxicity to the predator species.

We also assume that the growth of detritus is assumed to follow a logistic type of growth equation and the Ivlev-type uptake function is considered for predator's functional response. Here, $\frac{d(\alpha x_2{}^2)}{dx_2} = 2\alpha x_2 > 0$, and $\frac{d^2(\alpha x_2{}^2)}{dx_2{}^2} = 2\alpha > 0$, which shows the accelerated growth of

116

toxicant, and as a result, the species consume the toxic-effected food more.

For simplicity, we convert our system into a non-dimensional system using the following transformations:

$x_1 = \frac{mX}{a}$, $x_2 = \frac{Y}{g}$, $x_3 = \frac{mZ}{fg}$, $t = \frac{T}{m}$.

Then the system (6.1) converted into

$$
\begin{aligned}
{}_{T_0}^{c}D_T^p X(T) &= X(\eta - X) + \gamma Z. \\
{}_{T_0}^{c}D_T^p Y(T) &= Y\left(\sigma - \frac{\phi Y}{X}\right) - Z\{1 - e^{-(1-\delta)Y}\} - \mu_1 Y^2. \\
{}_{T_0}^{c}D_T^p Z(T) &= Z\left[-1 + \psi\{1 - e^{-(1-\delta)Y}\}\right] - \mu_2 Z,
\end{aligned}
\tag{6.2}
$$

where $X(0) > 0, Y(0) \geq 0,\ Z(0) \geq 0$.

Here, $\eta = \frac{r_1}{m}$, $\gamma = \frac{ka}{mfg}$, $\sigma = \frac{r_2}{m}$, $\phi = \frac{b}{gm^2}$, $\mu_1 = \frac{\alpha}{mg^2}$, $\psi = \frac{f}{m}$, $\mu_2 = \frac{\beta}{fg}$.

6.3 Preliminaries

In this section, definition and some fundamental properties of Caputo derivative are discussed briefly.

Definition 6.1

Let's examine a continuous function $H(X) \in C^n([T_0 + \infty), \mathbb{R})$ with fractional order $p > 0$ (Petras, 2011).

Then the Caputo derivative of $H(X)$ is defined as

$$
{}_{T_0}^{c}D_T^p H(T) = \frac{1}{\Gamma(q - p)} \int_{T_0}^{T} \frac{H^q(s)}{(T - s)^{p-q+1}} ds,
$$

where $\Gamma(q - p)$ is the gamma function, $q \in \mathbb{Z}^+$, $p \in (q - 1, q)$ and $T \geq T_0$.

When $q = 1$, then the mathematical form of the Caputo derivative is as follows:

$$_{T_0}^{c}D_T^p H(T) = \frac{1}{\Gamma(1-p)} \int_{T_0}^{T} \frac{H'(s)}{(T-s)^p} ds,$$

where $p \in (0, 1)$.

Lemma 6.1

Suppose $_{T_0}^{c}D_T^p H(T) \in C[a, b] \ \forall \ T \in (a, b)$, where $0 < p \leq 1$ and $H(T) \in C[a, b]$ (Odibat and Shawagfeh, 2007). Then

(i) If $_{T_0}^{c}D_T^p H(T) \geq 0$, then $H(T)$ is increasing function $\forall \ T \in [a, b]$.

(ii) If $_{T_0}^{c}D_T^p H(T) \leq 0$, then $H(T)$ is decreasing function $\forall \ T \in [a, b]$.

Theorem 6.1

Let us consider that $H(T) \in C_n[a, b]$, and $_{T_0}^{c}D_T^p H(T)$ is piecewise continuous in $[T_0, \infty)$, where p is positive and $n - 1 < p < n \ \forall \ n \in \mathbb{N}$ (Liang et al., 2015). Then

$$\mathcal{L}\left\{ _{T_0}^{c}D_T^p H(T)\right\} = s^p F(s) - \sum_{j=0}^{n-1} s^{p-j-1} H^j(T_0),$$

where $\mathcal{L}$ stands for Laplace transform and $F(s) = \mathcal{L}\left\{H(T)\right\}$.

Here, $\Re(s) \geq 0$, where $\Re(s)$ stands for the real part of s.

Theorem 6.2

For each $M \in \mathbb{C}^{n \times n}$, we can write (Kexue and Jigen, 2011)

$$\mathcal{L}\left\{T^{v-1} E_{u,v}(MT^u)\right\} = \frac{s^{u-v}}{s^u - M} \ \ \forall \ u > 0, v > 0,$$

118

where s is a complex number. The real part of s, i.e., $\Re(s) > \| M \|^{\frac{1}{u}}$, and $E_{u,v}$ is the Mittag-Leffler function (Podlubny, 1999).

Definition 6.2

Let us assume a system of equations

$$
{}^{c}_{T_0}D^p_T H(T) = \Psi(T, H),
$$

which represents a dynamical system with Caputo fractional order p and $H(T_0) > 0$. By solving $\Psi(T, H) = 0$, we get the system's equilibria H^* (Li et al., 2009).

Theorem 6.3

Assume a fractional-order system $\frac{d^p(x)}{dt^p} = g(x)$, $x(0) = x_0$ with $0 < p < 1$ and $x \in \mathbb{R}^n$ (Petras, 2011). An equilibrium point is called locally asymptotically stable if the Jacobian matrix $J = \frac{\partial g}{\partial x}$ possesses the eigenvalues λ_i for all the equilibrium points satisfying $|arg(\lambda_i)| > \frac{p\pi}{2}$.

6.4   Positivity of solutions

Theorem 6.4

All the solutions of the system (6.2) starting in $\mathbb{R}^{+3}$ are always positive.

Proof

Let $P(T_0) = (X_{T_0}, Y_{T_0}, Z_{T_0}) \in \Omega^+ = \left\{ (X, Y, Z) \in \Omega^+ : X, Y, Z \in \mathbb{R}^+ \right\}$ is the initial value of $X(T)$, $Y(T)$, and $Z(T)$, where $\mathbb{R}^+ = \left\{ X \in \mathbb{R} : X \geq 0 \right\}$. To show $X(T), Y(T), Z(T) \geq 0$ $\forall\, T \geq 0$, let's assume that $Z(T) \geq 0\ \forall\, T \geq 0$ is not true. Then $\exists$ a constant T_1 satisfying

$T_0 \leq T < T_1$ such that

$$
\begin{cases}
Z(T) > 0, & \text{when } T_0 \leq T < T_1, \\
Z(T_1) = 0, & \text{when } T = T_1, \\
Z(T_1{}^+) < 0, & \text{when } T \geq T_1.
\end{cases}
$$

For the system (6.2), it is clear that ${}_{T_0}^c D_T^p Z(T) \mid_{Z(T_1)=0} = 0$.

Thus, using Lemma 6.1, we have $Z\left(T_1{}^+\right) = 0$, which creates a contradiction in the fact $Z\left(T_1{}^+\right) < 0$. Thus, we can claim that $Z(T) \geq 0 \ \forall \ T \in [T_0, \infty)$.

In a similar way, we can prove that $Y(T) \geq 0 \ \forall \ T \in [T_0, \infty)$, and $X(T) \geq 0 \ \forall \ T \in [T_0, \infty)$.

Hence, the theorem is proved.

6.5 Boundedness of the solutions

Theorem 6.5

The system (6.2) possesses uniformly bounded solutions.

Proof

Suppose $Q(T) = X + \psi Y + Z$. Then

$$
\begin{aligned}
{}_{T_0}^c D_T^p Q(T) &= {}_{T_0}^c D_T^p X(T) + {}_{T_0}^c D_T^p Y(T) + {}_{T_0}^c D_T^p Z(T) \\
&= X(\eta - X) + \gamma Z + Y\left(\sigma - \frac{\phi Y}{X}\right) - \psi \mu_1 Y^2 - Z - \mu_2 Z \\
&\leq -m_1 Q(T) + 2\eta X - X^2 + \frac{\psi \sigma^2}{\phi} X,
\end{aligned}
$$

where $m_1 = \min\{\eta, \sigma, (1 + \mu_2 - \gamma)\}$.

Here, $(1 + \mu_2 - \gamma) > 0$ as $\gamma < 1$.

Let $G(X) = 2\eta X - X^2 + \frac{\psi\sigma^2}{\phi}X$.

Then G has maximum value $G_{max} = \left(\eta + \frac{\psi\sigma^2}{2\phi}\right)\left(2\eta + \frac{\psi\sigma^2}{\phi}\right) - \frac{1}{4}\left(2\eta + \frac{\psi\sigma^2}{\phi}\right)^2$,

at $X = \frac{1}{2}\left(2\eta + \frac{\psi\sigma^2}{\phi}\right)$.

Hence, it follows that ${}^{c}_{T_0}D^p_T Q(T) + m_1 Q(T) \leq G_{max}$.

Now applying the Laplace transformation, we get

$$s^p F(s) - s^{p-1}Q(0) + m_1 F(s) \leq G_{max}\frac{1}{s}, \text{where } F(s) = \mathcal{L}\{Q(T)\}$$

$$\Rightarrow F(s) \leq Q(0)\frac{s^{p-1}}{s^p + m_1} + G_{max}\frac{1}{s(s^p + m_1)}. \qquad (6.3)$$

Now applying the inverse Laplace transformation, we get

$$Q(T) \leq Q(0)\mathcal{L}^{-1}\left\{\frac{s^{p-1}}{s^p + m_1}\right\} + G_{max}\mathcal{L}^{-1}\left\{\frac{s^{p-(p+1)}}{s^p + m_1}\right\}.$$

Now using Theorem 6.2, we obtain

$$Q(T) \leq Q(0)E_{p,1}\{-m_1 T^p\} + G_{max}T^p E_{p,p+1}\{-m_1 T^p\}. \qquad (6.4)$$

Again, using Mittag-Leffer functions properly, we obtain

$$E_{p,1}\{-m_1 T^p\} = (-m_1 T^p)E_{p,p+1}\{-m_1 T^p\} + \frac{1}{\Gamma(1)}.$$

Thus, we have

$$T^p E_{p,p+1}\{-m_1 T^p\} = -\frac{1}{m_1}\left[E_{p,1}\{-m_1 T^p\} - 1\right]. \qquad (6.5)$$

From (6.4) and (6.5), we achieve

$Q(T) \leq \left\{Q(0) - \frac{1}{m_1}G_{max}\right\}E_{p,1}\{-m_1 T^p\} + \frac{1}{m_1}G_{max}$.

Since $E_{p,1} \to 0$ as $T \to \infty$, so, $Q(T) \leq \frac{1}{m_1}G_{max}$.

So, the system (6.2) possesses uniformly bounded solutions in the region

$\mathbb{B} = \{(X, Y, Z) \in \Omega^+ | X + \psi Y + Z \leq \frac{1}{m_1} G_{max} + \epsilon, \epsilon \geq 0\}.$

6.6 Uniqueness of the solutions

Theorem 6.6

Let us consider the system (6.2) has the solution $P(T) = (X(T), Y(T), Z(T)) \in \Omega^+$, and the initial condition is $P(T_0) = (X_{T_0}, Y_{T_0}, Z_{T_0}) \in \Omega^+ = \{(X, Y, Z) \in \mathbb{R}^{+3} | max\{|X|, |Y|, |Z|\} \leq U\}$, where $T \geq 0$ and U is sufficiently large. Then the solution $P(T) = (X(T), Y(T), Z(T)) \in \Omega^+$ is unique.

Proof

Let $P = (X, Y, Z) \in \Omega^+$, $\bar{P} = (\bar{X}, \bar{Y}, \bar{Z}) \in \Omega^+$, and consider a map $W(P) = (W_1(P), W_2(P), W_3(P))$ such that

$$
\begin{aligned}
W_1(P) &= X(\eta - X) + \gamma Z. \\
W_2(P) &= Y\left(\sigma - \frac{\phi Y}{X}\right) - Z\{1 - e^{-(1-\delta)Y}\} - \mu_1 Y^2. \\
W_3(P) &= Z\left[-1 + \psi\{1 - e^{-(1-\delta)Y}\}\right] - \mu_2 Z,
\end{aligned}
\tag{6.6}
$$

Now we have

$$\|W(P) - W(\bar{P})\| = |W_1(P) - W_1(\bar{P})| + |W_2(P) - W_2(\bar{P})|$$

$$+ |W_3(P) - W_3(\bar{P})|$$

$$= |X(\eta - X) - \bar{X}(\eta - \bar{X}) + \gamma(Z - \bar{Z})|$$

$$+ \left| Y\left(\sigma - \frac{\phi Y}{X}\right) - Z\{1 - e^{-(1-\delta)Y}\} - \mu_1 Y^2 \right.$$

$$\left. - \bar{Y}\left(\sigma - \frac{\phi \bar{Y}}{\bar{X}}\right) + \bar{Z}\{1 - e^{-(1-\delta)\bar{Y}}\} + \mu_1 \bar{Y}^2 \right|$$

$$+ \left| Z\big[-1 + \psi\{1 - e^{-(1-\delta)Y}\}\big] - \mu_2 Z \right.$$

$$\left. - \bar{Z}\big[-1 + \psi\{1 - e^{-(1-\delta)\bar{Y}}\}\big] + \mu_2 \bar{Z} \right|$$

$$\leq U_1|X - \bar{X}| + U_2|Y - \bar{Y}| + U_3|Z - \bar{Z}|$$

$$\leq L\|P - \bar{P}\|,$$

where $L = max\{U_1, U_2, U_3\}$, where

$$U_1 = \left(\eta + 2U + \phi U^2\right),$$

$$U_2 = \left(\sigma + 2\phi U^2 + 2\mu_1 U\right),$$

$$U_3 = \{2 + \gamma + \psi + (\psi + 1)Ue^{(1-\delta)U} + \mu_2\}.$$

Therefore, the Lipschitz condition is satisfied for $W(P)$ with respect to P.

Thus, the system (6.2) has a unique solution.

6.7   Equilibria and their feasibility

There exist three equilibria as follows:

(i) $E_1(\eta, 0, 0)$,

(ii) $E_2(\overline{X}, \overline{Y}, 0)$, where $\overline{X} = \eta$, $\overline{Y} = \frac{\sigma}{\frac{\phi}{\eta}+\mu_1}$.

(iii) $E_3(X^*, Y^*, Z^*)$, where $Y^* = \frac{1}{(1-\delta)} ln\left\{\frac{\psi}{\psi-(\mu_2+1)}\right\}$.

It is pretty challenging to find the exact value of X^* and Z^*, but we find a polynomial of Z, which is as follows:

$$D_1 Z^3 + D_2 Z^2 + D_3 Z + D_4 = 0,$$

where

$D_1 = \frac{4\gamma(\mu_2+1)^2}{\psi^2}$,

$D_2 = 4\gamma\left\{\frac{2\mu_1(\mu_2+1)}{\psi}Y^{*2} - 2\sigma Y^*\frac{\mu_2+1}{\psi}\right\}$,

$D_3 = 4\gamma\left\{\sigma^2 Y^{*2} + \mu_1{}^2 Y^{*4} - 2\sigma\mu_1 Y^{*3}\right\} - \frac{4\phi\eta(\mu_2+1)}{\psi}Y^{*2}$,

$D_4 = 4\phi Y^{*3}\left(\sigma\eta - \phi Y^* - \eta\mu_1 Y^*\right)$.

Here, $D_1 > 0$.

If any one of D_2, D_3, and D_4 are negative, then we can conclude that there exists at least one positive real root, say Z^*. So,

$$X^* = \frac{\eta+\sqrt{\eta^2+4\gamma Z^*}}{2}.$$

Here, $E_3(X^*, Y^*, Z^*)$ is feasible when $\mu_2 < (\psi - 1)$.

6.8   System's dynamical behaviour

This section covers the study of the local stability behaviour of our model system (6.2) around the equilibria.

The system (6.2) possesses the variational matrix

$$J = \begin{bmatrix} \eta - 2X & 0 & \gamma \\ \phi\frac{Y^2}{X^2} & \sigma - 2\phi\frac{Y}{X} - Z(1-\delta)e^{-(1-\delta)Y} - 2\mu_1 Y & -\left\{1 - e^{-(1-\delta)Y}\right\} \\ 0 & \psi(1-\delta)Ze^{-(1-\delta)Y} & -1 + \psi\left\{1 - e^{-(1-\delta)Y}\right\} - \mu_2 \end{bmatrix}.$$

Theorem 6.8

The system (6.2) shows a local asymptotic unstable behaviour around E_1.

Proof

At $E_1\left(\eta, 0, 0\right)$, the variational matrix J has the characteristic equation

$$(\lambda + \eta)(\lambda - \sigma)\left(\lambda + 1 + \mu_2\right) = 0.$$

Thus, the three eigenvalues are $\lambda_1 = -\eta$, $\lambda_2 = \sigma$, $\lambda_3 = -(1 + \mu_2)$. Thus,

$|arg(\lambda_1)| = \pi > \frac{p\pi}{2} \ \forall \ 0 < p < 1,$

$|arg(\lambda_2)| = 0 < \frac{p\pi}{2} \ \forall \ 0 < p < 1,$

$|arg(\lambda_3)| = \pi > \frac{p\pi}{2} \ \forall \ 0 < p < 1.$

Therefore, according to theorem 6.3, it follows that the equilibrium point E_1 shows an unstable behaviour.

Theorem 6.9

The system (6.2) shows a local asymptotic stable behaviour around E_2 for $M_1 < \delta < M_2$, where $M_1 = 1 - \frac{1}{\bar{Y}} ln\left[\frac{\psi}{\psi - \left\{1 + \mu_2 - \left(\sigma - \frac{2\phi\bar{Y}}{\eta} - 2\mu_1\bar{Y}\right)\right\}}\right]$, and $M_2 = 1 - \frac{1}{\bar{Y}} ln\{\frac{\psi}{\psi - (\mu_2 + 1)}\}$.

Proof

At E_2, the variational matrix J has the characteristic equation

$$(\lambda + \eta)\left[\lambda^2 + A_1\lambda + B_1\right] = 0.$$

Here,

$$A_1 = 1 - \psi\{1 - e^{-(1-\delta)\overline{Y}}\} + \mu_2 - \left(\sigma - \frac{2\phi}{\eta}\overline{Y} - 2\mu_1\overline{Y}\right),$$

$$B_1 = \left(\sigma - \frac{2\phi}{\eta}\overline{Y} - 2\mu_1\overline{Y}\right)\left[-1 + \psi\{1 - e^{-(1-\delta)\overline{Y}}\} - \mu_2\right].$$

Let the characteristic equation possesses three roots λ_1, λ_2, and λ_3, where one root $\lambda_1 = -\eta < 0$.

So, if $A_1 > 0$ and $B_1 > 0$, then

$|arg(\lambda_1)| = \pi > \frac{p\pi}{2} \ \forall \ 0 < p < 1$,

$|arg(\lambda_2)| = \pi > \frac{p\pi}{2} \ \forall \ 0 < p < 1$,

$|arg(\lambda_3)| = \pi > \frac{p\pi}{2} \ \forall \ 0 < p < 1$.

Now $A_1 > 0$ if $\delta > M_1$, and $B_1 > 0$ if $\delta < M_2$, where

$$M_1 = 1 - \frac{1}{\overline{Y}}ln\left[\frac{\psi}{\psi - \left\{1 + \mu_2 - \left(\sigma - \frac{2\phi\overline{Y}}{\eta} - 2\mu_1\overline{Y}\right)\right\}}\right],$$

and

$$M_2 = 1 - \frac{1}{\overline{Y}}ln\left\{\frac{\psi}{\psi - (\mu_2 + 1)}\right\}.$$

Therefore, according to theorem 6.3, it follows that the equilibrium point E_2 shows a local asymptotic stable behaviour for $M_1 < \delta < M_2$.

Theorem 6.10

The system (6.2) shows a conditional local asymptotic stable behaviour around $E_3(X^*, Y^*, Z^*)$.

Proof

The characteristic equation at E_3 is

$$\left\{\lambda - (\eta - 2X^*)\right\}\left(\lambda^2 + A_2\lambda + B_2\right) = 0,$$

where

$$A_2 = \left\{\frac{2\phi Y^*}{X^*} + Z^*(1-\delta)e^{-(1-\delta)Y^*} + 2\mu_1 Y^* - \sigma\right\},$$

$$B_2 = (1+\mu_2)\,Z^*(1-\delta)e^{-(1-\delta)Y^*} - \phi\gamma\frac{Y^{*2}}{X^{*2}}\psi Z^*(1-\delta)e^{-(1-\delta)Y^*}.$$

Let the characteristic equation possesses three roots λ_1, λ_2, and λ_3, where one root $\lambda_1 = -\sqrt{\eta^2 + 4\gamma Z^*} < 0$.

So, if $A_2 > 0$ and $B_2 > 0$, then

$|arg(\lambda_1)| = \pi > \frac{p\pi}{2} \ \forall \ 0 < p < 1$,

$|arg(\lambda_2)| = \pi > \frac{p\pi}{2} \ \forall \ 0 < p < 1$,

$|arg(\lambda_3)| = \pi > \frac{p\pi}{2} \ \forall \ 0 < p < 1$.

Therefore, according to theorem 6.3, it follows that the equilibrium point E_3 shows a local asymptotic stable behaviour if $A_2 > 0$ and $B_2 > 0$.

Hopf-bifurcation

The system (6.2) can be rewritten as

$$\,^c_{T_0}D^p_T P(T) = f(\delta, P(T)), \tag{6.7}$$

where $T > 0$, $P(T) = (X(T), Y(T), Z(T))$, and $0 < \delta \le 1$.

The system (6.2) experiences a Hopf-bifurcation around $E_3(X^*, Y^*, Z^*)$, when δ meets the

critical value δ^*, and the subsequent conditions are satisfied concurrently.

(i) Equation (6.7) comprises one eigenvalue λ_1 which is real, and two eigenvalues that are complex conjugate to one another, i.e., $\lambda_{2,3}(\delta) = \mu(\delta) \pm iv(\delta)$,

(ii) $\mu_{1,2,3}(p, \delta^*) = 0$, where $\mu_{1,2,3} = \frac{p\pi}{2} - \left| arg\left(\lambda_j(\delta)\right)\right|$, $j = 1, 2, 3$,

(iii) $\frac{\partial \mu}{\partial \delta}\big|_{\delta=\delta^*} \neq 0$.

6.9   Numerical simulations

To validate the theoretical findings, this section includes numerical simulations that have been done using the Predictor-Corrector method applicable to differential equations with fractional order. For this purpose, a set of parameter values have been considered, which is $\eta = 3.5$, $\phi = 0.68$, $\sigma = 2.2$, $\gamma = 0.5$, $\mu_1 = 0.05$, $\psi = 1.1$, and $\mu_2 = 0.005$.

Then we have calculated the critical value of δ, i.e., $\delta^* = 0.457$. The only two parameters
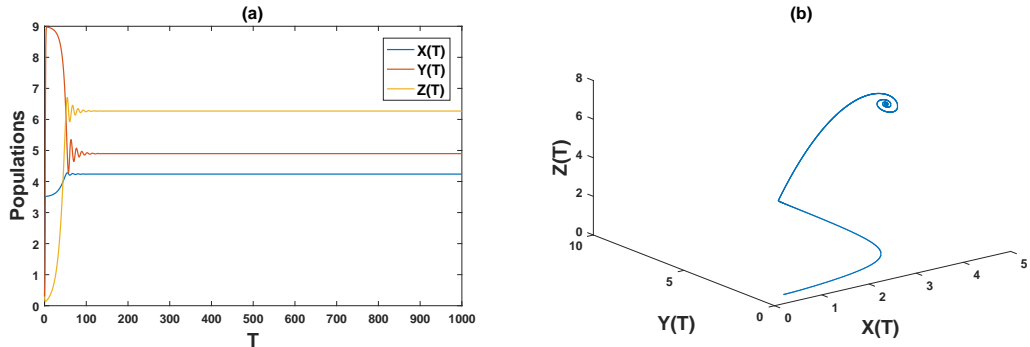
Figure 6.1: Stable state of the system (6.2) around E_3 for $p = 1$, $\eta = 3.5$, $\phi = 0.68$, $\sigma = 2.2$, $\gamma = 0.5$, $\psi = 1.1$, $\mu_1 = 0.05$, $\mu_2 = 0.005$, and $\delta = 0.5 > \delta^* = 0.457$ with the initial values $(0.3, 0.3, 0.3)$: (a) Time series plot, (b) Phase diagram plot.

that change during the whole numerical simulations are p and δ, while the other parameters remains constant.

For Figure 6.1, we take $\delta = 0.5 > \delta^* = 0.457$, $p = 1$. Figure 6.1 shows the system (6.2) is stable when $\delta > \delta^*$ and $p = 1$.

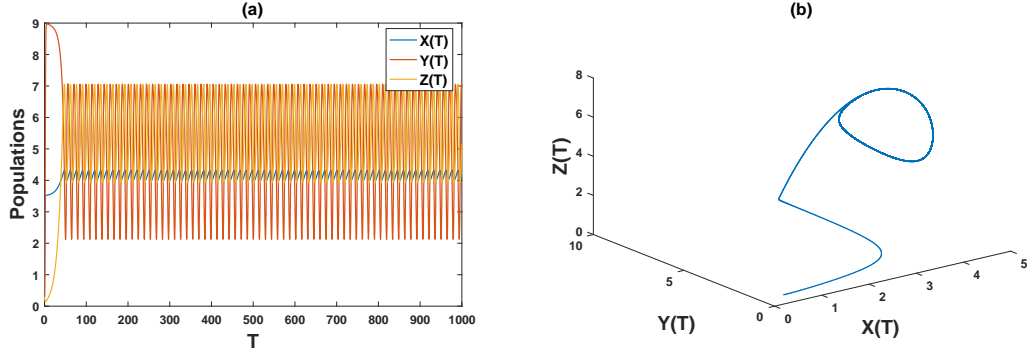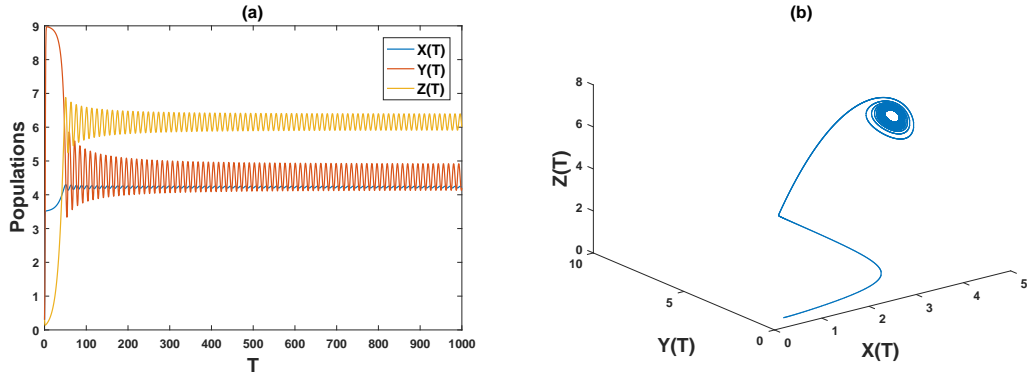Next we set the value $\delta = 0.4 < \delta^*$, and $p = 1$. Now from the Figure 6.2, we have seen that

Figure 6.2: Chaotic solution of the system (6.2) around E_3 for $p = 1$, $\eta = 3.5$, $\phi = 0.68$, $\sigma = 2.2$, $\gamma = 0.5$, $\psi = 1.1$, $\mu_1 = 0.05$, $\mu_2 = 0.005$, and $\delta = 0.4 < \delta^* = 0.457$ with the initial values $(0.3, 0.3, 0.3)$: (a) Time series plot, (b) Phase diagram plot.

Figure 6.3: Hopf-bifurcation diagram of the model system (6.2) at $\delta = 0.457$ and other parameters are fixed as $p = 1$, $\eta = 3.5$, $\phi = 0.68$, $\sigma = 2.2$, $\gamma = 0.5$, $\psi = 1.1$, $\mu_1 = 0.05$, $\mu_2 = 0.005$ with the initial values $(0.3, 0.3, 0.3)$: (a) Time series plot, (b) Phase diagram plot.
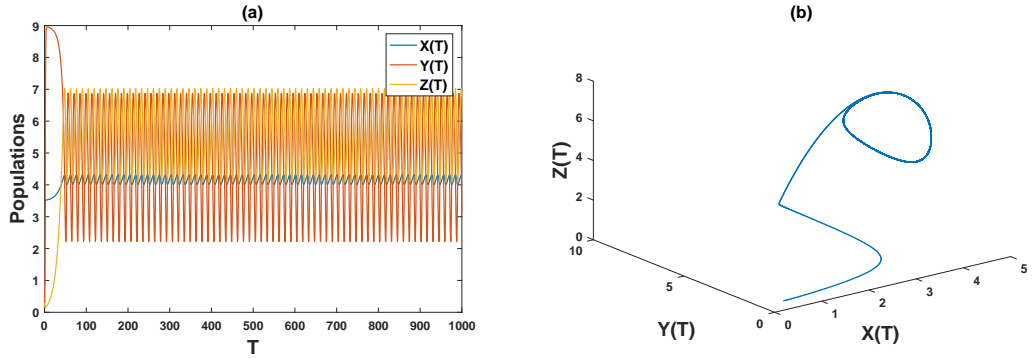
Figure 6.4: Chaotic solution of the system (6.2) around E_3 for $\eta = 3.5$, $\phi = 0.68$, $\sigma = 2.2$, $\gamma = 0.5$, $\psi = 1.1$, $\mu_1 = 0.05$, and $\mu_2 = 0.005$, $\delta = 0.4$, and $p = 0.99$, with the initial values $(0.3, 0.3, 0.3)$: (a) Time series plot, (b) Phase diagram plot.

Figure 6.5: Chaotic solution of the system (6.2) around E_3 for $\eta = 3.5$, $\phi = 0.68$, $\sigma = 2.2$, $\gamma = 0.5$, $\psi = 1.1$, $\mu_1 = 0.05$, and $\mu_2 = 0.005$, $\delta = 0.4$, and $p = 0.95$ with the initial values $(0.3, 0.3, 0.3)$: (a) Time series plot, (b) Phase diagram plot.
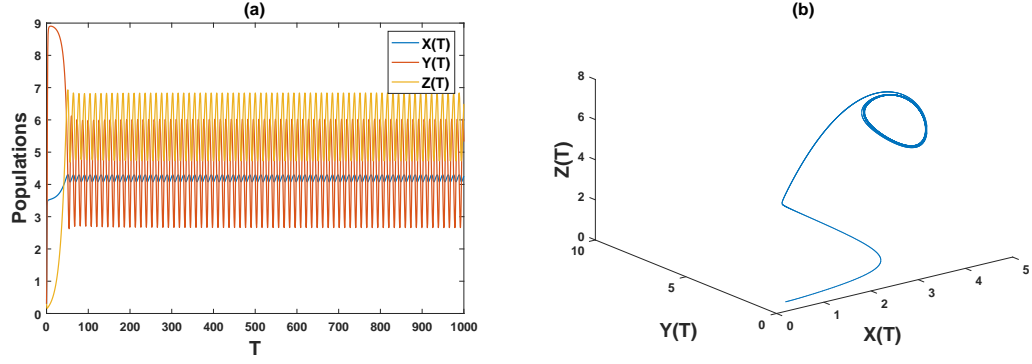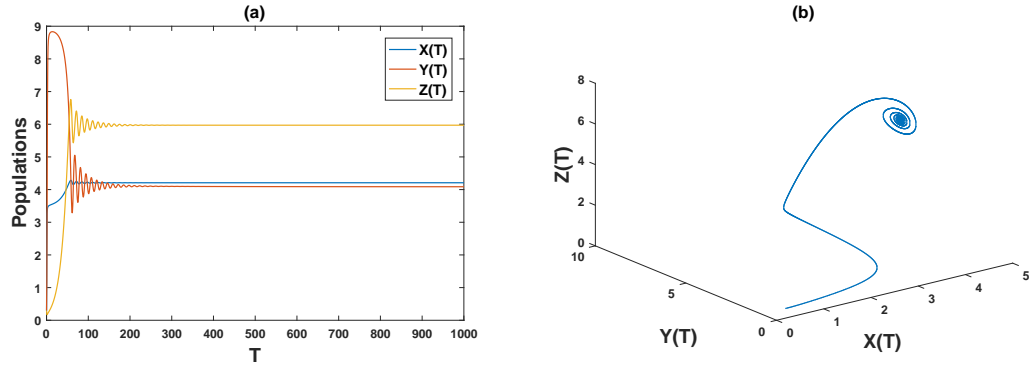

Figure 6.6: Stable state of the system (6.2) around E_3 for $\eta = 3.5$, $\phi = 0.68$, $\sigma = 2.2$, $\gamma = 0.5$, $\psi = 1.1$, $\mu_1 = 0.05$, and $\mu_2 = 0.005$, $\delta = 0.4$, and $p = 0.88$ with the initial values $(0.3, 0.3, 0.3)$: (a) Time series plot, (b) Phase diagram plot.

Figure 6.7: Stable state of the system (6.2) around E_3 for $\eta = 3.5$, $\phi = 0.68$, $\sigma = 2.2$, $\gamma = 0.5$, $\psi = 1.1$, $\mu_1 = 0.05$, and $\mu_2 = 0.005$, $\delta = 0.4$ and $p = 0.84$ with the initial values $(0.3, 0.3, 0.3)$: (a) Time series plot, (b) Phase diagram plot.

Figure 6.8: Hopf-bifurcation diagram of model system (6.2) at $p = 0.91$, and other parameters are fixed as $\eta = 3.5$, $\phi = 0.68$, $\sigma = 2.2$, $\gamma = 0.5$, $\psi = 1.1$, $\mu_1 = 0.05$, $\mu_2 = 0.005$, $\delta = 0.4$ with the initial values $(0.3, 0.3, 0.3)$: (a) Time series plot, (b) Phase diagram plot.

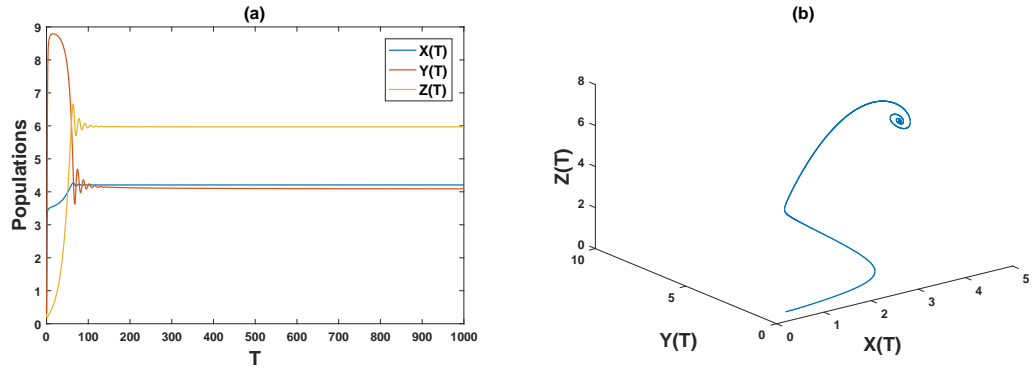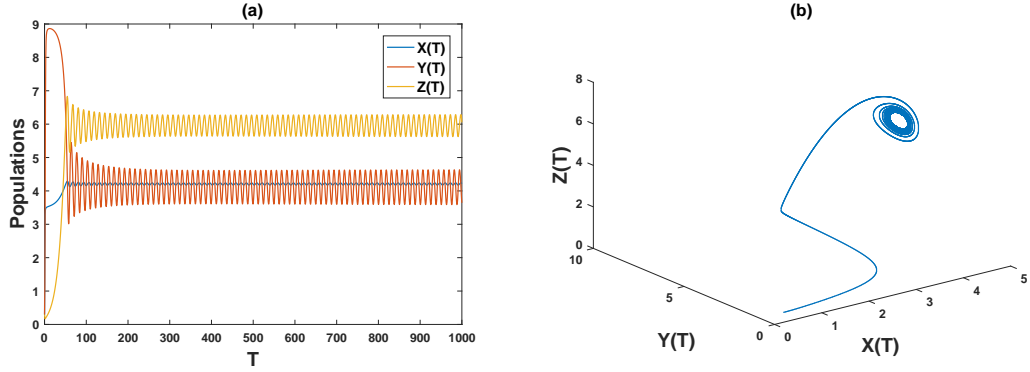the system (6.2) is unstable for $\delta < \delta^*$.

Figure 6.3 demonstrates the existence of Hopf-bifurcation at $\delta = \delta^* = 0.457$, treating the parameter δ as the bifurcation parameter.

We have now changed the system (6.2)'s order p to show the effect of it. Figure 6.4 illustrates the instability of the system (6.2) at $\delta = 0.4$ and $p = 0.99$. For $\delta = 0.4$, and $p = 0.95$, Figure 6.5 illustrates the system (6.2)'s instability, while Figure 6.6 shows the system (6.2) is stable at $\delta = 0.4$, and $p = 0.88$. Additionally, the system is stable for $\delta = 0.4$, and $p = 0.84$ (Figure 6.7).

Therefore, we may state that the fractional order p highly influences the system (6.2)'s dynamic characteristics. We can change an unstable system into a stable system by lowering the fractional order. Figure 6.8 demonstrates the existence of Hopf-bifurcation at $p = 0.91$, treating the parameter p as the bifurcation parameter.

6.10   Conclusion

This work introduces a model that examines the relationship between predator and prey in the Sundarban mangrove forest and the nearby estuary, taking into account the existence of

toxicity. The phrase "prey refuge," which arises as a result of the tidal wave, is also included in our model. The analysis focuses on the existence of positive, unique, and bounded solution. We have determined the various equilibria and their corresponding feasibility conditions. This chapter demonstrates the dynamics of our suggested model for various equilibrium points and conditions. This research primarily examines how the prey-refuge term can affect the dynamics. Distinct dynamics can be observed with varying prey-refuge rates. The stability behaviour undergoes a significant change when the prey-refuge rate is altered. An integer order system exhibits stability above a certain critical value of prey-refuge rate, while instability occurs below that critical value. At the critical value, a Hopf-bifurcation with a little amplitude occurs.

The fractional order is another crucial characteristic of our system. This fractional order can alter a system's steady-state behaviour. While the system may be unstable for integer order derivatives, even a little change in the fractional order can cause the instability to become stable. In our study, we have shown the impact of fractional order on stability. Thus, this study concludes with a remark that the memory property of fractional order regulates the dynamics of our proposed model with high efficiency.

Chapter 7

Discussion

In this thesis, we have mainly formulated some detritus-based prey-predator models which are deterministic in nature in Sundarban mangrove forest and the nearby estuary. In every model, the primary energy source is detritus, whereas the micro-organism pool and invertebrates, in turn, represent the roles of prey and predator, respectively. These models are based on different conditions and parameters. Here, we have discussed the summary of key findings that we have got throughout the six chapters.

Chapter 1 discusses some general and fundamental topics including definitions which have been used throughout the thesis. A brief idea and scope of the chapters are also discussed.

In **Chapter 2**, a predator-prey model based on detritus is discussed. It is assumed that the loss of detritus follows a Holling type-II functional response, and the invertebrate predator's uptake function is an Ivlev-type function. This uptake function has a complex ecological interpretation and demonstrates the complexity of the model system, leading to some intricate mathematical results that are, from an ecological perspective, extremely plausible. We obtain the conditions of the global attractor, periodic orbit, and Hopf-bifurcation under specific circumstances in the study. Here, we can observe that the micro-organism pool's growth rate serves as a bifurcation parameter and is a significant variable that may impact the stability of the mangrove ecosystem. To interpret our analytical results' qualitative behaviour, numerical simulations are run with various system parameter values.

In **Chapter 3**, a model is presented wherein the growth of micro-organisms is expected to

follow donor-controlled type function, whereas the detritus is considered to follow logistic type growth. A gestation time delay that is incorporated into the invertebrate predator's functional response term is used to analyse the model. Both the local and global stability of several feasible equilibria are included in the mathematical study. It is shown that a stable limit cycle surrounds the interior equilibrium point. Additionally, a critical value for the micro-organism pool's food conversion efficiency rate has been identified, and for this value, Hopf-bifurcation behaviour is observed near the equilibrium point. It can be claimed that in the real situation, we can also observe the same dynamical behaviour in the Sundarban estuary. We have shown that the dynamics of time-delay differential equation model is more complicated and rich compare to the ordinary-differential equation model. Here, it is shown that the discrete time-delay has a deep impact on the dynamics of ecosystem. It even destabilizes the stable equilibrium point $E_3(X^*, Y^*, Z^*)$. When the delay parameter passes its critical value $\hat{\tau}^0$, small-amplitude periodic oscillations known as Hopf-bifurcating oscillations occur. Due to presence of instability, a limit cycle is formed. All the analytical results are verified through numerical simulations for various system parameter values.

Chapter 4 discusses a model, where it is assumed that though the leading source of detritus is the plant litter of mangrove forest, a small amount of detritus is also formed from the dead bodies of invertebrate predators by the recycling process. The beauty of this chapter is that we have incorporated two different valued discrete time delays for the gestation of prey (micro-organism pool) and predator (invertebrate predator). Due to the time lag, our proposed model possesses more complicated dynamics than the ordinary differential equations system. We have made a thorough theoretical and numerical investigation without time delay and with time delay throughout the chapter. From the analysis of our model, some engrossing and functional outcomes have been obtained. From the biological aspect, the most salient fact from our study is that the time lag plays a leading role in shaping the dynamics of our proposed model. Without delays, the system is locally asymptotically stable

134

under some circumstances. These delays demolish the dynamical ecosystem's stability and give rise to periodic oscillations. It has been noted that the dynamical system is stable for both delays, under the critical values of the delay parameters. When the delay parameter passes its critical value, the dynamical system becomes unstable. A periodic oscillation is found with increasing delay, which leads to a complex dynamical system. A Hopf-bifurcation with small amplitude occurs at the critical values for both the delay parameters. Numerical illustrations also ensure our theoretical observations that the dynamics of our model are widely influenced by taking distinct values of delay parameters.

In **Chapter 5**, a model with fractional order is formulated. We have derived the approximate solution of the fractional order system using Homotopy Perturbation method (HPM) with high accuracy. This HPM is better than any other perturbation methods generally used in fractional calculus. As HPM is a rapid convergence method, we have done only a few iterations to get approximate analytical series solutions of the system. Numerical simulations have been experimented with different valued fractional orders to better understand our analytical findings.

Chapter 6 presents a model influenced by prey-refuge and toxicity. Throughout the chapter, the dynamics of our proposed model has been illustrated for different equilibrium points and conditions. The primary topic of this research is how prey-refuge affects the dynamics. For different values of prey-refuge rate, different types of dynamics can be seen. Changes in the prey-refuge rate cause a significant change in the stability behaviour. For an integer order system, a critical prey-refuge rate value is determined. Below that critical value, the system is stable; beyond it, the system is unstable; and at that critical value, a small-amplitude Hopf-bifurcation occurs.

Fractional order is the another important parameter for our system. This fractional order is capable to change the stability of a system. Even if the system is stable for integer order derivative, the stability may convert into instability with the slight change of fractional or-

der. In this chapter, the influence of fractional order in the matter of stability is observed. Thus, this chapter concludes with a remark that the memory effect of fractional order plays a significant role in terms of dynamical stability of our proposed model. Ultimately, numerical simulations are run in order to confirm the analytical findings.

Future scope of research work

Using an enhanced model, new tools, and techniques, the research conducted for this thesis can be developed into a more thorough study. These are a few possible areas of future research that may be covered.

• This research can be extended to formulate models under the effect of diffusion in Sundarban mangrove estuary. Diffusion theory is predicated on the idea that individuals within a population move randomly and isotropicallythat is, without favouring any particular direction.

• The effect of Seasonality can also be examined for a detritus-based model in future. As the amount of plant litter which falls on the ground can be different for different seasons, the amount of detritus can be changed with the change of season.

Bibliography

Agarwal, M., & Pathak, R. (2012). Persistence and optimal harvesting of prey-predator model with Holling Type III functional response. International Journal of Engineering, Science and Technology, 4(3), 78-96.

Agarwal, M., & Pathak, R. (2017). Harvesting and Hopf Bifurcation in a prey-predator model with Holling Type IV Functional Response. International journal of mathematics and soft computing, 2(1), 99.

Alsakaji, H. J., Kundu, S., & Rihan, F. A. (2021). Delay differential model of one-predator two-prey system with Monod-Haldane and holling type II functional responses. Applied Mathematics and Computation, 397, 125919.

Arqub, O. A., & El-Ajou, A. (2013). Solutions of the fractional epidemics model by homotopy analysis method. J King Saud Univ-Sci., 25(1), 7381.

Assila, C., Lemnaouar, M. R., Benazza, H., & Hattaf, K. (2024). Hopf bifurcation of a delayed fractional-order preypredator model with Holling type II and with reserved area for prey in the presence of toxicity. International Journal of Dynamics and Control, 12(5), 1239-1258.

Atangana, A., & Secer, A. (2013). A note on fractional order derivatives and table of fractional derivatives of some special functions. Abstract and Applied Analysis, 18.

Awawdeh, F., Adawi, A., & Mustafa, Z. (2009). Solutions of the SIR models of epidemics using HAM. Chaos Solitons Fractals, 42(5), 3047-3052.

Balci, E., (2023). Predation fear and its carry-over effect in a fractional order preypredator model with prey refuge. Chaos, Solitons & Fractals, 175, 114016.

Baldy, V., & Gessner, M. O. (1997). Towards a budget of leaf litter decomposition in a first-order woodland stream. C. R. Acad. Sci. Ser. III. SCi. Vie/Life Sci., 320, 747-758.

Bandyopadhyay, M., Bhattacharya, R., & Chakrabarti, C. G. (2003). A nonlinear two-species oscillatory system: bifurcation and stability analysis. International Journal of Mathematics and Mathematical Sciences, 31, 1981-1991.

Banerjee, M., & Takeuchi, Y. (2017). Maturation delay for the predators can enhance stable coexistence for a class of preypredator models. Journal of theoretical biology, 412, 154-171.

Batiha, B., Noorani, M. M., & Hashim, I. (2007). Variational iteration method for solving multispecies LotkaVolterra equations. Computers & Mathematics with Applications, 54(7-8), 903-909.

Biazar, J. (2006). Solution of the epidemic model by adomian decomposition method. Appl Math Comput, 173(2), 1101-1106.

Braza, P. A. (2003). The bifurcation structure of the HollingTanner model for predatorprey interactions using two-timing. SIAM J. Appl. Math, 63, 889-904.

Canale, R. (1969). Predator-prey relationships in a model for the activated process. Biotechnology and Bioengineering, 11(5), 887-907.

Cantrell, R. S., & Cosner, C. (2001). On the dynamics of predatorprey models with the BeddingtonDeAngelis functional response. Journal of Mathematical Analysis and Applications, 257(1), 206-222.

Caputo, M. (1967). Linear models of dissipation whose Q is almost frequency independent-II. Geophys J R Astron Soc., 13, 529539.

Caputo, M., & Mainardi, F. (1971). A new dissipation model based on memory mechanism. Pure and Applied Geophysics, 91, 134147.

Charles, F. (1993). Utilisation of fresh detritus derived from Cystoseira mediterranea and Posidonia oceania by deposit-feeding bivalve Abra ovata. Journal of Experimental Marine Biology and Ecology, 174(1), 4364.

Chauhan, R. P., Singh, R., Kumar, A., & Thakur, N. K. (2024). Role of prey refuge and fear level in fractional preypredator model with anti-predator. Journal of Computational Science, 81, 102385.

Choi, S. K., Kang, B., & Koo, N. (2014). Stability for Caputo fractional differential systems. Abstr Appl Anal, 16.

Chun, C., Jafari, H., & Kim, Y. I. (2009). Numerical method for the wave and nonlinear diffusion equations with the homotopy perturbation method. Computers & Mathematics with Applications, 57(7), 1226-1231.

Cole, K. S. (1993). Electric conductance of biological systems. In: Cold Spring Harbor Symposium on quantitative biology, 107116.

Collings, J. B. (1995). Bifurcation and stability analysis of temperature-dependent mite predatorprey interaction model incorporating a prey refuge. Bull. Math. Biol., 57, 6376.

Conway, E. D., & Smoller, J. A., (1986). Global analysis of a system of predatorprey equations. SIAM Journal on Applied Mathematics, 46(4), 630-642.

Das, B. K., Sahoo, D., Santra, N., & Samanta, G. (2023). Modeling predatorprey interaction: effects of perceived fear and toxicity on ecological communities. International Journal of Dynamics and Control, 1-33.

Das, K., & Gazi, N. H. (2011). Random excitations in modelling of algal blooms in estuarine systems. Ecological modelling, 222(14), 2495-2501.

Das, K., & Ray, S. (2008). Effect of delay on nutrient cycling in phytoplankton−zooplankton interactions in estuarine system. ecological modelling, 215(1-3), 69-76.

Das, K., Sabarmathi, A., Srinivas, M. N., Gazi, N. H., & Kumar B. R. (2015). Trophic cascades scenario of a detritus-based stage-structured model in marine ecology. Journal of Nonlinear Evolution Equations and Applications, 2014(6), 77-100.

Das, S. (2007). Functional Fractional Calculus for System Identification and Controls. Springer.

Das, S., & Gupta, P. K. (2011). A mathematical model on fractional LotkaVolterra equations. Journal of Theoretical Biology, 277, 16.

Das, T., Mukherjee, R. N., & Chaudhuri, K. S. (2009). Harvesting of a preypredator fishery in the presence of toxicity. Appl. Math. Modell., 33(5), 22822292.

Dash, M. C. (2001). Fundamentals of Ecology. Tata McGraw Hill, New Delhi.

Datta, J., Jana, D., & Upadhyay, R. K. (2019). Bifurcation and bio-economic analysis of a prey-generalist predator model with Holling type IV functional response and nonlinear age-selective prey harvesting. Chaos, Solitons & Fractals, 122, 229-235.

DeAngelis, D. L. (1969). Dynamics of nutrient cycling and food webs. Chapman and Hall, New York, USA.

Du, Y. H., & Hsu, S. B. (2004). A diffusive predatorprey model in heterogeneous environment. J. Differential Equations, 203(2), 331-364.

Dubey, B., & Kumar, A. (2019). Dynamics of preypredator model with stage structure in prey including maturation and gestation delays. Nonlinear Dynamics, 96(4), 2653-2679.

Dubey, V. P., Kumar, R., & Kumar, D. (2020). Numerical solution of time-fractional three-species food chain model arising in the realm of mathematical ecology. International Journal of Biomathematics, 13(02), 2050011.

El-Sayed, A. M. A., El-Mesiry, A. E. M., & El-Saka, H. A. A. (2007). On the fractional-order logistic equation. Applied mathematics letters, 20(7), 817-823.

Faust, M. A., & Gulledge, R. A. (1996). Associations of microalgae and meiofauna in floating detritus at a mangrove Island, Twin Cays, Belize. Journal of Experimental Marine Biology and Ecology, 197(2), 159175.

Fedri, Y. (2012). Some applications of fractional order calculus to design digital flters for biomedical signal processing. J Mech Med Biol, 12(2), 13.

Findlay, S. E. G., & Arsuffi, T. L. (1989). Microbial growth and detritus transformations during decomposition of leaf litter in a stream. Freshwat. Biol., 21, 261-269.

Findlay, S. E. G., Dye, S., & Kuehn, K. A. (2002). Microbial growth and nitrogen retention in litter of Phragmites australis compared to Typha angustifolia. Wetlands, 22, 616-625.

Forde, J. (2005). Delay differential equation models in mathematical biology. PhD thesis, University of Michigan.

Freedman, H. I. (1980). Deterministic Mathematical Models in Population Ecology. Marcel Dekker, New York, NY.

Freedman, H. I., & Shukla, J. B. (1990). Models for the effect of toxicant in single-species and predator-prey systems. J. Math. Biol., 30(1), 1530.

Gazi, N. H., & Bandyopadhyay, M. (2006). Effect of time delay on a detritus-based ecosystem. International journal of mathematics and mathematical sciences.

Gazi, N. H., & Das, K. (2010). Control of parameters of a delayed diffusive autotroph herbivore system. Journal of Biological systems, 18(02), 509-529.

Ghosh, D., & Sarkar, A. K. (1997). Oscillatory behaviour of an autotroph-herbivore system with a type-III uptake function. International journal of systems science, 28(3), 259-264.

Golmankhaneh, A. K., Golmankhaneh, A. K., & Baleanu, D. (2011). On nonlinear fractional KleinGordon equation. Signal Processing, 91(3), 446-451.

Gompertz, B. (1825). On the Nature of the Function Expressive of the Law of Human Mortality, and on a New Mode of Determining the Value of Life Contingencies. philosophical Transactions of the Royal Society of London, 115, 513-583.

Gonzalez-Olivares, E., & Ramos-Jiliberto, R. (2003). Dynamics consequences of prey refuge in a simple model system: more prey and few predators and enhanced stability. Ecol. Model., 166, 135146.

Gonzlez-Olivares, E., & Ramos-Jiliberto, R. (2004). Consequences of prey refuge use on the dynamics of some simple predator-prey models: Enhancing stability?. Proceedings of the Third Brazilian Symposium on Mathematical and Computational Biology, E-Papers Services Editorials, Ltda, 2, 75-98.

Gonzlez-Olivares, E., & Rojas-Palma, A. (2011). Multiple limit cycles in a Gause type predatorprey model with Holling type III functional response and Allee effect on prey. Bulletin of Mathematical Biology, 73(6), 1378-1397.

Gulis, V., & Suberkropp, K. (2003). Effect of inorganic nutrients on relative contributions of fungi and bacteria to carbon flow from submerged decomposing leaf litter. Microbial Ecology, 45, 11-19.

Haeckel, E. H. P. A. (1866). Generelle Morphologie der Organismen. Allgemeine Grundzge der organischen Formen-Wissenschaft, mechanische Begrndet durch die von Charles Darwin reformirte Descendenz-Theorie. Volume I: Allgemeine Anatomie der Organismen. 32 + 574 pages; volume II: Alllgemeine Entwickelungsgeschichte der Organismen. 140 + 462 pages. Georg Reimer, Berlin, Germany.

Hale, J. K. (1969). Ordinary Differential Equations. Wiley-Interscience, New York, NY, 242.

Haque, M. (2011). A detailed study of the BeddingtonDeAngelis predatorprey model. Mathematical Biosciences, 234(1), 1-16.

Haque, M. (2012). Existence of complex patterns in the BeddingtonDeAngelis predatorprey model. Mathematical biosciences, 239(2), 179-190.

Haque, M., Sarwardi, S., Preston, S., & Venturino, E. (2011). Effect of delay in a Lotka-Volterra type predatorprey model with a transmissible disease in the predator species. Mathematical Biosciences, 234(1), 47-57.

Hassard, B. D., Hassard, B. D., Kazarinoff, N. D., Wan, Y. H., & Wan, Y. W. (1981). Theory and applications of Hopf bifurcation. CUP Archive, (Vol. 41).

Hassell, M. P., & May, R. M. (1973). Stability in insect host-parasite modes", The Journal of Animal Ecology. 693-726.

He, J. H. (1999). Homotopy perturbation technique. Comput. Meth. Appl. Mech. Eng., 178, 257-262.

He, J. H. (2005). Homotopy perturbation method for bifurcation of nonlinear problems. Int. J. Nonlin. Sci. Numer. Simul., 6, 207-208.

He, J. H. (2005). Application of homotopy perturbation method to nonlinear wave equations. Chaos, Solitons & Fractals, 26(3), 695-700.

Hieber, M., & Gessner, M. O. (2002). Contribution of stream detrivores, fungi, and bacteria to leaf breakdown based on biomass estimates. Ecology, 83, 1026-1038.

Hifer, R. (2000). Application of Fractional Calculus in Physics, World Scientific.

Hofbauer, J. (1981). A general cooperation theorem for hypercycles. Monatsh. Math., 91, 233-240.

Hooker, P. F. (1965). Benjamin Gompertz: 5 March 1779-14 July 1865. Journal of the Institute of Actuaries, 91, 203-212.

Hsu, S. B., & Huang, T. W. (1995). Global stability for a class of predatorprey systems. SIAM J. Appl. Math, 55, 763-783.

Hsu, S. B., Hwang, T. W., & Kuang, Y. (2008). Global dynamics of a predator-prey model with Hassell-Varley type functional response. Discrete Contin. Dyn. Syst. Ser. B, 10(4), 857-871.

Hu, H., & Huang, L. (2010). Stability and Hopf bifurcation in a delayed predatorprey system with stage structure for prey. Nonlinear Analysis: Real World Applications, 11(4), 2757-2769.

Huang, K. G., Cai, Y. L., Rao, F., Fu, S. M., & Wang W. M. (2018). Positive steady states of a density-dependent predatorprey model with diffusion. Discrete Contin. Dyn. Syst. Ser. B, 23(8), 3087-3107.

Huang, Y., Chen, F., & Zhong, L. (2006). Stability analysis of a preypredator model with Holling type III response function incorporating a prey refuge. Applied Mathematics and Computation, 182(1), 672-683.

Hutchinson, G. E. (1948). Circular causal systems in ecology. Ann. NY Acad. Sci, 50(4), 221-246.

Hutson, V., & Vickers, G. T. (1983). A criteria for permanent coexistence of species, with an application to a two prey one predator system. Math. Biosci., 63, 253-269.

Hwang, T. W. (2003). Global analysis of the predatorprey system with BeddingtonDeAngelis functional response. Journal of Mathematical Analysis and Applications, 281(1), 395-401.

Ishteva, M. (2005). Properties and applications of the Caputo fractional operator. Master thesis, Department of Mathematics, University of Karlsruhe, Karlsruhe.

Isik, S., & Kangalgil, F. (2024). Dynamical analysis and chaos control of a fractional-order Leslie-type predatorprey model with Caputo derivative. International Journal of Biomathematics, 17(4).

Ivlev, V. S. (1961). Experimental Ecology of the Feeding of Fishes. Yale University Press, New Haven.

Jana, D., Dolai, P., Pal, A. K., & Samanta, G. P. (2016). On the stability and Hopf-bifurcation of a multi-delayed competitive population system affected by toxic substances with imprecise biological parameters. Model. Earth Syst. Environ., 2(3), 110.

Jana, S., Chakraborty, M., Chakraborty, K., & Kar, T. K. (2012). Global stability and bifurcation of time delayed preypredator system incorporating prey refuge. Mathematics and Computers in Simulation, 85, 57-77.

Jayaprakasha, P. C., & Baishya, C. (2020). The Elzaki Transform with Homotopy Perturbation Method for Nonlinear Volterra Integrow-Differential Equations. Advances in Differential Equations & Control Processes, 23(2).

Jiang, X. Y., & Xu, M. Y. (2006). Analysis of fractional anomalous diffusion caused by an instantaneous point source in disordered fractal media. International Journal of Non-Linear Mechanics, 41, 156165.

Joint, I. R. (1978). Microbial production of an estuarine mudflat. Estuarine Coastal and Marine Science, 7(2), 185195.

Kar, T. K. (2005). Stability analysis of a pre-predator model incorporating a prey refuge. Commun. Nonlinear Sci. Numerical Simulation, 10, 681691.

Kexue, L., & Jigen, P. (2011). Laplace transform and fractional differential equations. Appl Math Lett, 24(12), 201923.

Khan, N. A., Razzaq, O. A., Mondal, S. P., & Rubbab, Q. (2019). Fractional order ecological system for complexities of interacting species with harvesting threshold in imprecise environment. Advances in Difference Equations, 1-34.

Kilbas, A. A., & Srivastava, H. M., & Trujilo, J. J. (2006). Theory and Applications of Fractional Differential Equations. Elsevier.

Ko, W., & Ryu, K. (2007). Non-constant positive steady-states of a diffusive predatorprey system in homogeneous environment. J. Math. Anal. Appl, 327, 539-549.

Kominkova, D., Kuehn, K. A., Busing, N., Steiner, D., & Gessner, M. O. (2000). Microbial biomass, growth, and respiration associated with submerged litter of Phragmites australis decomposing in a littoral reed stand of a large lake. Aquat. Microb. Ecol., 22, 271-282.

Kooi, B., & Kooijman, S. (1994). Existence and stability of microbial prey-predator systems. Journal of Theoretical Biology, 170(1), 75-85.

Kooij, R. E., & Zegeling, A. (1996). A predator-prey model with Ivlev's functional response. Journal of Mathematical Analysis and Applications, 198(2), 473-489.

Kuang, Y. (1993). Delay Differential Equations: With Applications in Population Dynamics. Academic Press.

Kuehn, K. A., Lemka, M. J., Suberkropp, K., & Wetzel, R. G. (2000). Microbial biomass and production associated with decaying leaf litter of the emergent macrophyte Juncus effusus, Limnol. Oceanorg., 45, 862-870.

Kumar, P., & Agrawal, O. P. (2006). An approximate method for numerical solution of fractional differential equations. Signal Process, 6, 26022610.

Kumar, S., Kumar, A., Samet, B., & Dutta, H. (2021). A study on fractional hostparasitoid population dynamical model to describe insect species. Numerical Methods for Partial Differential Equations, 37(2), 1673-1692.

Kundu, S., & Maitra, S. (2018). Dynamical behaviour of a delayed three species predator-prey model with cooperation among the prey species. Nonlinear Dyn, 92, 627643.

Li, H. L., Zhang, L., Hu, C., Jiang, Y. L., & Teng, Z. (2017). Dynamical analysis of a fractional-order predator-prey model incorporating a prey refuge. Journal of Applied Mathematics and Computing, 54, 435-449.

Li, S., Wang, X., Li, X., & Wu, K. (2021). Relaxation oscillations for Leslie-type predatorprey model with Holling Type I response functional function. Applied Mathematics Letters, 120, 107328.

Li, Y., Chen, Y., & Podlubny, I. (2009). Mittagleffler stability of fractional order nonlinear dynamic systems. Automatica, 45(8), 19651969.

Liang, S., Wu, R., & Chen, L. (2015). Laplace transform of fractional order differential equa- tions. Electron J Differ Equ, 139, 115.

Linley, J. R. (1968). Studies on larval biology of Leptoconops (Kieff.)(Diptera: Ceratopogonidae). Bulletin of Entomological Research, 58(1), 124.

Linley, J. R., & Adams, G. M. (1997). Ecology and behaviour of immature Culicoides melleus(Coq.)(Diptera: Ceratogonidae). Bulletin of Entomological Research, 62(1), 113127.

Liu, W., Jiang, Y., & Chen, Y. (2016). Dynamic properties of a delayed predatorprey system with Ivlev-type functional response. Nonlinear Dynamics, 84(2), 743-754.

Liu, X., & Huang, Q. (2020). Analysis of optimal harvesting of a predator-prey model with Holling type IV functional response. Ecological Complexity, 42, 100816.

Lotka, A. J. (1925). Elements of Physical Biology. Williams and Wilkins, Baltimore, USA.

Magin, R. L. (2004). Fractional calculus in bioengineering part 2. Crit. Rev. Biomed. Eng., 2,105193.

Maiti, A. P., Dubey, B., & Chakraborty, A. (2019). Global analysis of a delayed stage structure preypredator model with CrowleyMartin type functional response. Mathematics and Computers in Simulation, 162, 58-84.

Majumdar, P., Debnath, S., Sarkar, S., & Ghosh, U. (2022). The complex dynamical behavior of a prey-predator model with Holling type-III functional response and non-linear predator harvesting. International Journal of Modelling and Simulation, 42(2), 287-304.

Malthus, T. R. (1973). An essay on the Principle of Population. London: J. Johnson.

Maynard-Smith J. (1974). Models in Ecology. Cambridge University Press.

Miller, K., & Ross, B. (1993). An Introduction to the Fractional Calculus and Fractional Differential Equations. Wiley-Interscience Publication.

Milton, J. (2015). Time delays and the control of biological systems: An overview. IFAC-Papers OnLine, 48, 8792.

Mishra, H. K., & Tripathi, R. (2020). Homotopy perturbation method of delay differential equation using hes polynomial with laplace transform. Proceedings of the National Academy of Sciences, India Section A: Physical Sciences, 90, 289-298.

Molla, H., Rahman, M. S., & Sarwardi, S. (2019). Dynamics of a predatorprey model with Holling type II functional response incorporating a prey refuge depending on both the species. International Journal of Nonlinear Sciences and Numerical Simulation, 20(1), 89-104.

Moussaoui A. et al. (2010). Effect of a toxicant on the dynamics of a spatial fishery. Afr. Diaspora J. Math. New Ser., 10(2), 122134.

Mukhopadhyay, B., Bera, A., & Bhattacharyya, R. (2010). Diffusive instability and traveling waves in a mangrove ecosystem food-chain model with delayed detritus recycling. International Journal of Biomathematics, 3(02), 225-241.

Murmu, T., Sarkar, A. K. (2020). Qualitative Behaviour of a Detritus-Based Prey-Predator Model of Sundarban Mangrove Forest, India. Global Journal of Pure and Applied Mathematics, 16(1), 9-25.

Newell, S. Y., Fallon, R. D., & Miller, J. D. (1989). Decomposition and microbial dynamics for standing naturally positioned leaves of the salt-marsh grass Spartina alterniflora. Mar. Biol., 101, 471-482.

Noor, M. A., & Mohyud-Din, S. T. (2008). Homotopy perturbation method for solving sixth-order boundary value problems. Computers & Mathematics with Applications, 55(12), 2953-2972.

Odibat, Z., & Momani, S. (2008). Modified homotopy perturbation method: application to quadratic Riccati differential equation of fractional order. Chaos, Solitons & Fractals, 36(1), 167-174.

Odibat, Z. M., & Shawagfeh, N. T. (2007). Generalized taylors formula. Appl Math Comput, 186(1), 28693.

Ogunmiloro, O. M., Fadugba, S. E., & Titiloye, E. O. (2021). On the existence, uniqueness and computational analysis of a fractional order spatial model for the squirrel population dynamics under the Atangana-Baleanu-Caputo operator. Math. Model. Comput, 8(3), 432-443.

Owolabi, K. M. (2017). Mathematical modelling and analysis of two-component system with Caputo fractional derivative order. Chaos, Solitons & Fractals, 103, 544-554.

Pal, P. J., & Mandal, P. K. (2014). Bifurcation analysis of a modified LeslieGower predator-prey model with BeddingtonDeAngelis functional response and strong Allee effect. Mathematics and Computers in Simulation, 97, 123-146.

Pal, S., Majhi, S., Mandal, S., & Pal, N. (2019). Role of fear in a predatorprey model with BeddingtonDeAngelis functional response. Zeitschrift fr Naturforschung A, 74(7), 581-595.

Panja, P. (2021). Dynamics of a predatorprey model with crowleymartin functional response, refuge on predator and harvesting of super-predator. Journal of Biological Systems, 29(03), 631-646.

Peng, R., & Wang, M. X. (2005). Positive steady-states of the HollingTanner preypredator model with diffusion. Proc. Roy. Soc. Edinburgh Sect. A, 135, 149-164.

Peng, R., & Wang, M. X. (2007). Global stability of the equilibrium of a diffusive Holling-Tanner preypredator model. Appl. Math. Lett, 20, 664-670.

Petras, I. (2011). Fractional-Order nonlinear systems. Beijing: Higher Education Press, Beijing and Springer-Verlag Berlin Heidelberg.

Podlubny, I. (1999). Fractional differential equations, vol. 198 of mathematics in science and engineering. Academic Press, San Diego, Calif, USA.

Rafei, M., Ganji, D. D., & Daniali, H. (2007). Variational iteration method for solving the epidemic model and the prey and predator problem. Appl Math Comput, 186, 1701-1709.

Rafei, M., Ganji, D. D., & Daniali, H. (2007). Solution of the epidemic model by homotopy perturbation method. Appl Math Comput, 187, 1056-1062.

Rai, B., Freedman, H. I., & Addicott, J. F. (1983). Analysis of three species models of mutualism in predator-pre and competitive systems. Math. Biosci, 65, 13-50.

Ray, S., & Choudhury, A. (1998). Salinity tolerance of Culex sitiens (Weid.) (Diptera: Culicidae) larvae in laboratory condition. Current Science, 57(3), 159160.

Rida, S. Z., El-Sherbiny, H. M., & Arafa, A. A. M. (2008). On the solution of the fractional nonlinear Schrodinger equation. Physics Letters A, 372(5), 553558.

Rivero, M., Trujillo, J. J., Vazquez, L., & Velasco, M. P. (2011). Fractional dynamics of populations. Appl. Math. Comput., 218, 10891095.

Ross, B., & Miller, K. S. (1993). An introduction to the fractional calculus and fractional differential equations. John Wiley and Sons, New York.

Roy, U., Sarwardi, S., Majee, N. C., & Ray, S., (2016). Effect of salinity and fish predation on zooplankton dynamics in HooghlyMatla estuarine system, India. Ecological informatics, 35, 19-28.

Saadatmandi, A., Dehghan, M., & Eftekhari, A. (2009). Application of Hes homotopy perturbation method for non-linear system of second-order boundary value problems. Nonlinear Analysis: Real World Applications, 10(3), 1912-1922.

Sabatier, J., Agrawal, O. P., & Tenreiro Machado, J. A. (2007). Advances in Fractional Calculus: Theoretical Developments and Applications in Physics and Engineering. Springer.

Saez, E., & Gonzalez-Olivares, E. (1999). Dynamics of a predatorprey model. SIAM J. Appl. Math., 59, 1867-1878.

Samanta, G. P. (2010). A two-species competitive system under the influence of toxic substances. Appl. Math. Comput., 216(1), 291299.

Samko, S., Kilbas, A., & Marichev, O. (1993). Fractional Integrals and Derivatives. Gordon and Breach Science Publishers.

Santra, P. K., Mahapatra, G. S., & Phaijoo, G. S. (2020). Bifurcation and chaos of a discrete predator-prey model with CrowleyMartin functional response incorporating proportional prey refuge. Mathematical Problems in Engineering, 1-18.

Sarkar, A. K., & Ghosh, D. (1997). Role of detritus in a general prey-predator model of Sunderban Estuary, India. Biosystems, 44(2), 153-160.

Sarkar, A. K., Mitra, D., & Roy, A. B. (1990). Stability of partially closed producer-consumer system via decomposer. Ganit. Journal of Bangladesh Mathematical Society, 10(1-2), 21-27.

Sarkar, A. K., Mitra, D., Ray, S., & Roy, A. B. (1991). Permanence and oscillatory co-existence of a detritus-based prey-predator model. Ecological modelling, 53, 147-156.

Sarwardi, S., Mandal, P. K., & Ray, S. (2012). Analysis of a competitive preypredator system with a prey refuge. Biosystems, 110(3), 133-148.

Sayevand, K., Fardi, M., Moradi, E., & Boroujeni, F. H. (2013). Convergence analysis of homotopy perturbation method for Volterra integro-differential equations of fractional order. Alexandria Engineering Journal, 52(4), 807-812.

Seo, G., & DeAngelis, D. L. (2003). A PredatorPrey Model with a Holling Type I Functional Response Including a Predator Mutual Interference. J Nonlinear Sci, 21, 811833.

Seo, G., & Kot, M. (2008). A comparison of two predatorprey models with Hollings type I functional response. Mathematical biosciences, 212(2), 161-179.

Shawagfeh, N. T., & Adomian G. (1996). Nonperturbative analytical solution of the general Lotka-Volterra three-species system. App. Math. Comput., 76, 251-266.

Tanner, J. T. (1975). The stability and the intrinsic growth rates of prey and predator populations. Ecology, 56, 855-867.

Tenreiro Machado, J. A. (2010). Entropy analysis of integer and fractional dynamical systems. Nonlinear Dynamics, 62, 371-378.

Tenreiro Machado, J. A., & Galhano, A. M. (2012). Fractional order inductive phenomena based on the skin effect. Nonlinear Dynamics, 68(1), 107-115.

Thakur, N. K., Ojha, A., Jana, D., & Upadhyay, R. K. (2020). Modeling the planktonfish dynamics with top predator interference and multiple gestation delays. Nonlinear Dynamics, 100, 4003-4029.

Thakur, N. K., Tiwari, S. K., Dubey, B., & Upadhyay, R. K. (2017). Diffusive three species plankton model in the presence of toxic prey: application to Sundarban mangrove wetland. Journal of Biological Systems, 25(02), 185-206.

Thingstad, T. F., & Langeland, T. I. (1974). Dynamics of chemostat culture: The effect of a delay in cell response. Journal of Theoretical Biology, 48(1), 149-159.

Vetter, E. W. (1998). Population dynamics of a dense assemblage of marine detritivores. Journal of Experimental Marine Biology and Ecology, 226(1), 131161.

Volterra, V. (1926). Fluctuations in the abundance of species considered mathematically. Nature, 118, 157-158.

Wang, S., & Xu, M. (2009). Axial Couette flow of two kinds of fractional viscoelastic fluids in an annulus. Nonlinear Analysis: Real World Applications, 10(2), 10871096.

Wang, W., Zhang, L., Wang, H., & Li, Z. (2010). Pattern formation of a predator-prey system with Ivlev-type functional response, Ecological Modelling, 221(2), 131-140.

Wang, Y. H. (2009). Numerical algorithm based on Adomian decomposition for fractional differential equations. Comput. Mathem. Appl., 57, 16271681.

Xie, B., Wang, Z., Xue, Y., & Zhang, Z. (2015). The dynamics of a delayed predator−prey model with double Allee effect. Discrete Dynamics in Nature and Society.

Xu, C., & Li, P. (2015). Oscillations for a delayed predatorprey model with HassellVarley-type functional response. Comptes rendus biologies, 338(4), 227-240.

Yan, X. P., & Li, W. T. (2006). Hopf bifurcation and global periodic solutions in a delayed predatorprey system. Applied Mathematics and Computation, 177(1), 427-445.

Yan, X. P., & Zhang, C. H. (2008). Hopf bifurcation in a delayed LoktaVolterra predatorprey system. Nonlinear Analysis: Real World Applications, 9(1), 114-127.

Yzbasi, S., & Karaayir, M. (2017). Application of homotopy perturbation method to solve two models of delay differential equation systems. International Journal of Biomathematics, 10(06), 1750080.

Zhao, J., & Shao, Y. (2023). Bifurcations of a prey-predator system with fear, refuge and additional food. Math. Biosci. Eng, 20, 3700-3720.

Zhou, Y., Sun, W., Song, Y., Zheng, Z., Lu, J., & Chen, S. (2019). Hopf bifurcation analysis of a predatorprey model with Holling-II type functional response and a prey refuge. Nonlinear Dynamics, 97(2), 1439-1450.

List of publications

1. **Tanushree Murmu** and Ashis Kumar Sarkar (2020), Qualitative Behaviour of a Detritus-Based Prey-Predator Model of Sundarban Mangrove Forest, India, **Global Journal of Pure and Applied Mathematics**, 16 (1): 9-25.

2. **Tanushree Murmu** and Ashis Kumar Sarkar (2022), Qualitative Analysis of Micro-Organism Pool and Its Invertebrate Predator with Discrete Time-Delay in Sundarban Estuary, India, **Bull. Cal. Math. Soc.**, 114 (6): 919-942.

3. **Tanushree Murmu** and Ashis Kumar Sarkar (2024), Approximate Analytical Solution of a Fractional Order Detritus-Based Predator-Prey Model Using Homotopy Perturbation Method, **Journal of Research in Applied Mathematics**, 10(3): 01-12.

4. **Tanushree Murmu** and Ashis Kumar Sarkar, Dynamical Complexity of a Detritus-Based Predator-Prey Model with Multiple Time Delays in Sundarban Mangrove Ecosystem, India. This paper is presented at **"International Conference on Mathematical Modelling and Emerging Trends in Computing (ICMMETC-2023),"** School of Technology, Woxsen University, Hyderabad, India. This paper is accepted for publication in conference proceedings.

5. **Tanushree Murmu** and Ashis Kumar Sarkar, Effect of Prey Refuge on a Fractional Order Detritus-Based Predator-Prey Model in Presence of Toxicity. This paper is submitted in Journal of Mathematical Biology for publication.